

SYNTHESIS AND CHARACTERIZATION OF OLIGO/POLYTHIOPHENES
BEARING STABLE RADICALS

by

Somaiah Almubayedh

A thesis submitted in partial fulfillment
of the requirements for the degree of
Master of Science (MSc) in Chemical Sciences

The School of Graduate Studies
Laurentian University
Sudbury, Ontario, Canada

© Somaiah Almubayedh, 2014

THESIS DEFENCE COMMITTEE/COMITÉ DE SOUTENANCE DE THÈSE
Laurentian University/Université Laurentienne
Faculty of Graduate Studies/Faculté des études supérieures

Title of Thesis Titre de la thèse	Synthesis and Characterization of Oligo/Polythiophenes Bearing Stable Radicals	
Name of Candidate Nom du candidat	Almubayedh, Somaiah	
Degree Diplôme	Master of Science	
Department/Program Département/Programme	Chemical Sciences	Date of Defence Date de la soutenance August 25, 2014

APPROVED/APPROUVÉ

Thesis Examiners/Examineurs de thèse:

Dr. M'hamed Chahma
(Supervisor/Directeur(trice) de thèse)

Dr. Hélène Joly
(Committee member/Membre du comité)

Dr. Gerardo Ulibarri
(Committee member/Membre du comité)

Dr. Martin Lemaire
(External Examiner/Examineur externe)

Approved for the Faculty of Graduate Studies
Approuvé pour la Faculté des études supérieures
Dr. David Lesbarrères
M. David Lesbarrères
Acting Dean, Faculty of Graduate Studies
Doyen, Faculté des études supérieures

ACCESSIBILITY CLAUSE AND PERMISSION TO USE

I, **Somaiah Almubayedh**, hereby grant to Laurentian University and/or its agents the non-exclusive license to archive and make accessible my thesis, dissertation, or project report in whole or in part in all forms of media, now or for the duration of my copyright ownership. I retain all other ownership rights to the copyright of the thesis, dissertation or project report. I also reserve the right to use in future works (such as articles or books) all or part of this thesis, dissertation, or project report. I further agree that permission for copying of this thesis in any manner, in whole or in part, for scholarly purposes may be granted by the professor or professors who supervised my thesis work or, in their absence, by the Head of the Department in which my thesis work was done. It is understood that any copying or publication or use of this thesis or parts thereof for financial gain shall not be allowed without my written permission. It is also understood that this copy is being made available in this form by the authority of the copyright owner solely for the purpose of private study and research and may not be copied or reproduced except as permitted by the copyright laws without written authority from the copyright owner.
droit d'auteur

Abstract

Two categories of verdazyl radical functionalized oligothiophenes have been prepared: 1,5-diisopropyl-6-oxoverdazyl radical directly linked to terthiophene (**2.6**), and 1,5-diisopropyl-6-oxoverdazyl radical attached to terthiophene through a π system bridge, e.g., pyridine (**2.11**).

Compound radical **2.6** was prepared by a two step process starting with the condensation of terthiophene carboxaldehyde and 2,4-diisopropylcarbonhydrazide bis-hydrochloride to give the tetrazane **2.5**, which was subsequently oxidized chemically to give the corresponding verdazyl radical grafted at the 3' position of the terthiophene moiety. The latter displays excellent stability toward organic solvents and moisture.

The electropolymerization of radical **2.6** resulted in the formation of its polymer (poly(**2.6**)), which was characterized by cyclic voltammetry and infrared spectroscopy. The electrochemical oxidation of the tetrazane, **2.5**, yielded surprisingly a poly(terthiophene) bearing verdazyl radical, with similar electrochemical and infrared properties of those found for the polymer produced in the electro-oxidation of the terthiophene bearing verdazyl radical (poly(**2.6**)). Moreover, the electrochemical oxidation of **2.5** (beyond its oxidation potential of the tetrazane motif) affords the radical **2.6**.

A similar strategy has been used for the synthesis and the characterization of tetrazane **2.10** and its corresponding verdazyl **2.11**.

Acknowledgments

Foremost, I would like to express my sincere gratitude to my supervisor Dr. M'hamed Chahma for the continuous support of my M.Sc. study and research, for his patience and immense knowledge. His guidance helped me in all the time of research and writing of this thesis.

I would like also to thank the rest of my thesis committee Dr. Helen Joly and Dr. Gerardo Ulibarri for their suggestions and discussions over the past two years.

It is also important that I thank my husband Mohammed and my two lovely kids Ritaj and Rakan for supporting me all the time.

Last but not the least; I would like to thank my family: my parents Sondos and Khalid, for giving birth to me at the first place and supporting me spiritually throughout my life.

Table of Contents

List of Tables.....	vii
List of Figures.....	viii
List of Schemes.....	x
List of Appendices.....	xii
Abbreviations and Symbols.....	xiii
Chapter 1. General Introduction.....	1
1 Stable Free Radicals.....	1
1.1 Hydrocarbon-Based Radicals.....	1
1.1.1 Triphenylmethyl and Related Radicals.....	1
1.1.2 Phenalenyl and Related Radicals.....	3
1.1.3 Phenoxy Radicals.....	3
1.2 Radicals with Spin Density on Nitrogen and Sulfur “Thiazyls”: Thioaminyl Radicals.....	5
1.3 Radicals Based on Nitrogen and/or Oxygen: Nitroxide and Nitronyl-Nitroxide Radicals.....	5
1.4 Verdazyl Radicals.....	6
1.4.1 Synthesis of Triaryl Verdazyl Radicals.....	7
1.4.2 Synthesis of 6-Oxo- and 6-Thioxoverdazyl Radicals.....	8
1.4.3 Synthesis of 1, 3, 5-Triaryl-6-oxoverdazyl Radicals.....	9
1.4.4 Synthesis of 1, 5-Diisopropyl-6-oxoverdazyl Radicals.....	9
1.5 Oligo/Polythiophene Grafted Stable Radical.....	10
1.5.1 Polythiophenes Bearing Phenoxy Radicals.....	11
1.5.2 Poly(3-Radical-Amino Thiophene).....	11
1.6 Applications and Uses of Stable Radicals.....	12
1.6.1 EPR Applications.....	12
1.6.2 Applications of Verdazyl Radicals.....	14
1.7 Objectives.....	17
Chapter 2. Synthesis of Verdazyl Radical Functionalized Terthiophene.....	19
2 Introduction.....	19
2.1 Nomenclature.....	19
2.2 Electrophilic Aromatic Substitution.....	19
2.3 Electron Paramagnetic Resonance.....	21

2.3.1	EPR of Pyrimidine-Verdazyl Radical.....	22
2.4	Synthesis of Radical Functionalized Terthiophenes.....	23
2.4.1	Synthesis of Verdazyl Radical Functionalized Terthiophene.....	23
2.4.2	Synthesis of Verdazyl Radical Functionalized Terthiophene Bridged by Pyridine.....	32
2.5	Summary.....	46
2.6	Experimental Section.....	47
2.6.1	Generalities.....	47
2.6.2	Synthesis of 2, 4-diisopropyl-6-terthiophene-3-oxotetrazane (2.5).....	47
2.6.3	Synthesis of 1,5-diisopropyl-3-terthiophene-6-oxoverdazyl (2.6).....	48
2.6.4	Synthesis of 6-(2,5-dibromo-thiophene-3-yl)pyridine-2-carboxaldehyde (2.8).....	48
2.6.5	Synthesis of 6-[2, 2': 5', 2'']terthiophen-3'-ylpyridine-2-carboxaldehyde (2.9).....	48
2.6.6	Synthesis of 2, 4-diisopropyl-6-terthiophene-3'-pyridine-2-yl-3-oxotetrazane (2.10).....	49
2.6.7	Synthesis of 1,5-diisopropyl-3-terthiophene-3'-pyridine-2-yl-6-oxoverdazyl (2.11).....	50
Chapter 3. Electropolymerization of Terthiophene Bearing a Verdazyl Radical.....		51
3	Introduction.....	51
3.1	Cyclic Voltammetry.....	51
3.2	Electropolymerization.....	54
3.3	Electrochemical Properties of Stable Radicals.....	55
3.4	Electrochemistry of Verdazyl Radical.....	56
3.5	Summary.....	71
3.6	Experimental Section.....	72
3.6.1	Generalities:.....	72
3.6.2	Electrochemical oxidation of all new monomers.....	72
3.6.3	Infrared spectroscopy (IR) of the polymers.....	72
Chapter 4. Conclusions and Future Work.....		73
4	Conclusions.....	73
References.....		76
Appenices: ¹ H and ¹³ C NMR Spectra Expansion.....		82

List of Tables

Table 2.1	Assignments of ^1H NMR signals for compound 2.5	25
Table 2.2	Assignments of ^{13}C NMR signals for compound 2.5	25
Table 2.3	HRMS data for compounds 2.5 and 2.6	29
Table 2.4	Assignment of ^1H NMR signals for compound 2.8	33
Table 2.5	Assignment of ^{13}C NMR signals for compound 2.8	34
Table 2.6	Assignment of ^1H NMR signals for compound 2.9	37
Table 2.7	Assignment of ^{13}C NMR signals for compound 2.9	37
Table 2.8	HRMS data for compounds 2.8 to 2.11	40
Table 2.9	Assignment of ^1H NMR signals for compound 2.10	42
Table 2.10	Assignment of ^{13}C NMR signals for compound 2.10	42
Table 3.1	Electrochemical properties of prepared terthiophene monomers and their corresponding polymers in ACN. [Scan rate of 0.1 V/s, WE = Platinum electrode, RE = Silver wire, and CE = Platinum wire]	57

List of Figures

Figure 2.1	EPR spectrum of pyrimidine-verdazyl radical taken from reference 74	22
Figure 2.2	500 MHz ^1H NMR spectrum of compound 2.5 in DMSO	26
Figure 2.3	500 MHz ^1H NMR expansion of CH_3 region of compound 2.5	27
Figure 2.4	500 MHz ^{13}C NMR spectrum of compound 2.5 in DMSO	28
Figure 2.5	A) IR spectra of compounds 2.5 (dashed line) and 2.6 (solid line), B) Expansion of $\text{C}=\text{O}$ region, and C) Expansion of NH region	30
Figure 2.6	Experimental EPR spectrum of compound 2.6 recorded at room temperature ($\nu = 9143 \mu\text{Hz}$, microwave power = 1 mw) (top) and simulated spectrum (bottom)	31
Figure 2.7	500 MHz ^1H NMR spectrum of compound 2.8 in CDCl_3	35
Figure 2.8	500 MHz ^{13}C NMR spectrum of compound 2.8 in CDCl_3	36
Figure 2.9	500 MHz ^1H NMR spectrum of compound 2.9 in CDCl_3	38
Figure 2.10	500 MHz ^{13}C NMR spectrum of compound 2.9 in CDCl_3	39
Figure 2.11	500 MHz ^1H NMR spectrum of compound 2.10 in CDCl_3	41
Figure 2.12	500 MHz ^{13}C NMR spectrum of compound 2.10 in CDCl_3	43
Figure 2.13	A) IR spectra of compounds 2.10 (dashed line) and 2.11 (solid line), B) Expansion of NH region, and C) Expansion of $\text{C}=\text{O}$ region	44
Figure 2.14	Experimental EPR spectrum of compound 2.11 recorded at room temperature ($\nu = 9086 \mu\text{Hz}$, microwave power = 1 mw) (top) and simulated spectrum (bottom)	45
Figure 3.1	Components of an electrochemical cell	51
Figure 3.2	Cyclic voltammetry of a reversible system	53
Figure 3.3	Cyclic voltammetry of a quasi-reversible system	53
Figure 3.4	Cyclic voltammetry of an irreversible system	54
Figure 3.5	A 20 scan electrochemical oxidation of 2.3 in ACN. [Scan rate = 0.1 V/s, WE = Platinum electrode, RE = Silver wire, and CE = Platinum wire]	58
Figure 3.6	A 20 scan electrochemical oxidation of 2.9 in ACN. [Scan rate = 0.1 V/s, WE = Platinum electrode, RE = Silver wire, and CE = Platinum wire]	59
Figure 3.7	The first CV scan of 2.5 in ACN. [Scan rate = 0.1 V/s, WE = Platinum electrode, RE = Silver wire, and CE = Platinum wire]	59
Figure 3.8	A 10 scan electrochemical oxidation of 2.5 in ACN. [Scan rate = 0.1 V/s, WE = Platinum electrode, RE = Silver wire, and CE = Platinum wire]	61
Figure 3.9	The first CV scan of 2.6 in ACN. [Scan rate = 0.1 V/s, WE = Platinum electrode, RE = Silver wire, and CE = Platinum wire]	62
Figure 3.10	A 10 scan electrochemical oxidation of 2.6 in ACN. [Scan rate = 0.1 V/s, WE = Platinum electrode, RE = Silver wire, and CE = Platinum wire]	63

	wire]	
Figure 3.11	One scan CV of poly(2.5) in monomer free solution using ACN. [Scan rate = 0.1 V/s, WE = Platinum electrode, RE = Silver wire, and CE = Platinum wire]	64
Figure 3.12	One scan CV of poly(2.6) in monomer free solution using ACN. [Scan rate = 0.1 V/s, WE = Platinum electrode, RE = Silver wire, and CE = Platinum wire]	65
Figure 3.13	IR spectra of poly(2.5) (dashed line) and poly(2.6) (solid line)	66
Figure 3.14	The first CV scan of 2.10 in ACN. [Scan rate = 0.1 V/s, WE = Platinum electrode, RE = Silver wire, and CE = Platinum wire]	67
Figure 3.15	The electropolymerization of 2.10 in ACN. [Scan rate = 0.1 V/s, WE = Platinum electrode, RE = Silver wire, and CE = Platinum wire]	68
Figure 3.16	The first CV scan of 2.11 in ACN. [Scan rate = 0.1 V/s, WE = Platinum electrode, RE = Silver wire, and CE = Platinum wire]	69
Figure 3.17	A 10 scan electrochemical oxidation of 2.11 in ACN. [Scan rate = 0.1 V/s, WE = Platinum electrode, RE = Silver wire, and CE = Platinum wire]	70

List of Schemes

Scheme 1.1	Equilibrium of the triphenylmethyl radical with its dimer	1
Scheme 1.2	Delocalization of unpaired electron on <i>ortho</i> - and <i>para</i> - phenyl positions of triphenylmethyl radicals	2
Scheme 1.3	<i>Para</i> -substituted (1.3) and the perchlorinated (1.4) derivatives of the triphenyl radical	2
Scheme 1.4	Polychlorinated triphenyl radicals	2
Scheme 1.5	Equilibrium of phenalenyl radical with its dimeric species	3
Scheme 1.6	Delocalized resonance over the six α -carbons in phenalenyl radicals	3
Scheme 1.7	Phenoxy radical 1.10 and its peroxide dimers 1.11	4
Scheme 1.8	Delocalization of the unpaired electron over <i>ortho</i> - and <i>para</i> -carbons in phenoxy radical	4
Scheme 1.9	Delocalization of the unpaired electron in galvinoxyl radical	4
Scheme 1.10	Combination of two thioaminy radicals results in a σ -bond formation between two nitrogen atoms	5
Scheme 1.11	Examples of nitroxide and nitronyl-nitroxide radicals	5
Scheme 1.12	Decomposition of nitroxide radical	6
Scheme 1.13	Structure of di- <i>t</i> -butyl nitroxide (1.21) and TEMPO (1.22)	6
Scheme 1.14	Verdazyl backbone with known modifications	6
Scheme 1.15	Structures of a non-planar (1.24) and planar (1.25) verdazyl radicals	7
Scheme 1.16	Formazan alkylation attempt; the synthesis of triaryl verdazyl radical	7
Scheme 1.17	Synthesis of 3-oxo or 3-thioxotetrazanes	8
Scheme 1.18	Oxidation of tetrazane through the intermediacy of leucoverdazyl, 1.28	8
Scheme 1.19	Synthesis of 1,3,5-triaryl-6-oxoverdazyl radical (1.30) from the oxidation of the 1,3,5-triaryl-6-oxotetrazane (1.33)	9
Scheme 1.20	Synthesis of 1,5-diisopropyl-6-oxoverdazyl radicals (1.40)	10
Scheme 1.21	Poly(3-radical-substituted thiophene)s	10
Scheme 1.22	Formation of polythiophenes bearing phenoxy radicals (1.47)	11
Scheme 1.23	Amino-substituted thiophenes	12
Scheme 1.24	Examples of spin traps	13
Scheme 1.25	Radical trapping using 5,5-dimethyl-2-pyrroline-N-oxide (1.52)	13
Scheme 1.26	Chemical structure of spin label used in biological study	14
Scheme 1.27	Verdazyl-mediated stable free radical polymerization (SFRP) system	14
Scheme 1.28	Formation of dihydrotetrazinone heterocyclic structures via cycloaddition reactions	15
Scheme 1.29	Polymerization of styrene and <i>n</i> -butyl acrylate under LRP condition in the presence of verdazyl unimer BSV	15

Scheme 1.30	Formation of copper (I) complex 1.65	16
Scheme 1.31	Formation of air-stable complexes, 1.67 , using $M(\text{hfac})_2 \cdot 2\text{H}_2\text{O}$	16
Scheme 1.32	The structure of an oligo/polythiophene bearing stable radical	17
Scheme 1.33	The chemical structure of poly(2.6) and poly(2.11)	17
Scheme 1.34	Synthesis of a verdazyl radical using electrochemical oxidation	18
Scheme 2.1	Nomenclature of thiophene, bithiophene and terthiophene	19
Scheme 2.2	Electron density on thiophene	20
Scheme 2.3	Electrophilic attack at α and β of a thiophene monomer	20
Scheme 2.4	The synthetic routes of terthiophene bearing 1,5-diisopropyl-6-oxoverdazyl radical (2.6)	23
Scheme 2.5	Verdazyl radical-oligo/polythiophene cross-conjugated via pyridine	32
Scheme 2.6	Synthetic route of terthiophene-3'-pyridine bearing verdazyl radical, 2.11	33
Scheme 3.1	General mechanism of electropolymerization via radical cation-radical cation (RC-RC) coupling	55
Scheme 3.2	Oxidation and reduction of neutral radical	56
Scheme 3.3	Electrochemical oxidation of terthiophene bearing 2,4-diisopropyl-3-oxotetrazane 2.5	60
Scheme 3.4	Mechanism of the oxidation of aliphatic amines	60
Scheme 3.5	Electrochemical oxidation of verdazyl 2.6	62
Scheme 3.6	Formation of poly(terthiophene) bearing verdazyl radical	63
Scheme 3.7	Electrochemical oxidation of tetrazane 2.10 to its radical 2.11	67
Scheme 3.8	Electrochemical oxidation of verdazyl 2.11	69
Scheme 3.9	Formation of poly(2.11) at the surface of platinum electrode	70
Scheme 4.1	Verdazyl radical functionalized oligo/polythiophenes	73
Scheme 4.2	Electrosynthesis of verdazyl radicals	74
Scheme 4.3	Synthetic route of thiophene bearing formazan radical	75

List of Appendices

Appendix 1	¹ H NMR spectrum expansion of compound 2.5 in DMSO	82
Appendix 2	¹³ C NMR spectrum expansion of compound 2.5 in DMSO	83
Appendix 3	¹ H NMR spectrum expansion of compound 2.8 in CDCl ₃	84
Appendix 4	¹³ C NMR spectrum expansion of compound 2.8 in CDCl ₃	85
Appendix 5	¹ H NMR spectrum expansion of compound 2.9 in CDCl ₃	86
Appendix 6	¹³ C NMR spectrum expansion of compound 2.9 in CDCl ₃	87
Appendix 7	¹ H NMR spectrum expansion of compound 2.10 in CDCl ₃	88
Appendix 8	¹³ C NMR spectrum expansion of compound 2.10 in CDCl ₃	89

Abbreviations and Symbols

<i>a</i>	Hyperfine coupling constant
ACN	Acetonitrile
AIBN	2,2'-Azobis(2-methylpropionitrile)
B ₀	Magnetic field
BPO	Benzoyl peroxide
BST	1-Benzoyloxy-2-phenyl-2-(2',2',6',6'-tetramethyl-1'-piperidinyloxy)ethane
BSV	Benzoyl-styrene-1,5-dimethyl-3-phenyl-6-oxoverdazyl radical
CE	Counter electrode
CV	Cyclic voltammetry
d	Doublet
dd	Doublet of doublet
DMF	Dimethyl formamide
DMSO	Dimethyl sulfoxide
E _p ^a	Anodic peak potential
E _p ^c	Cathodic peak potential
EPR	Electron paramagnetic resonance
Fc	Ferrocene
FT-IR	Fourier transform-infrared
g	Proportionality factor, g-value
G	Gauss
hfac	Hexafluoroacetylacetonate
HOMO	Highest occupied molecular orbital
<i>i</i> _p	Peak current
<i>i</i> _p ^a	Anodic peak current
<i>i</i> _p ^c	Cathodic peak current
IUPAC	International Union of Pure and Applied Chemistry
LRP	Living-radical polymerization process
LUMO	Lowest unoccupied molecular orbital
M	Molarity
m	Multiplet
MHz	Mega-hertz
m _I	Nuclear spin quantum number
MMA	Methyl methacrylate
M _s	Electron spin quantum number
NBS	N-bromosuccinimide
ox	Oxidation
NMR	Nuclear magnetic resonance
Pd(PPh ₃) ₄	Tetrakis(triphenylphosphine)palladium(0)

ppm	Parts per million
Pt	Platinum electrode
RC-RC	Radical cation-radical cation
RE	Reference electrode
red	Reduction
s	Singlet
SASL	2-(3-Carboxypropyl)-4,4-dimethyl-2-tridecyl-3-oxazolidinyloxy
SFRP	Stable free radical polymerization
SiO ₂	Celite
SOMO	Singly occupied molecular orbital
t	Triplet
<i>t</i> -Boc	<i>Tert</i> -butoxycarbonyl
TEMPO	(2,2,6,6-Tetramethylpiperidin-1-yl)oxy
TLC	Thin-layer chromatography
WE	Working electrode
μ	Magnetic moment
μ _B	Bohr magneton
ν	Frequency

Chapter 1. General Introduction

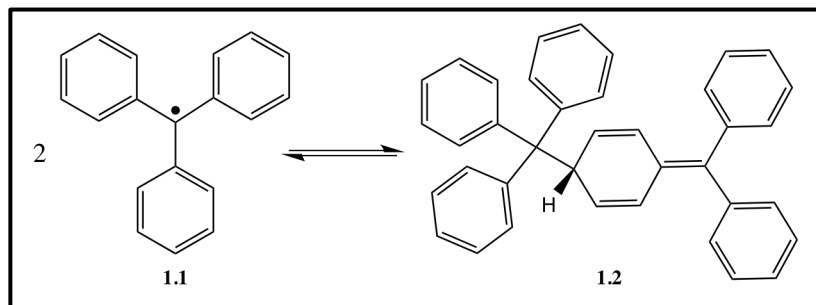
1 Stable Free Radicals

Radicals are compounds that have one or more unpaired electron(s), i.e. they have fewer bonds than expected. Radicals that are sufficiently long lived to be observed by conventional spectroscopic techniques are defined as persistent, while a stable radical can be isolated as a pure compound, and they are unreactive in air and water.^{1,2} Stable free radicals have been known for over a century. However, they are still new in many chemical communities. There are various families of stable radicals, which have been described for decades.¹

1.1 Hydrocarbon-Based Radicals

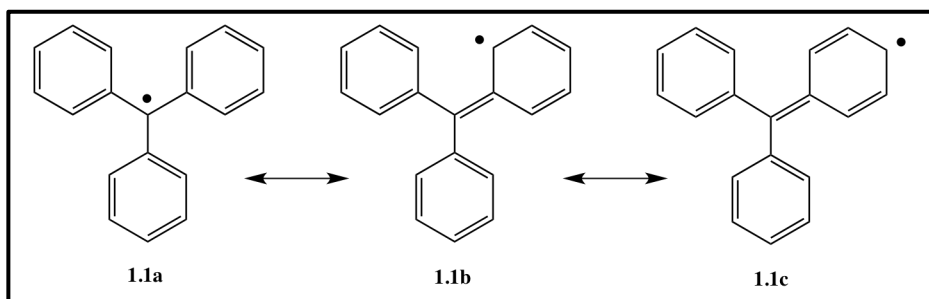
1.1.1 Triphenylmethyl and Related Radicals

Gomberg discovered the first organic free radicals of triphenylmethyl chloride in 1900.³ Triphenylmethyl, **1.1**, and its derivatives cannot be isolated, so they are characterized as persistent rather than stable radicals. In dilute and deoxygenated solution, **1.1** is in equilibrium with the dimer **1.2**, Scheme 1.1.¹ The intra-dimer bond of species **1.2** is weak with a bond dissociation enthalpy of 11 kcal mol⁻¹.⁴



Scheme 1.1 Equilibrium of the triphenylmethyl radical with its dimer

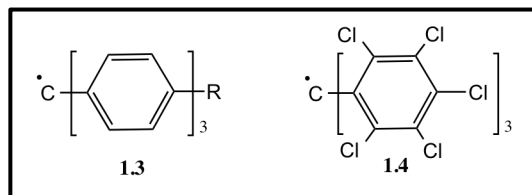
It is suggested that the unpaired electron does not exist on the central carbon, but is delocalized on the *ortho*- and *para*- phenyl positions (**1.1a-c** in Scheme 1.2). This delocalization is consistent with EPR studies that show larger hyperfine coupling constants for *ortho*- and *para*-hydrogens than for *meta*-hydrogens.^{4,5}



Scheme 1.2 Delocalization of unpaired electron on *ortho*- and *para*- phenyl positions of triphenylmethyl radicals

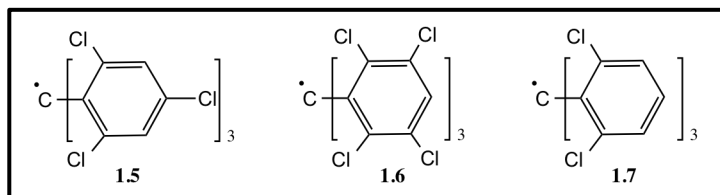
The stability of triphenylmethyl radicals can be enhanced by blocking the *para*-phenyl positions involved in the dimerization. Derivatives with *para*-substituents (**1.3**) are monomeric in solution, even though they are sensitive to oxygen (Scheme 1.3).⁶

The perchlorinated derivative, **1.4**, Scheme 1.3, is not sensitive to oxidation. Indeed, this radical is chemically inert compared to the parent compound, except when it is subjected to harsh reaction conditions.⁷



Scheme 1.3 *Para*- substituted (**1.3**) and the perchlorinated (**1.4**) derivatives of the triphenyl radical

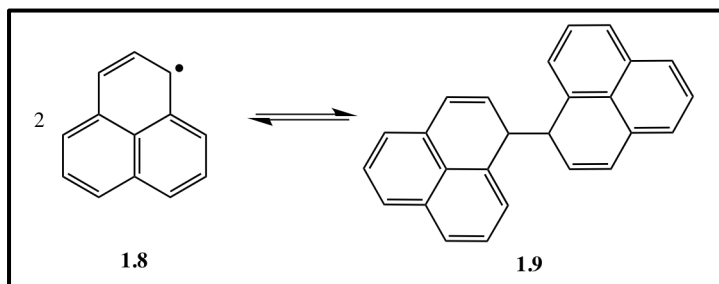
Other polychlorinated triphenyl radicals such as **1.5** and **1.6** (Scheme 1.4) have been studied. They display excellent stability.⁸ Moreover, it has been reported that triphenyl radicals with chlorine atoms on the *ortho*-position **1.7** are also very stable.⁹



Scheme 1.4 Polychlorinated triphenyl radicals

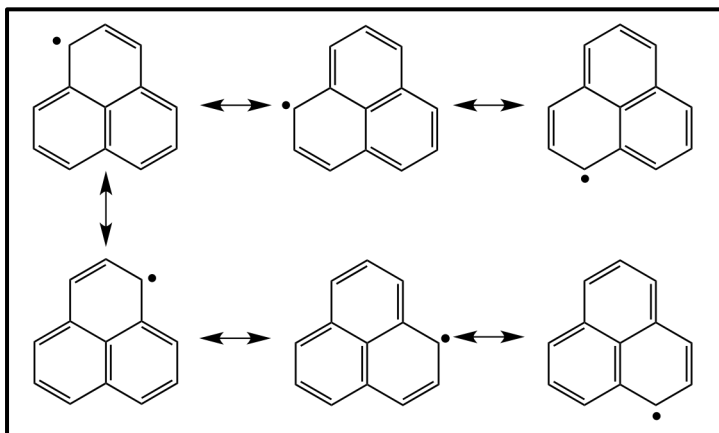
1.1.2 Phenalenyl and Related Radicals

The first example of a phenalenyl radical (**1.8**) was reported in the 1950s. The phenalenyl radical (**1.8**), resulting from the oxidation of phenalene,¹⁰⁻¹² was prepared by Reid *et al.*¹⁰ and detected by Calvin *et al.*¹¹ Radical **1.8** is very sensitive to oxygen and is in equilibrium with a σ -bond dimer **1.9** (Scheme 1.5).



Scheme 1.5 Equilibrium of phenalenyl radical with its dimeric species

The unpaired electron in phenalenyl radicals is delocalized over the six α -carbons, and a small spin density was found in the central and β -carbons, Scheme 1.6. Moreover, the molecular orbital calculations show no spin density on the central carbon.¹⁰

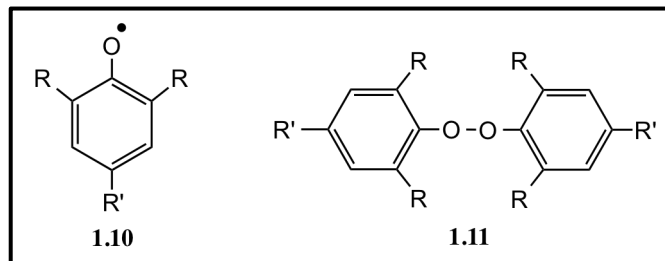


Scheme 1.6 Delocalized resonance over the six α -carbons in phenalenyl radicals

1.1.3 Phenoxy Radicals

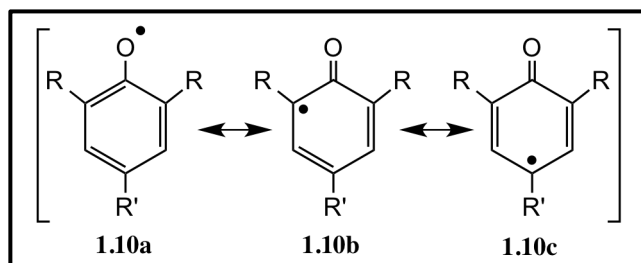
Phenoxy radicals (**1.10**) have been widely studied and are still extensively used.¹³ In order to prevent radical decomposition, *para*- and *ortho*-substituents must be present. Peroxide dimers of phenoxy radicals (**1.11**) are not ordinarily detected for three reasons: (i) the presence of bulky *ortho*-substituents (e.g. R = Me, Bu, or OMe), (ii) the lone pair

repulsion between oxygen atoms, and (iii) the delocalization of the radical on the aryl ring.



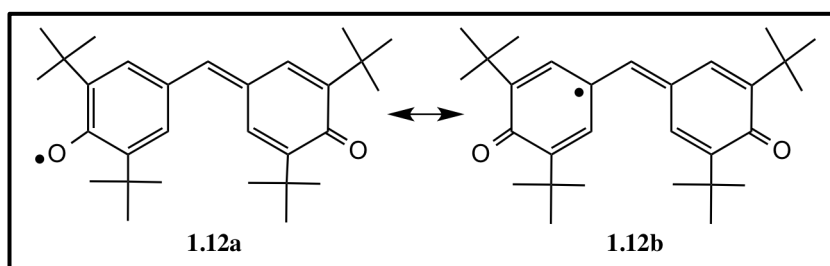
Scheme 1.7 Phenoxyl radical **1.10** and its peroxide dimers **1.11**

The unpaired electron in the phenoxyl radicals is delocalized through resonance (**1.10a-c** in Scheme 1.8). The oxygen atom carries slightly more spin density than the *ortho*- and *para*-carbons.¹⁴



Scheme 1.8 Delocalization of the unpaired electron over *ortho*- and *para*-carbons in phenoxyl radical

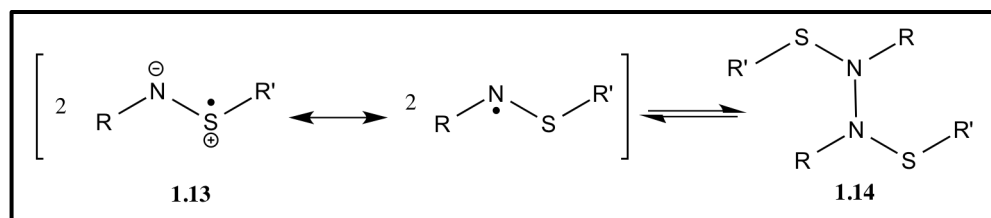
In association with phenoxyl radicals, the galvinoxyl radical **1.12a** (Coppinger's radical)¹⁵ has received special attention due to its unusual magnetic properties and its stability, i.e., it is insensitive to oxygen and can be isolated.¹⁶ Computational studies show that, like common phenoxyls, the galvinoxyl radical has substantial spin density on the *para*-carbon atoms as shown in Scheme 1.9 (**1.12a, b**), implying that the radical has some allyl character.¹⁷



Scheme 1.9 Delocalization of the unpaired electron in galvinoxyl radical

1.2 Radicals with Spin Density on Nitrogen and Sulfur “Thiazyls”: Thioaminyll Radicals

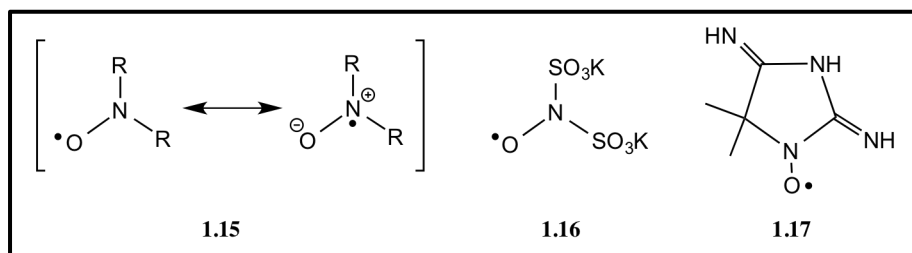
Thioaminyll radicals (**1.13**) have been extensively studied by Miura *et al.*¹⁸⁻²⁰ These radicals are usually persistent. They are in equilibrium with hydrazine-like dimers (**1.14**) in solution (Scheme 1.10)²⁰ resulting from a σ -bond formation between the nitrogen atoms of two different thioaminyll radicals. Bulky substituents such as triphenylmethyl,¹⁸ 2,4,6-trisubstituted phenyl,²¹ and substituted pyrenyl²² attached to the N atom of the thioaminyll radical, render the radical stable enough to be isolated and prevent dimerization.



Scheme 1.10 Combination of two thioaminyll radicals results in a σ -bond formation between two nitrogen atoms

1.3 Radicals Based on Nitrogen and/or Oxygen: Nitroxide and Nitronyl-Nitroxide Radicals

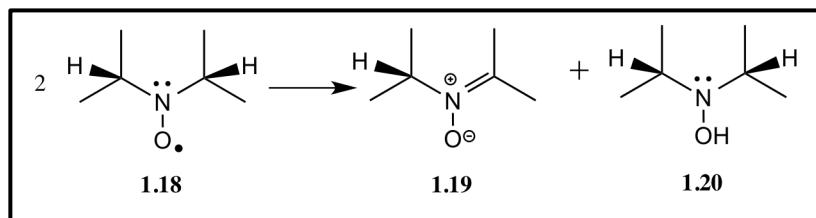
Nitroxide (**1.15**) is a major class of stable radicals where R is an alkyl or aryl groups.²³ Fermi's salt (**1.16**)²⁴ was discovered over 150 years ago. After radical **1.15**, the first synthesized organic derivative was radical **1.17** (Scheme 1.11).²⁵



Scheme 1.11 Examples of nitroxide and nitronyl-nitroxide radicals

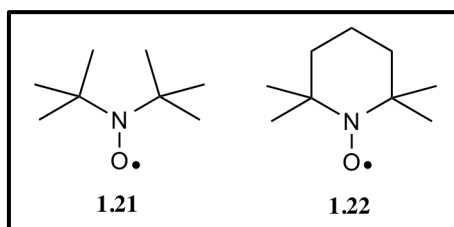
The spin density of nitroxide radicals resides on the nitrogen and oxygen atoms. σ -Dimers of nitroxides have not been seen, which therefore demonstrates their high stability. Due to the lone pair repulsion associated with the N-O-O-N heteroatom sequence, the peroxide bond is very weak.²⁶

The stability of nitroxide radicals depends on the substituents on the nitrogen atom. Nitroxides with alkyl substituents possessing α -hydrogen atoms, e.g., **1.18**, can abstract an α -hydrogen atom from a second radical resulting in the formation of a nitrene (**1.19**) and hydroxylamine (**1.20**) as shown in Scheme 1.12.



Scheme 1.12 Decomposition of nitroxide radical

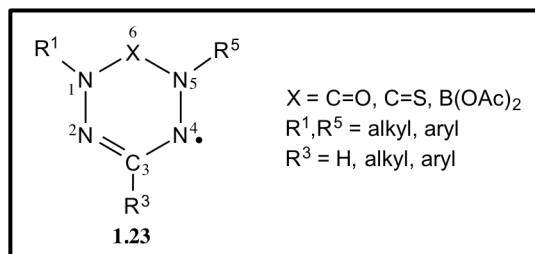
Nitroxides with substituents on nitrogen atom that do not include α -hydrogen atoms are stable in the presence of air and moisture. Consequently, many derivatives are commercially available, e.g., di-*t*-butyl nitroxide (**1.21**) and (2,2,6,6-tetramethylpiperidin-1-yl)oxy (TEMPO, **1.22**)²⁷ (Scheme 1.13).



Scheme 1.13 Structure of di-*t*-butyl nitroxide (**1.21**) and TEMPO (**1.22**)

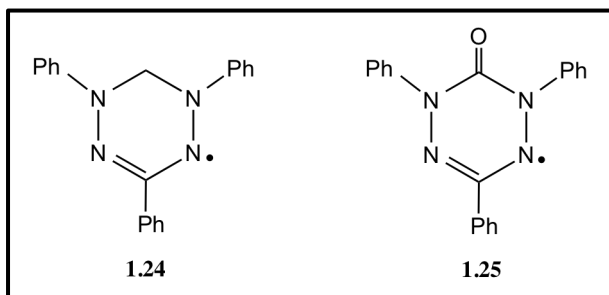
1.4 Verdazyl Radicals

Verdazyl radicals (**1.23**) are a new family of radicals that have attracted a lot of interest since their discovery in the 1960s. The family of verdazyl radicals is stable and can be isolated, stored, and handled without any decomposition. The main backbone of verdazyl radicals is a six-membered ring having four nitrogen atoms at positions 1, 2, 4, and 5 (Scheme 1.14).²⁸



Scheme 1.14 Verdazyl backbone with known modifications

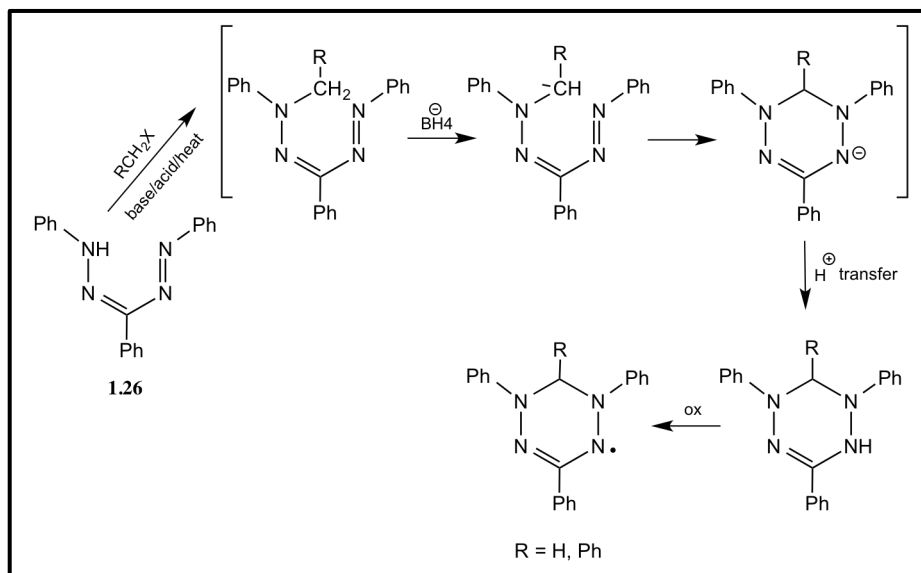
The stability of verdazyl is due to the delocalization of the spin density over the four nitrogen atoms.²⁹⁻³² In addition, it is protected by steric hindrance of the R groups at positions 1, 3, and 5. A broad range of synthetic methods has been reported for the synthesis of verdazyl radicals with a variety of structures.³³⁻³⁵ The color of the verdazyl radicals range from green, the color of the first verdazyl radical discovered,³³ to reddish orange,³⁴ and purple.³⁵ The origin of the name verdazyl stems from the French word for green, i.e., *vert*. Their conformation can be non-planar (**1.24**) or planar (**1.25**) depending on the substituent groups that are attached (Scheme 1.15).³⁶



Scheme 1.15 Structure of a non-planar (**1.24**) and planar (**1.25**) verdazyl radical

1.4.1 Synthesis of Triaryl Verdazyl Radicals

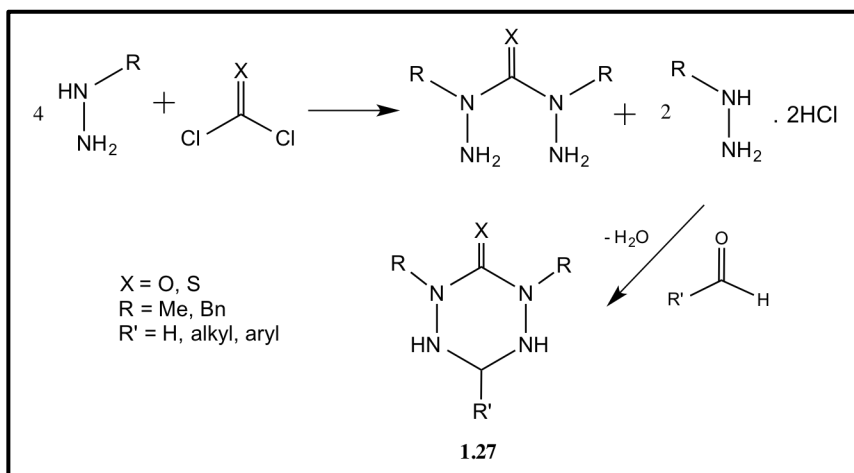
Kuhn and Trischmann (1963) discovered the first verdazyl radical in their effort to alkylate formazan (**1.26**) (Scheme 1.16).³³ After that, many studies were focused on the synthesis and characterization of verdazyl radicals.



Scheme 1.16 Formazan alkylation attempt; the synthesis of triaryl verdazyl radical

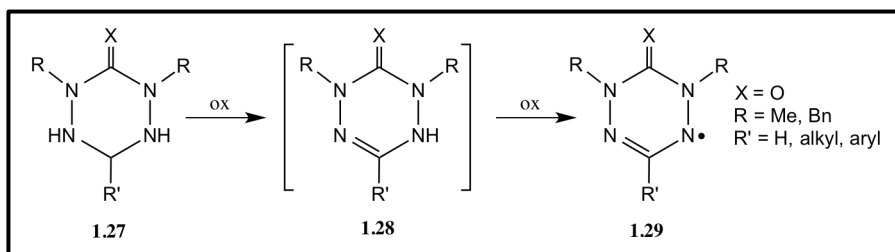
1.4.2 Synthesis of 6-Oxo- and 6-Thioxoverdazyl Radicals

The synthesis of 6-oxo and 6-thioxoverdazyl radicals was reported in 1983.³⁷ In the first step, hydrazines such as methyl- and benzyl-hydrazines are reacted with phosgene or thiophosgene to form the bis-alkylhydrazides of carbonic acid or thiocarbonic acid, respectively. The condensation of the bis-alkylhydrazine of carbonic acid or thiocarbonic acid with an alkyl- or aryl- aldehyde (Scheme 1.17) results in the formation of 3-oxo or 3-thioxotetrazane (**1.27**).



Scheme 1.17 Synthesis of 3-oxo or 3-thioxotetrazanes

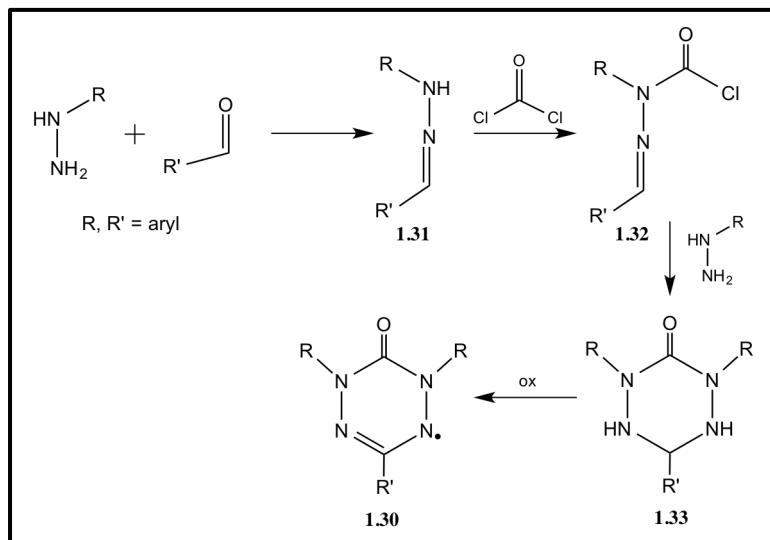
The 6-oxoverdazyl radical precursors (**1.27**, X=O), tetrazanes, are stable in organic solvent and in the presence of air. With different oxidizing agents, tetrazanes can be oxidized to the corresponding radicals. Potassium ferricyanide and periodates were commonly used as oxidizing agents.²⁸ During the oxidation, an intermediate, leucoverdazyl, **1.28**, forms which is subsequently oxidized by oxygen (Scheme 1.18) to form the radical **1.29**.



Scheme 1.18 Oxidation of tetrazane through the intermediacy of leucoverdazyl, **1.28**

1.4.3 Synthesis of 1, 3, 5-Triaryl-6-oxoverdazyl Radicals

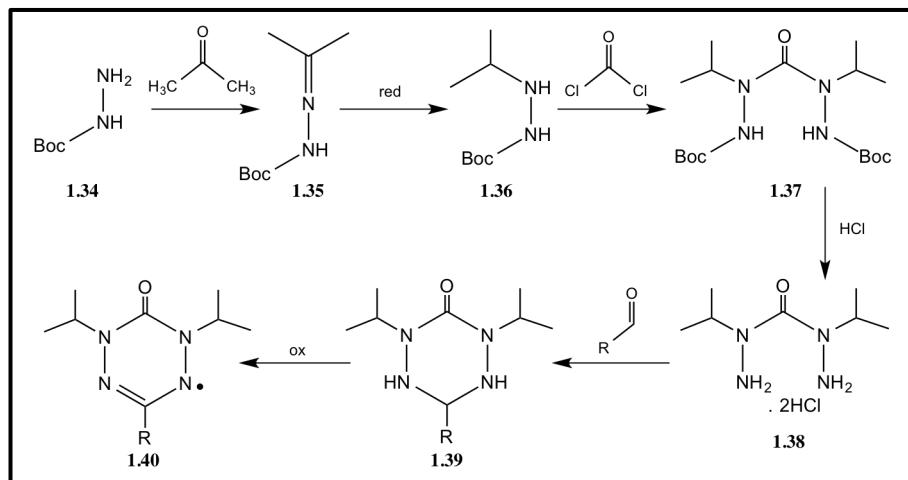
In 1994, Milcent *et al.*³⁵ reported the synthesis of 1, 3, 5-triaryl-6-oxoverdazyl radicals, **1.30**, (Scheme 1.19). It was suggested that the addition of benzaldehyde to form the arylhydrazone, **1.31**, eliminates the undesired chemoselectivity of arylhydrazines. Addition of phosgene, followed by a second mole of arylhydrazine results in the formation of 1,3,5-triaryl-6-oxotetrazane, **1.33**. The oxidation of **1.33** gives the corresponding 1, 3, 5-triaryl-6-oxoverdazyl radicals, **1.30**.



Scheme 1.19 Synthesis of 1,3,5-triaryl-6-oxoverdazyl radical (**1.30**) from the oxidation of the 1,3,5-triaryl-6-oxotetrazane (**1.33**)

1.4.4 Synthesis of 1, 5-Diisopropyl-6-oxoverdazyl Radicals

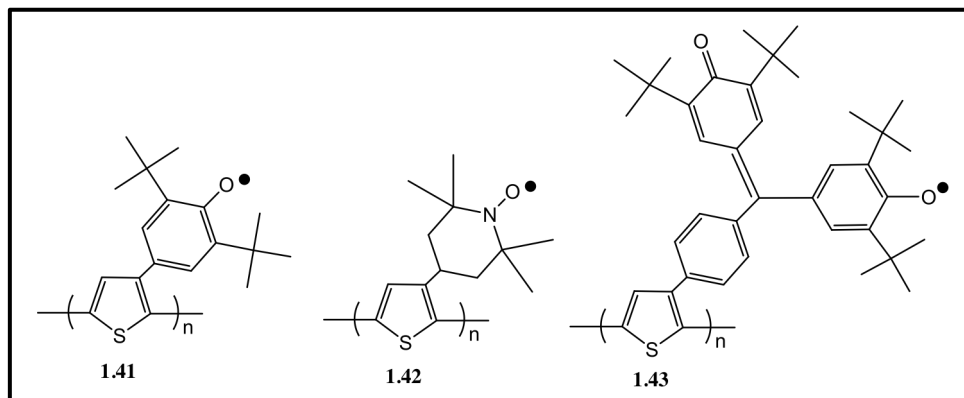
The synthesis of dialkyl 6-oxoverdazyl radicals was reported by Brook *et al.*³⁸ (Scheme 1.20). The condensation reaction of *t*-butylcarbazate, **1.34**, a protected derivative of hydrazine, with ketones or aldehydes can give hydrazine **1.35**. The reduction of **1.35** with sodium cyanoborohydride affords *t*-butyl-2-isopropylhydrazinecarboxylate, **1.36**.³⁹ The reaction of **1.36** with phosgene followed by the removal of the *t*-Boc group with acid, produces the bis(1-alkylhydrazides) of carbonic acid, **1.38**, which then undergoes condensation reactions with different aldehydes to give 2,4-dialkyl-3-oxotetrazanes, **1.39**. The oxidation of the latter produces 1,5-dialkyl-6-oxoverdazyl radicals, **1.40**.



Scheme 1.20 Synthesis of 1,5-diisopropyl-6-oxoverdazyl radicals (**1.40**)

1.5 Oligo/Polythiophene Grafted Stable Radical

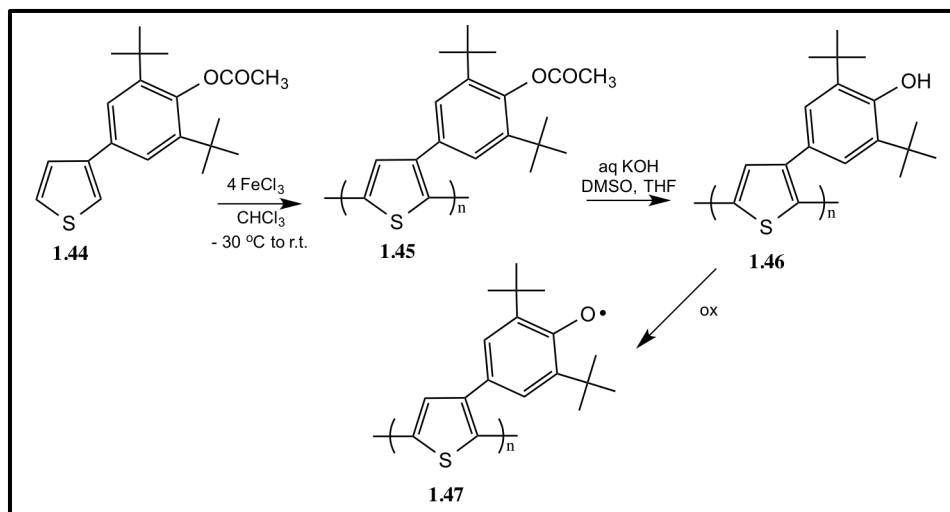
Due to their electronic and optical properties, π -conjugated polymers have attracted considerable interest in many fields of science and industry.⁴⁰ Poly(3-substituted thiophene)s are an example of the π -conjugated polymers. It has been found that the 3-radical-substituted polythiophenes can afford high spin and electrically conductive polyradicals.⁴¹ There are a variety of radical groups that were introduced in the 3-position of thiophene such as phenoxyl (**1.41**), TEMPO (**1.42**), and galvinoxyl (**1.43**) (Scheme 1.21). The thiophene derivatives were polymerized chemically to give poly(3-radical-substituted thiophene)s. The oxidative polymerization was carried out with ferric chloride as the oxidizing agent. However, some thiophene derivatives, i.e. amino-substituted thiophenes, do not polymerize when are treated with this oxidizing agent.⁴¹



Scheme 1.21 Poly(3-radical-substituted thiophene)s

1.5.1 Polythiophenes Bearing Phenoxy Radicals

The polythiophene grafted phenoxy radical was successfully synthesized in 2000 by Miyasaka *et al.*⁴² using the processes outlined in Scheme 1.22. The corresponding monomer 3-(3',5'-di-*t*-butyl-4'-acetoxyphenyl)thiophene, **1.44**, was oxidatively polymerized with 4 equivalents of ferric chloride in a dilute chloroform solution at temperatures between -30 °C to room temperature. Poly(3-(3',5'-di-*t*-butyl-4'-acetoxyphenyl) thiophene), **1.45**, a red-orange powder, was converted to the corresponding hydroxyl polymer, **1.46**, after the elimination of the protecting acetyl group. The heterogeneous oxidation of **1.46** yielded polythiophenes bearing phenoxy radicals, **1.47**.

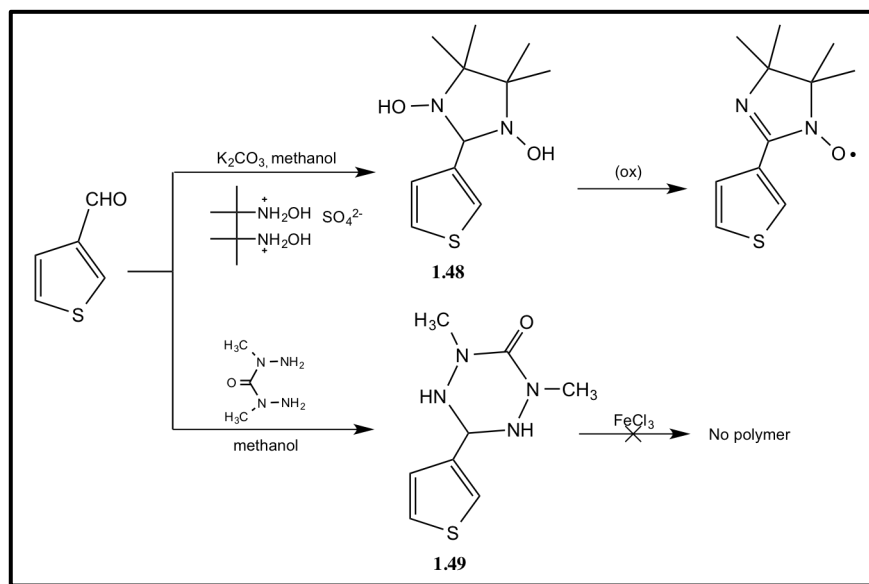


Scheme 1.22 Formation of polythiophenes bearing phenoxy radicals (**1.47**)

It was found that the π -conjugated polythiophene bearing phenoxy radical, **1.47**, possesses a ferromagnetic connectivity of the unpaired electrons. It has a spin quantum number (S) value of $2/2$ to $3/2$, which indicates a high-spin ground state and an intramolecular ferromagnetic spin coupling through the polythiophene backbone.⁴²

1.5.2 Poly(3-Radical-Amino Thiophene)

In 2001, Miyasaka *et al.*⁴¹ reported the synthesis of new thiophene monomers substituted in position 3 with amino-based radical precursors (Scheme 1.23).



Scheme 1.23 Amino-substituted thiophenes

The dihydroxyimidazoline derivative, **1.48**, was obtained by the condensation of the aldehyde group of thiophene-3-carboxaldehyde with bis(hydroxyamino)dimethylbutane. It was immediately oxidized to yield the nitronyl nitroxide, which could not be isolated. On the other hand, it has been reported that an aromatic aldehyde produced the corresponding tetrazanes with bis (1-methylhydrazide) **1.49**.⁴³

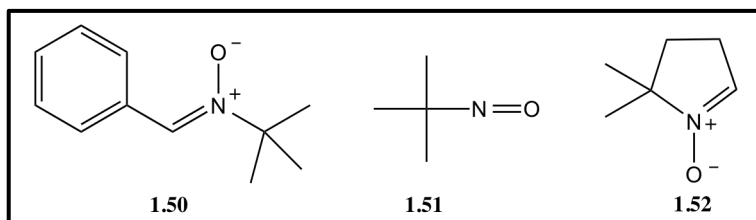
Unfortunately, the oxidative polymerization of the amino-substituted thiophenes, **1.48** and **1.49**, with ferric chloride was not successful even with high concentration of the oxidizing agents. Ferric chloride acts as a Lewis acid in the presence of the amine derivatives to form adducts. The 3-substituted amino groups were oxidized to give their corresponding radicals, but the oxidative polymerization of the amino-functionalized thiophene was difficult due to the higher oxidation potential of the thiophene ring compared to the amino group.⁴¹

1.6 Applications and Uses of Stable Radicals

1.6.1 EPR Applications

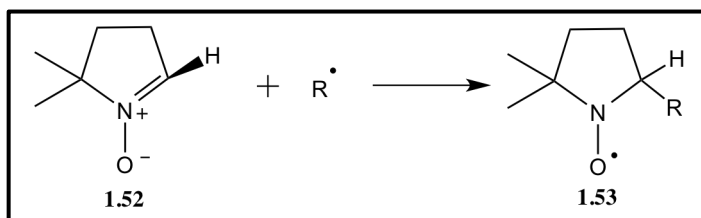
Electron paramagnetic resonance (EPR) spectroscopy gives structural, dynamic, and reactivity information for stable radicals.⁴⁴ Radicals are used as molecular markers in

techniques such as spin trapping, spin labeling, and EPR imaging. The spin trapping technique includes the reaction of a diamagnetic molecule (radical trap) with a highly reactive radical to produce a new persistent or stable radical.⁴⁵ Phenyl-*t*-butylnitrone (**1.50**),⁴⁶ 2-methyl-2-nitrosopropane (**1.51**),⁴⁷ and 5,5-dimethyl-2-pyrroline-N-oxide (**1.52**)⁴⁸ are the most common spin traps (Scheme 1.24).



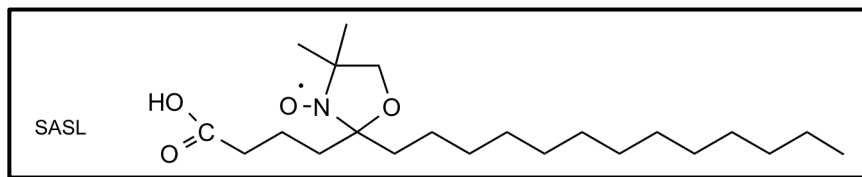
Scheme 1.24 Examples of spin traps

Scheme 1.25 shows an example of using **1.52** as a spin trap, which illustrates the generation of a new radical species, **1.53**. It should be noted that spin trapping provides indirect evidence of the existence of the trapped species. It provides little to no structural information about the trapped species as it is observed indirectly.



Scheme 1.25 Radical trapping using 5,5-dimethyl-2-pyrroline-N-oxid (**1.52**)

A technique such as spin labeling has been used to study biological systems.⁴⁹ A stable radical is introduced into a biological system allowing for EPR spectra to be recorded, supplying information about the environment around the label (the radical), dynamic processes, and hydrophobicity/hydrophilicity.⁵⁰ Scheme 1.26 illustrates an example of the lipophilic spin label, 2-(3-carboxypropyl)-4,4-dimethyl-2-tridecyl-3-oxazolidinyloxy (SASL), used in a biological system by Vishnyakova *et al.*⁵¹ as a probe of membrane structure. The hydrophilic part in these structures is the carboxyl group (Scheme 1.26). The hydrophilic group of the spin labels is introduced into the polar headgroup region of the membrane.

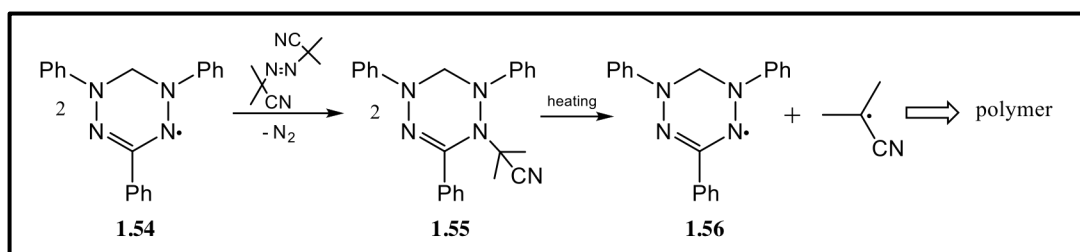


Scheme 1.26 Chemical structure of spin label used in biological study

Unfortunately, the number of radicals that can be used in this technique is limited by their compatibility with biological methods. Only few radicals are stable over broad ranges of pH and temperature, and soluble in aqueous solutions.

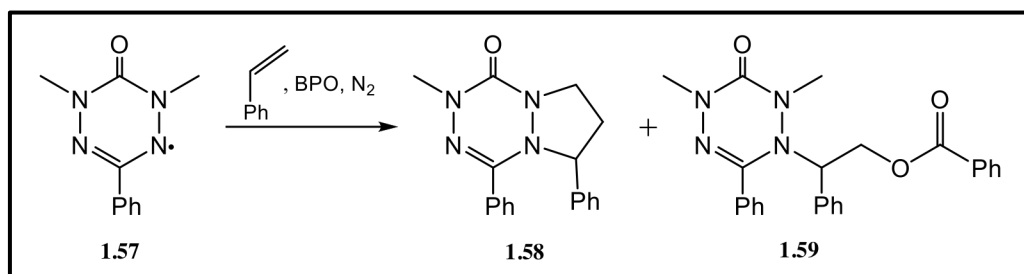
1.6.2 Applications of Verdazyl Radicals

The applications of verdazyl radicals vary from being radical traps,⁵² molecular magnets,⁵³ living radical polymerization mediators,⁵⁴ organic synthesis substrates,⁵⁵ to ultimately sacrificing their own backbones to create special heterocyclic structures.



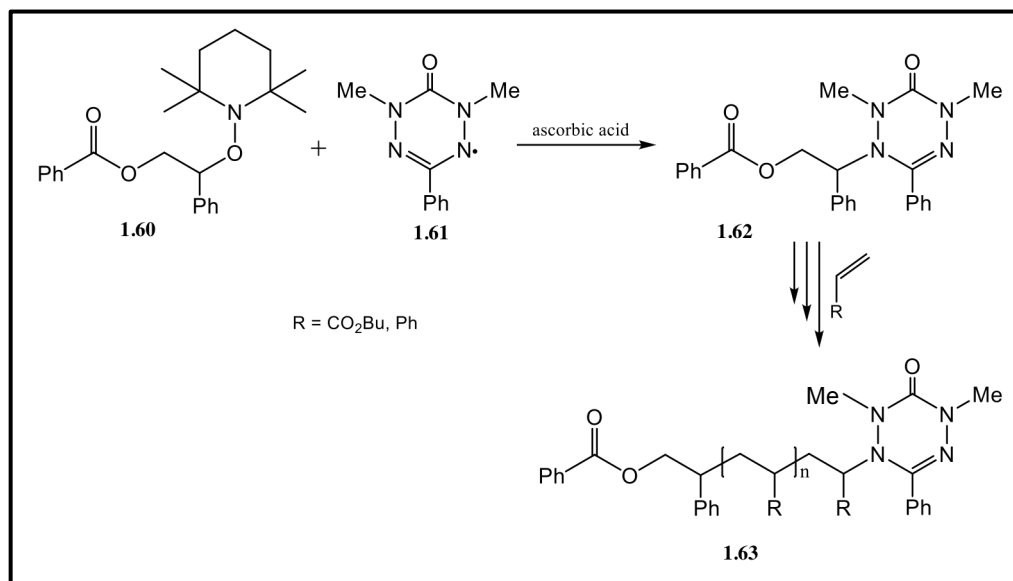
Scheme 1.27 Verdazyl-mediated stable free radical polymerization (SFRP) system

Researchers discovered the first applications of verdazyls as radical traps in kinetic experiments. This was done by the determination of initiation rates of AIBN in methyl methacrylate (MMA), acrylonitrile, styrene, and vinyl chloride polymerization.⁵⁶ Verdazyl radicals have also been applied as targets in the analysis of polymer end-groups. Yamada *et al.*⁵⁸ tried to use verdazyls as mediating agents in living radical polymerization processes (Scheme 1.27);^{57,58} however, initial results were not productive. Scheme 1.28 shows how verdazyl radicals can be used as substrates for organic synthesis. In this study, the 1,5-dimethyl-3-phenyl-6-oxoverdazyl radical (**1.57**) is successfully used as a precursor in forming the azomethine imine. The verdazyl radical undergoes cycloaddition reactions in the presence of dipolarophiles to produce dihydrotetrazinone heterocyclic structures **1.58**.⁵⁵ This study opened a new strategy to synthesize unique bicyclic and tricyclic heterocyclic compounds with different structural design.



Scheme 1.28 Formation of dihydrotetrazinone heterocyclic structures via cycloaddition reactions

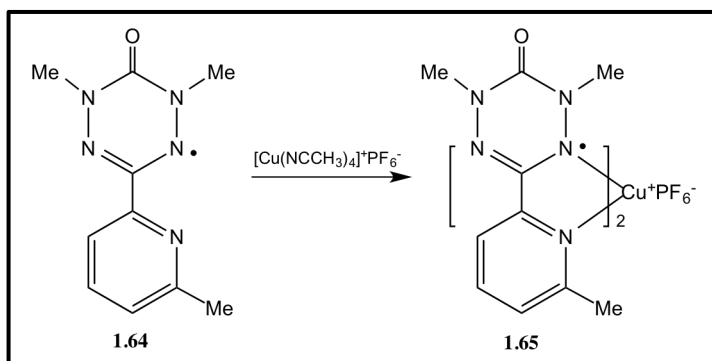
Scheme 1.29 shows an example of the use of verdazyl radical in a living-radical polymerization process (LRP). Due to its steric and electronic properties, 1,5-dimethyl-3-phenyl-6-oxoverdazyl radical (**1.61**) was successfully used as a mediating agent for styrene and *n*-butyl acrylate stable free radical polymerization.⁵⁴



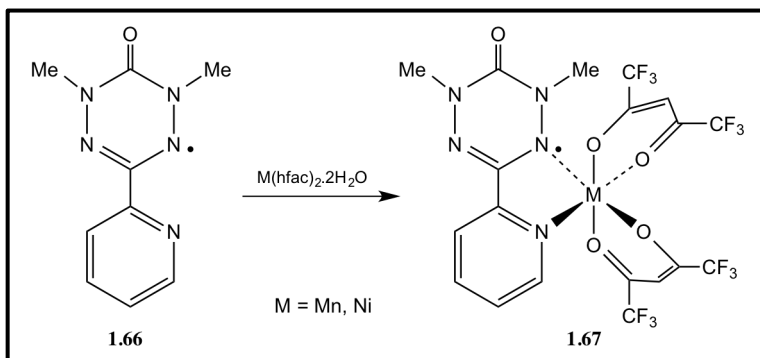
Scheme 1.29 Polymerization of styrene and *n*-butyl acrylate under LRP condition in the presence of verdazyl unimer BSV

The 1,5-dimethyl-3-phenyl-6-oxoverdazyl radical, **1.61**, was converted to its unimolecular initiator, benzoyl-styrene-1,5-dimethyl-3-phenyl-6-oxoverdazyl radical (BSV), **1.62**, via an exchange reaction with 1-benzoyloxy-2-phenyl-2-(2',2',6',6'-tetramethyl-1'-piperidinyloxy)ethane (BST), **1.60**, and in the presence of ascorbic acid. The polymerization of styrene and *n*-butyl acrylate under living-radical polymerization conditions in the presence of verdazyl unimer BSV, **1.62**, affords copolymer **1.63**. Furthermore, verdazyl radicals have a high stability, strong magnetic exchange with

coordinated metal ions,⁵⁹ and structural similarity to aromatic azine ligands such as pyridine and pyrimidine. These properties make verdazyl radicals an appealing building block for the synthesis of magnetic complex nanostructures.⁶⁰ Verdazyl coordination compounds can be divided into two groups: coordination compound with copper (I)⁶¹ (Scheme 1.30) and coordination compounds of other transition metals with hexafluoroacetylacetonate (hfac) ancillary ligands⁶²⁻⁶⁴ (Scheme 1.31).



Scheme 1.30 Formation of copper (I) complex **1.65**



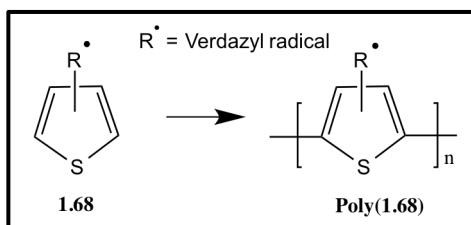
Scheme 1.31 Formation of air-stable complexes, **1.67**, using $M(\text{hfac})_2 \cdot 2\text{H}_2\text{O}$

These are some studies that make such verdazyl radicals interesting, in addition to its unique stability that is increased by:

1. The electronic stability provided by the delocalization of the unpaired electrons over the four nitrogen atoms.
2. The steric protection resulting from the substituents at the 1, 3 and 5 positions.

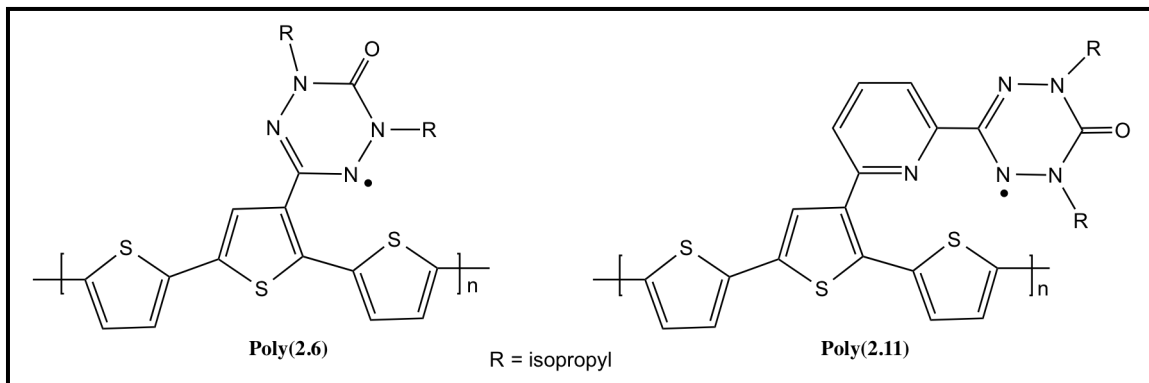
1.7 Objectives

Although there are many papers focused on the synthesis and the characterization of verdazyl radicals, there are relatively few studies involving the synthesis of verdazyl radical attached to highly conducting materials such as polythiophenes. The main objective of this thesis, is to design new conducting materials bearing a verdazyl radical (poly(**1.68**)), Scheme 1.32. The introduction of a radical on a polythiophene backbone may change the optical, electrical and electrochemical properties of these new materials. Moreover, the presence of the radical, that can be oxidized or reduced, may affect the electrical conductivity of the polythiophenes.



Scheme 1.32 The structure of an oligo/polythiophene bearing a stable radical

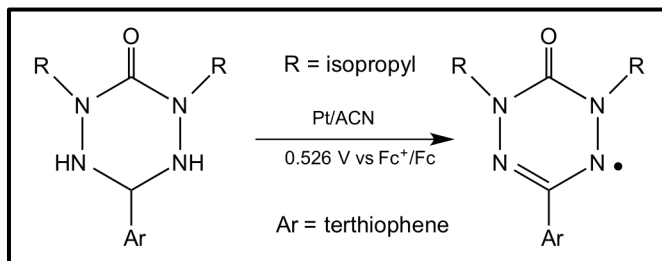
More specifically we are planning to prepare 1,5-diisopropyl-6-oxoverdazyl functionalized oligo/poly(terthiophene) (poly(**2.6**)), and 1,5-diisopropyl-6-oxoverdazyl functionalized oligo/poly(terthiophene) through pyridine bridge (poly(**2.11**)), Scheme 1.33.



Scheme 1.33 The chemical structure of poly(**2.6**) and poly(**2.11**)

By combining chemical and electrochemical methods, we have been able to prepare oligo/polythiophenes bearing verdazyl radicals. Moreover, we present the first synthesis

of a verdazyl radical using electrochemical oxidation as outlined in Scheme 1.34. The electrochemical oxidation method displays several advantages such as it is clean (no need to use an oxidizing agent) and very selective.



Scheme 1.34 Synthesis of a verdazyl radical using electrochemical oxidation

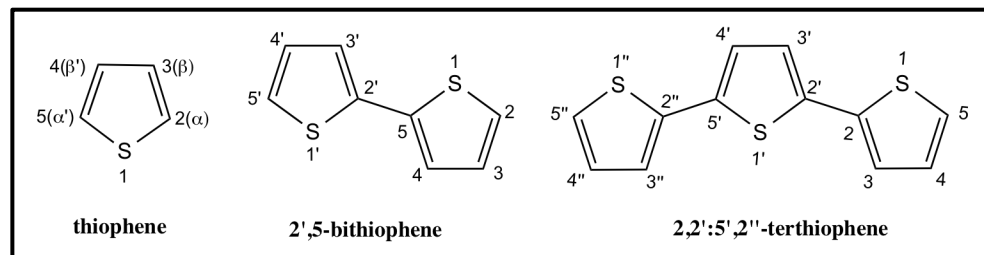
Chapter 2 describes the synthesis and characterization of 1,5-diisopropyl-6-oxoverdazyl radical functionalized oligothiophene monomers **2.6** and **2.11**. Their electropolymerization using cyclic voltammetry affords the corresponding polymers poly(**2.6**) and poly(**2.11**), which have been characterized with CV and FT-IR, (Chapter 3). The future work including the synthesis of new radical functionalized terthiophenes is presented in Chapter 4.

Chapter 2. Synthesis of Verdazyl Radical Functionalized Terthiophene

2 Introduction

2.1 Nomenclature

The universally accepted nomenclature of organic and inorganic molecules is based on the International Union of Pure and Applied Chemistry (IUPAC) rules. However, certain compounds are better known by a semi-systematic approach utilized by the authors that first introduced them to the scientific community. The nomenclature of thiophene, bithiophene and terthiophene is presented in Scheme 2.1.



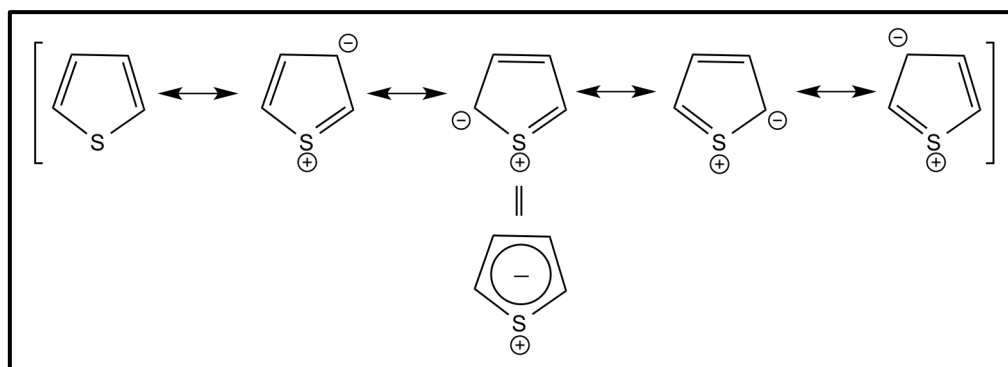
Scheme 2.1 Nomenclature of thiophene, bithiophene and terthiophene

For thiophene monomers, numbering begins at the sulfur atom and is labeled position 1. The 2 and 5 positions of thiophene monomers are known as α and α' , respectively, while positions 3 and 4 are referred to β and β' , respectively. Then naming thiophene derivatives with more than one thiophene ring, prefixes bi and ter are used to designate two and three rings, respectively. The numbering scheme for bithiophene and terthiophene is shown in Scheme 2.1.^{65,66}

2.2 Electrophilic Aromatic Substitution

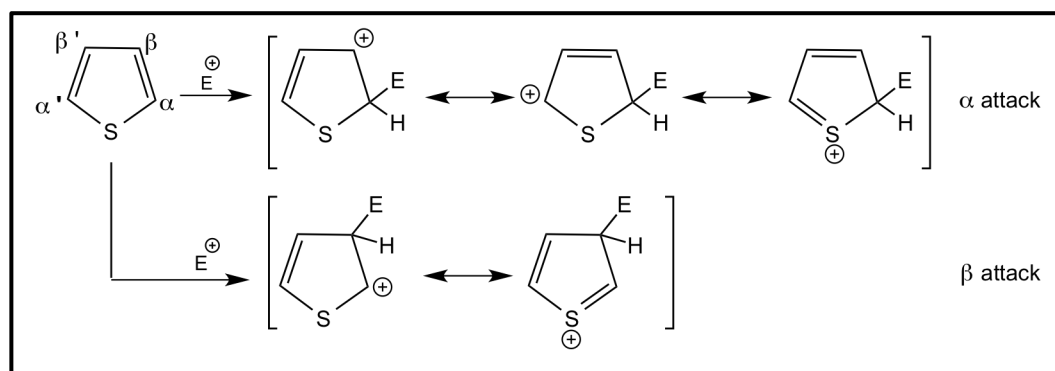
Thiophene can undergo many reactions such as electrophilic aromatic substitution reactions. It has been found that thiophene is more reactive than benzene due to the presence of the heteroatom (sulfur atom). As a result, the electrophilic substitution reaction occurs more easily in thiophene compared to benzene.⁶⁷ The substitution reaction

will occur at the carbons since the electron density on the carbon atoms is greater than on sulfur as seen in Scheme 2.2.



Scheme 2.2 Electron density on thiophene

There are two possible positions at which the substitution can occur: the α and β positions. The α position is more favorable than the β position, which is explained using the resonance structures, Scheme 2.3. Attack at the α position results in 3 different resonance structures; however, when the attack is at the β position only two structures are possible. Also, the substitution at the α position is preferred because stabilization through resonance is much stronger. Although the substitution at α is favored, β is also activated, but the yield of the β -substituted thiophene is smaller than that of the α -substituted thiophene. Furthermore, the negative partial charge carried by the α -carbon is larger in comparison to the β -carbon.⁶⁸



Scheme 2.3 Electrophilic attack at α and β of a thiophene monomer

2.3 Electron Paramagnetic Resonance

Electron paramagnetic resonance (EPR) is an important spectroscopic technique for the study of compounds and ions that have unpaired electron(s). It is also known as electron spin resonance (ESR). The radiation used in EPR spectroscopy is in the gigahertz range. In EPR spectroscopy, the frequency of the radiation is held constant while the magnetic field is varied in order to obtain an absorption spectrum.⁶⁹

The energy states of the electron, for a molecule with single unpaired electron in a magnetic field, is given by equation 2.1:

$$E = g\mu_B B_0 M_S = \pm \frac{1}{2} g\mu_B B_0 \quad \text{Equation 2.1}$$

where g is the proportionality factor (g -factor), μ_B is the Bohr magneton, B_0 is the magnetic field, and M_S is the electron spin quantum number ($M_S = \pm \frac{1}{2}$).

From equation 2.1, two important factors are noticeable: 1) the two spin states have the same energy in the absence of applied magnetic field, and 2) with increasing magnetic field strength, the energy difference between the two spin states increases linearly.

The proportionality factor (g -factor) provides useful information and unique identification of compounds. Using equation 2.2, the g -factor can be determined.⁷⁰

$$g = \frac{h\nu}{\mu_B B_0} \quad \text{Equation 2.2}$$

The value of the g -factor depends on the species. It is equal to 2.0023 for a free electron⁷¹ and ranging from 1.99-2.01 for organic radicals. However, it is different for transition metals ($g = 1.40$ - 3.00), due to the zero-field splitting and spin-orbit coupling.⁷²

Another important parameter that can be determined in EPR is the hyperfine coupling constant (a). It is resulting from the interactions between the unpaired electron and the magnetic nuclei present in the molecule. These hyperfine interactions can be used to offer information about the compound including data regarding the number and identity of

nuclei in a complex, and the distance between the unpaired electron and the nuclei. This interaction converts equation 2.1 to:

$$E = g\mu_B B_0 M_S + a M_S m_I \quad \text{Equation 2.3}$$

where a represents the hyperfine coupling constant and m_I is the nuclear spin quantum number of the neighboring nuclei.

The number of lines in an EPR spectrum can be determined using the $(2NI + 1)$ formula. N indicates the number of equivalent nuclei and I is the spin. From this formula, we can know the number of lines in the spectrum, but not their relative intensities. The intensities of the lines can be determined using a binomial distribution.⁷³

2.3.1 EPR of Pyrimidine-Verdazyl Radical

The EPR spectrum of verdazyl radical linked to chelating species such as pyrimidine has been reported by Hicks *et al.*⁷⁴ Figure 2.1 shows the EPR spectrum of this verdazyl radical recorded at 298 K. This radical has a g -value of 2.0037. The lines observed in this spectrum are due to the hyperfine coupling of the unpaired electron of the pyrimidine-verdazyl radical to the four nitrogen nuclei and six-methyl protons. The hyperfine coupling constants found are: $a(N_{2,4}) = 6.5$ G (2N), $a(N_{1,5}) = 5.3$ G (2N), $a(CH_3) = 5.3$ G (6H).

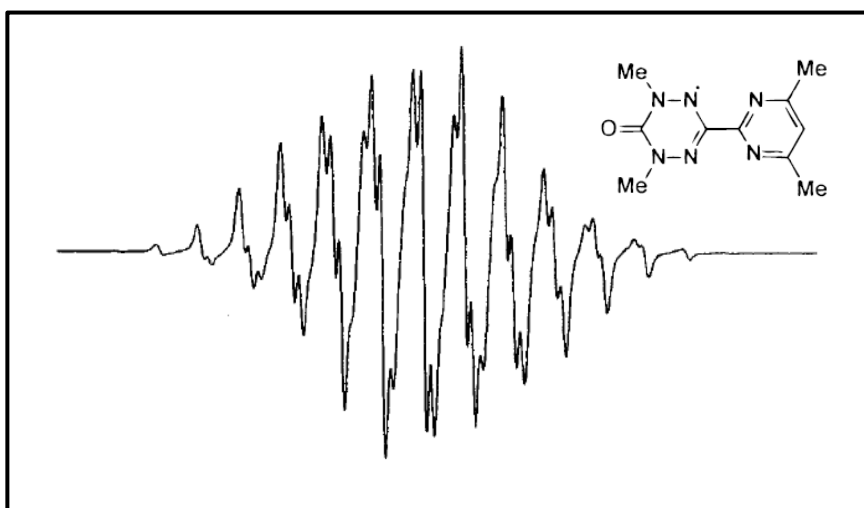
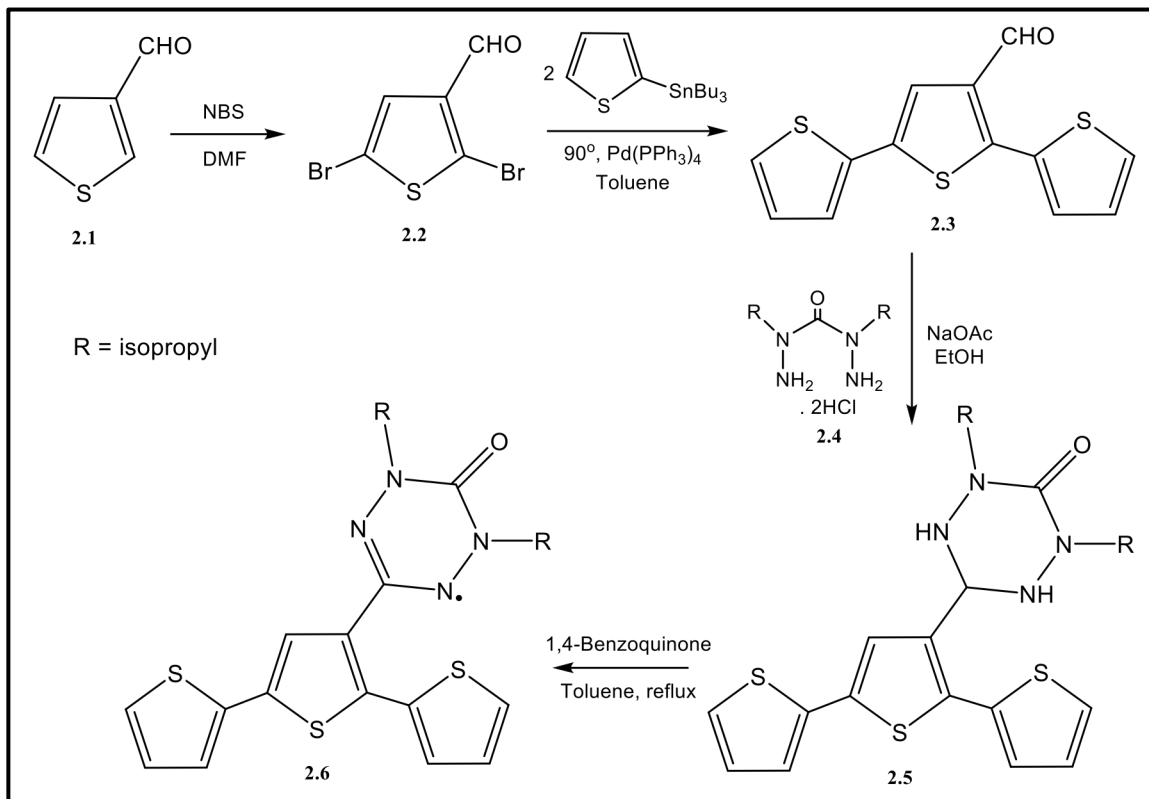


Figure 2.1 EPR spectrum of pyrimidine-verdazyl radical taken from reference 74

2.4 Synthesis of Radical Functionalized Terthiophenes

2.4.1 Synthesis of Verdazyl Radical Functionalized Terthiophene

The multi-step synthesis outlined in Scheme 2.4 describes the formation of the 1,5-diisopropyl-6-oxoverdazyl radical functionalized terthiophene **2.6**.



Scheme 2.4 The synthetic routes of terthiophene bearing 1,5-diisopropyl-6-oxoverdazyl radical (**2.6**)

In the first step, 2,5-dibromothiophene-3-carboxaldehyde, **2.2**, is synthesized by reaction of thiophene-3-carboxaldehyde, **2.1**, with N-bromosuccinimide (NBS).^{75,76} Even though there are various examples in the literature where thiophene monomers have been brominated in positions 2 and 5 using NBS, there were few examples of this being done with a thiophene substituted with electron withdrawing groups in position 3. It is worth noting that compound **2.2** is commercially available.

A Stille cross coupling reaction which involves treating the dibrominated thiophene monomer (**2.2**) with the commercially available 2-tributylstannyl thiophene yields terthiophene-3'-carboxaldehyde, **2.3**.^{77,78} The condensation of aldehyde **2.3** with bis(1-alkylhydrazide)s of carbonic acid, **2.4**, gives the corresponding 2, 4-diisopropyl-6-terthiophene-3-oxotetrazane **2.5**. The bis(1-alkylhydrazide) of carbonic acid used in this study, 2,4-diisopropylcarbonhydrazide bis-hydrochloride (**2.4**), was prepared using the procedure described by Brook *et al.*³⁸ The final step involved the oxidation of the tetrazane, **2.5**, to form the radical 1,5-diisopropyl-3-terthiophene-6-oxoverdazyl, **2.6**, (Scheme 2.4). Many conditions have been studied for the oxidation of 3-oxotetrazanes to 6-oxoverdazyl radicals. *Para*-benzoquinone in toluene has been found to be effective in the oxidation of 3-oxotetrazane. The benzoquinone is reduced to form hydroquinone adducts that were precipitated from the reaction mixture as it cooled overnight. Filtration and evaporation of the solvent gave 1,5-diisopropyl-6-oxoverdazyl radical functionalized terthiophene, which was purified by silica gel column chromatography. The purified 1,5-diisopropyl-6-oxoverdazyl radical functionalized terthiophene **2.6** was a red oil which crystallized upon sitting at room temperature. This verdazyl radical is stable in air and different organic solvents; it requires no special handling and can be stored for a long time without decomposition.

The heterocyclic tetrazane, **2.5**, has been characterized by ¹H/¹³C NMR and IR. The peaks in the ¹H NMR spectrum, Figure 2.2, assigned to the terthiophene and the tetrazane, are summarized in Table 2.1. The aromatic proton peaks are as follow: a) a doublet at 7.69 ppm with a coupling constant of 4.9 Hz represents the proton number 7, b) a singlet at 7.60 ppm represents the proton number 4, c) a doublet at 7.56 ppm with a coupling constant of 4.7 Hz represents the proton number 1, d) a multiplet at 7.30 ppm represents the 2H protons 3 and 5 e) two doublet of doublet at 7.12 ppm and 7.18 ppm with a coupling constant of 3.7 Hz correspond to proton 2 and 6, respectively. The ¹H NMR peaks of the tetrazane ring are: a) a doublet at 5.25 ppm ($J = 11.5$ Hz) corresponding to the 2 N-H protons 12, b) a multiplet at 4.45 ppm corresponding to the 2 CH protons of the isopropyl group, c) a triplet at 4.56 ppm corresponding to the CH proton linked to N atom ($J = 11.5$ Hz), and d) two doublets at 1.01 ($J = 6.7$ Hz) and 0.95

ppm ($J = 6.4$ Hz) corresponding to the non-equivalent protons of the isopropyl methyl groups.

Table 2.1 Assignments of ^1H NMR signals for compound **2.5**

Proton number	δ (ppm)	Multiplicity	Integration	J (Hz)
1	7.56	doublet	1H	4.7
2	7.12	doublet of doublet	1H	3.7
3,5	7.30	multiplet	2H	-
4	7.60	singlet	1H	-
6	7.18	doublet of doublet	1H	3.7
7	7.69	doublet	1H	4.9
8,8'	0.95	doublet	6H	6.4
9,9'	1.01	doublet	6H	6.7
10,10'	4.45	multiplet	2H	-
11	4.56	triplet	1H	11.5
12,12'	5.25	doublet	2H	11.5

Table 2.2 Assignments of ^{13}C NMR signals for compound **2.5**

Carbon number	δ (ppm)
1	128.2
2	133.0
3	124.6
4	124.0
5	128.0
6	135.6
7	135.5
8	131.9
9	126.2
10	127.6
11	134.2
12	128.5
13,13'	18.7
14,14'	19.5
15,15'	46.7
16	153.0
17	67.5

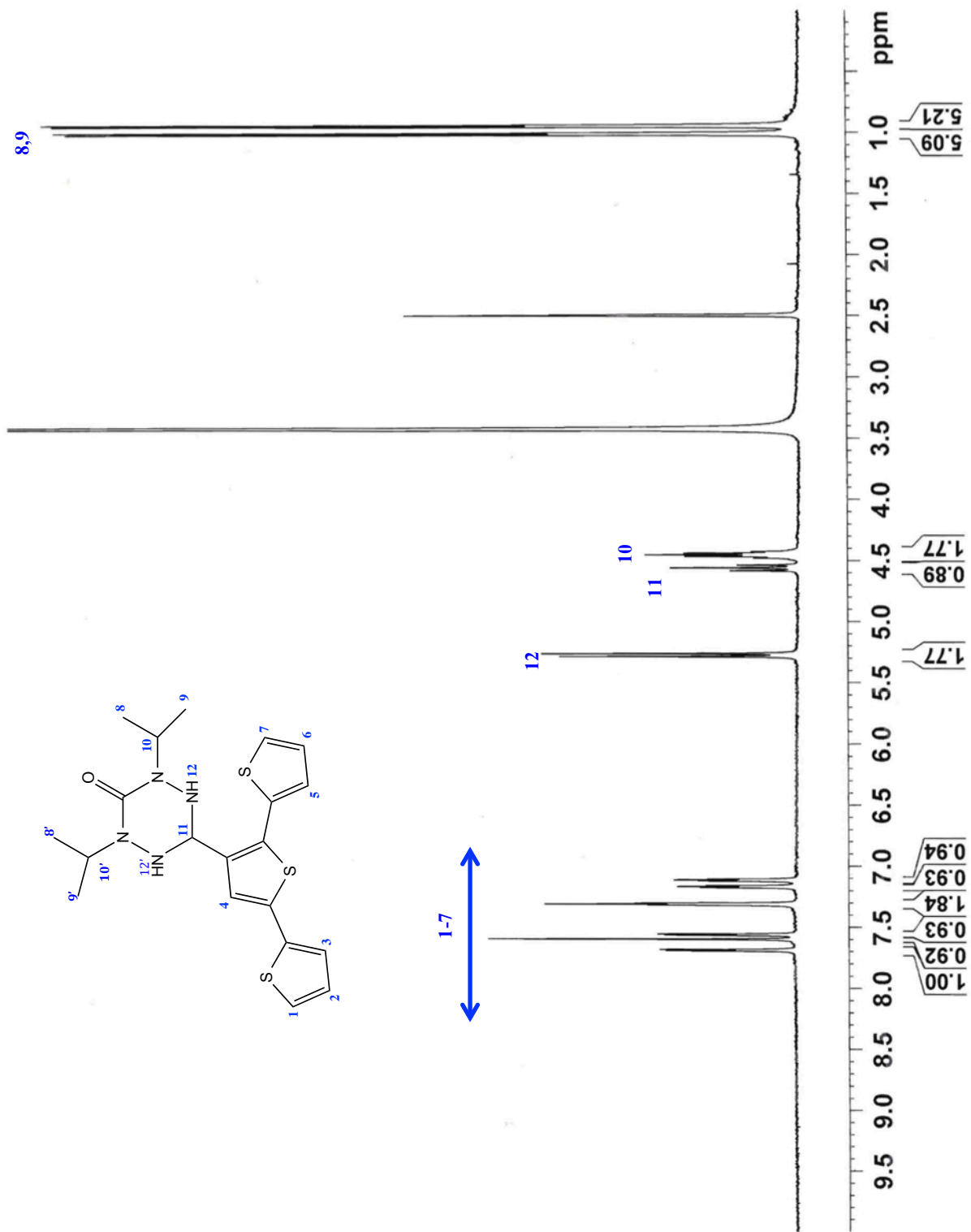


Figure 2.2 500 MHz ^1H NMR spectrum of compound 2.5 in DMSO

In addition to ^1H NMR, ^{13}C NMR confirms the structure of **2.5**, in Figure 2.4 and Table 2.2. The carbonyl group carbon has a chemical shift of 153.0 ppm. The chemical shifts between 124.0 ppm and 135.6 ppm correspond to the CH and C carbons of the terthiophene. The peak at 67.5 ppm corresponds to the C-N carbon of the tetrazane. The carbons of the isopropyl group are at 46.7 ppm (CH), 19.5 ppm (CH_3), and 18.7 ppm (CH_3). ^1H NMR and ^{13}C NMR values are in agreement with the NMR values found in the literature for the terthiophene^{77,78} and the heterocyclic tetrazane³⁸.

It has been reported that the isopropyl substituents make the verdazyl radical more stable in comparison to the methyl and phenyl groups.⁷⁹ This stability is due to the conformation of these radicals. Surprisingly, the two isopropyl methyls are not equivalent and are placed above and below the plane of the verdazyl ring, providing a steric protection for the verdazyl ring.³⁸ This can be confirmed by the ^1H NMR in which two doublets have been observed for the methyls of the isopropyl group (Figure 2.3), whereas one peak has been observed for the two methyls in the ^1H NMR of **2.4**.³⁸ Moreover, two CH_3 peaks has been detected in ^{13}C NMR (Figure 2.4).

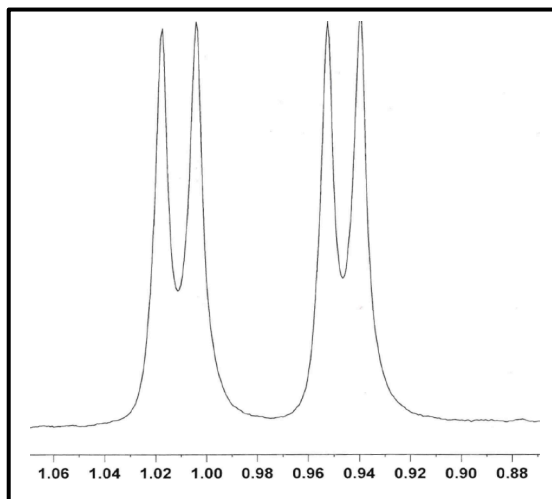


Figure 2.3 500 MHz ^1H NMR expansion of CH_3 region of compound **2.5**

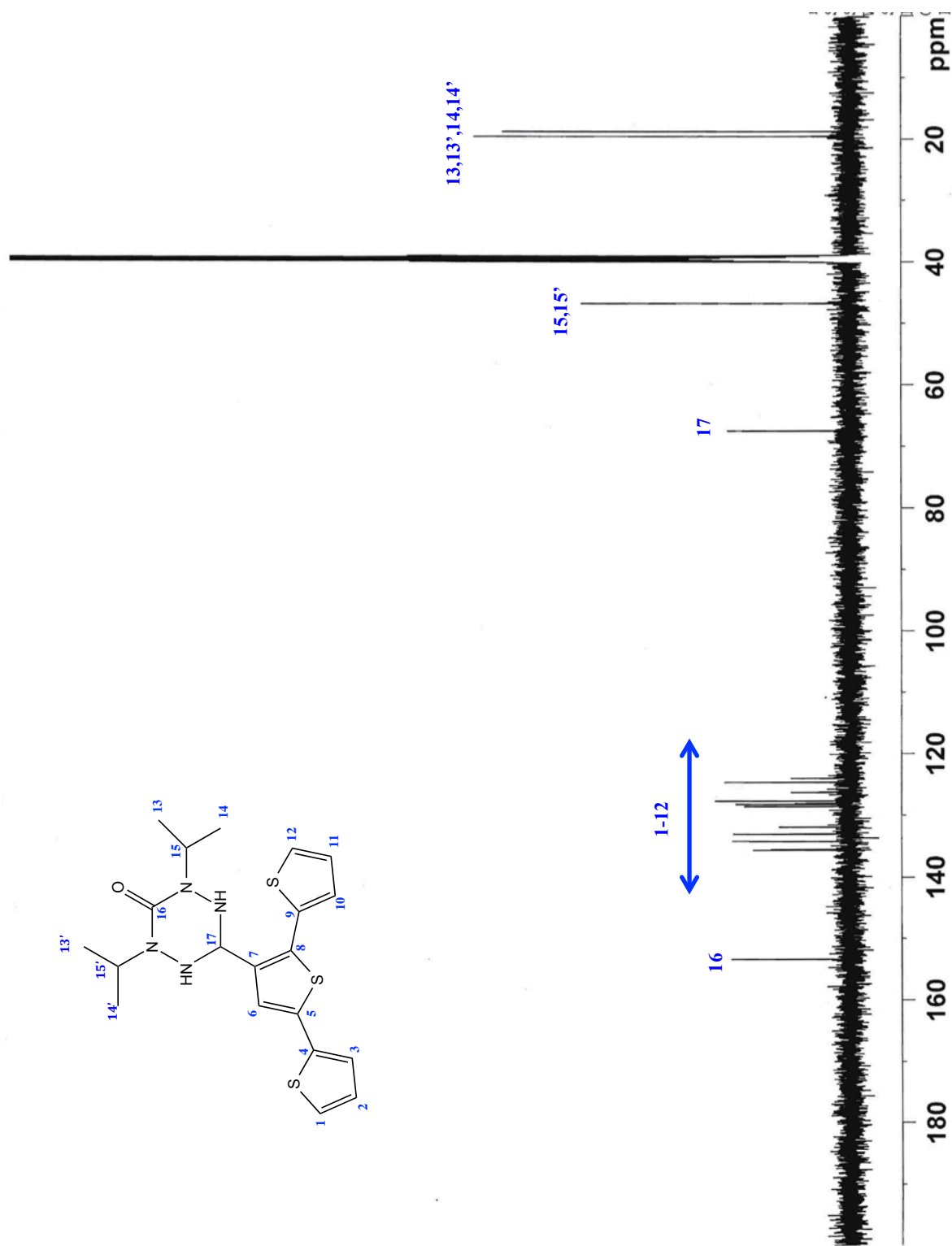


Figure 2.4 500 MHz ^{13}C NMR spectrum of compound 2.5 in DMSO

Figure 2.5 shows the IR spectra of compounds **2.5** (dashed) and **2.6** (solid) and confirms the successful conversion of tetrazane **2.5** to verdazyl radical **2.6**. After oxidation, the presence of the NH stretching absorption at 3250 cm^{-1} in the spectrum of tetrazane **2.5** disappears for verdazyl **2.6**. Moreover, the C=O stretching absorption shifts from 1607 cm^{-1} in the case of tetrazane **2.5** to 1680 cm^{-1} for the verdazyl radical **2.6**. The 73 cm^{-1} shift corresponds to the presence of an unpaired electron that makes the carbonyl stretching occur at a higher wavenumber.

Furthermore, to validate the presence of the radical, the EPR spectrum of 1,5-diisopropyl-6-oxoverdazyl radical functionalized terthiophene, **2.6**, has been recorded at room temperature (Figure 2.6). The top trace represents the experimental spectrum and the bottom trace represents the simulated spectrum obtained using the WINSIM program.⁸⁰ The multi-lined spectrum, centered at $g = 2.0020$ is due to the hyperfine coupling between the unpaired electron with four nitrogen atoms and the methane two hydrogen atoms of the isopropyl groups. The best agreement between the experimental and simulated spectrum occurred in using the following coupling constants $a(\text{N}_{2,4}) = 6.5\text{ G}$ (2N), $a(\text{N}_{1,5}) = 5.3\text{ G}$ (2N) and $a(\text{CH}) = 1.3\text{ G}$ (2H). These values are almost identical to those reported for other isopropyl substituted-verdazyls.^{81,82} In fact, the EPR magnetic parameters of the isopropyl substituted-verdazyl radicals are all very similar with the exception of the $a(\text{H})$. The value of $a(\text{H})$ is sensitive to the radical's conformation. Coupling between the methane hydrogen and the unpaired electron is a minimum when the C-H twists in the plane of the verdazyl ring.

$g = 0.7144775 * \nu (\mu\text{Hz})/H (\text{G})$ $g = 2.0020$ $\nu = 9143\ \mu\text{Hz}, H = 3263\ \text{G}$	Equation 2.4
---	---------------------

Moreover, HRMS experimental data are in agreement with the theoretical value found for the radical **2.6** and its precursor **2.5** (Table 2.3)

Table 2.3 HRMS data for compounds **2.5** and **2.6**

Compound	Formula	HRMS calcd.	HRMS found
2.5	$\text{C}_{20}\text{H}_{24}\text{N}_4\text{OS}_3$	433.1190	433.1186
2.6	$\text{C}_{20}\text{H}_{21}\text{N}_4\text{OS}_3$	429.0877	429.0870

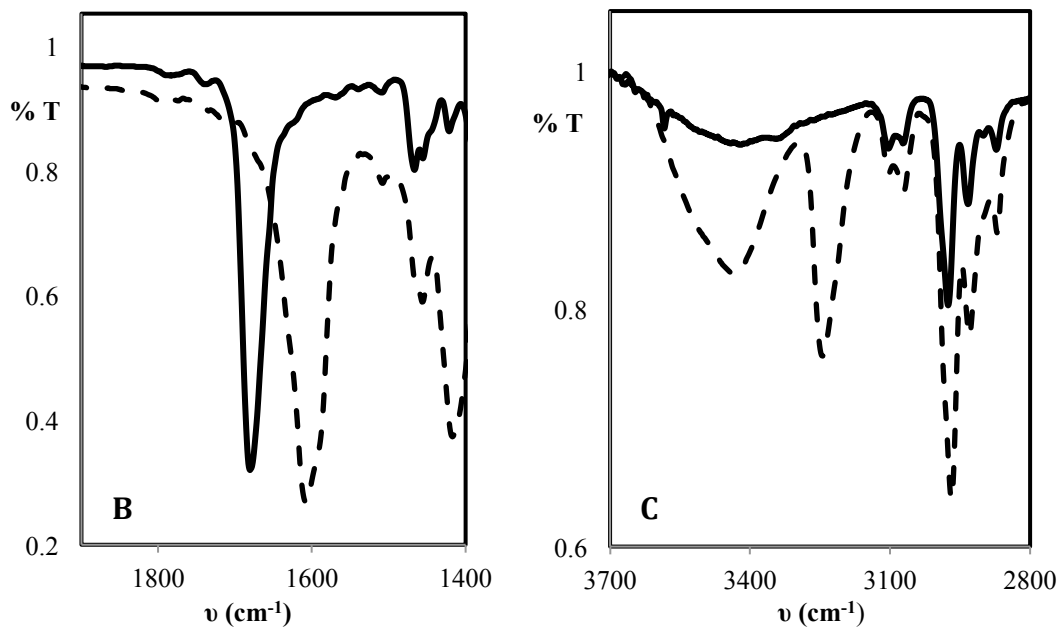
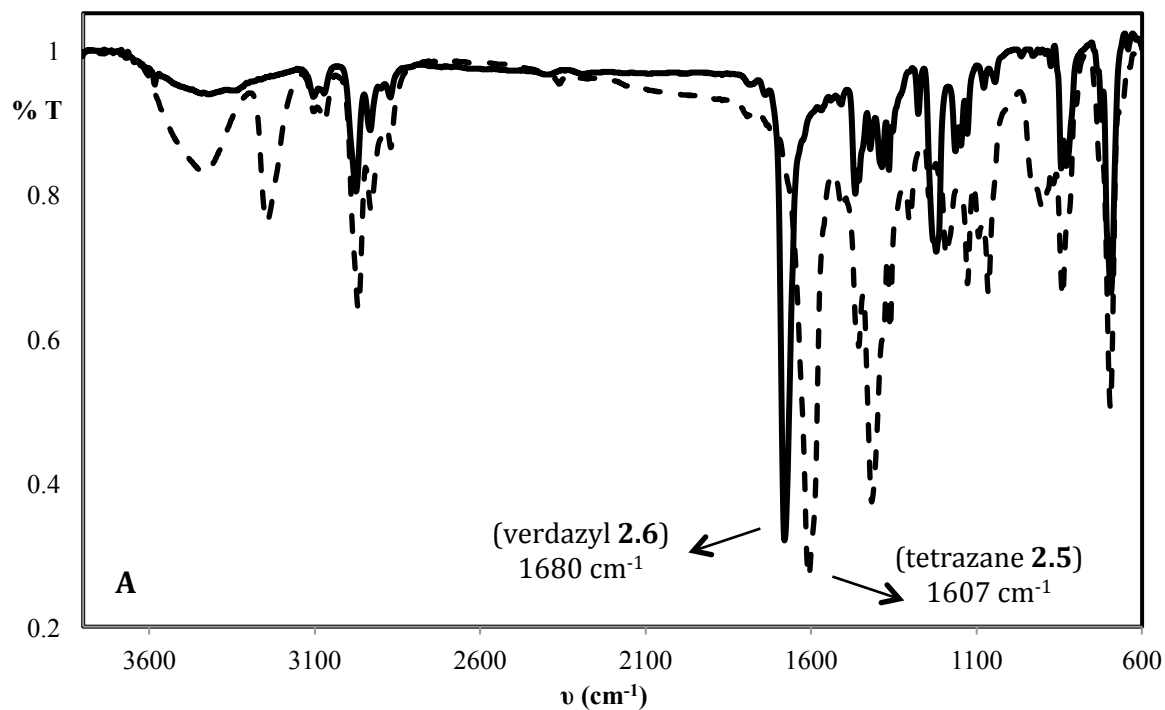


Figure 2.5 A) IR spectra of compounds 2.5 (dashed line) and 2.6 (solid line), B) Expansion of C=O region, and C) Expansion of NH region

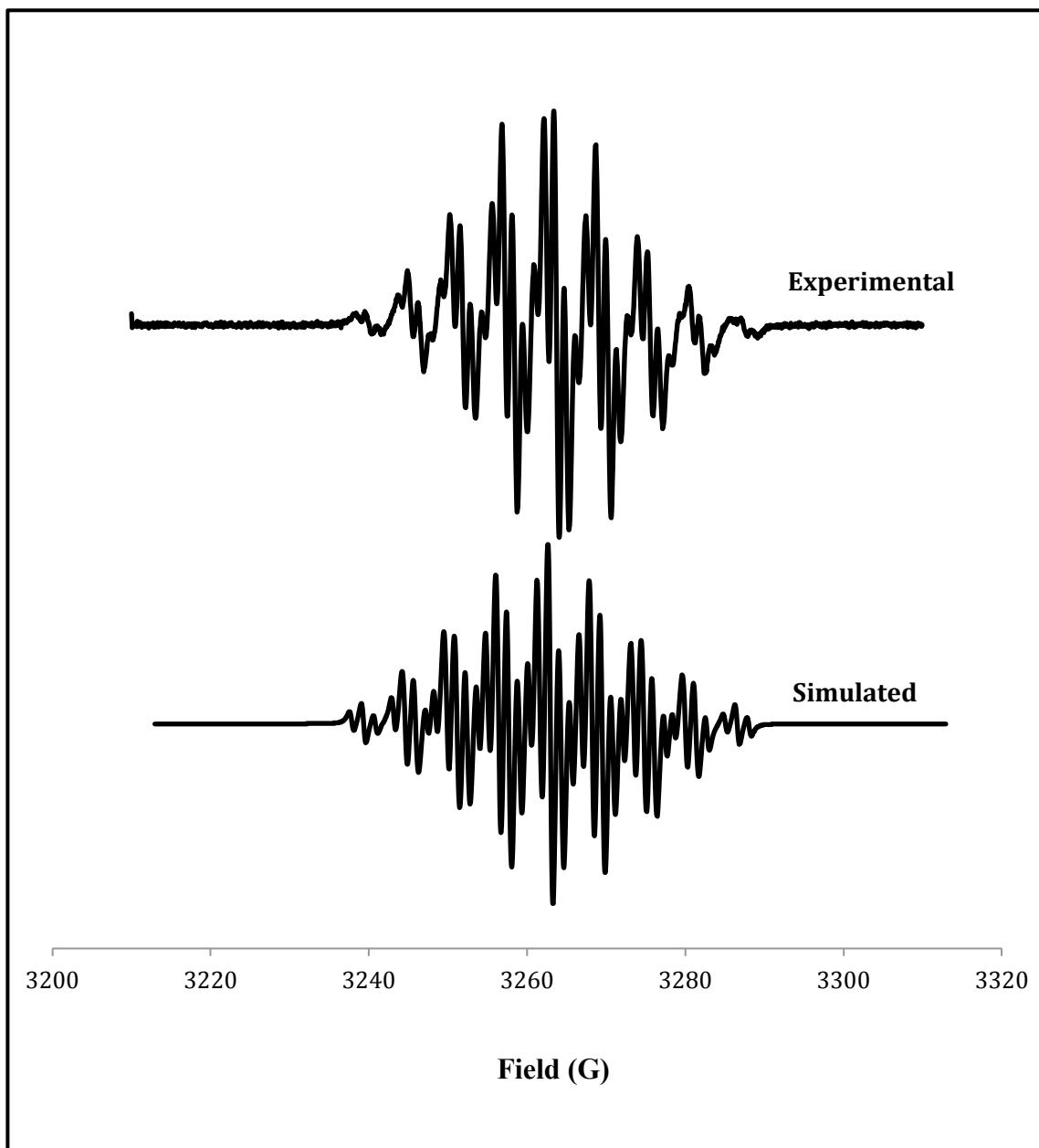
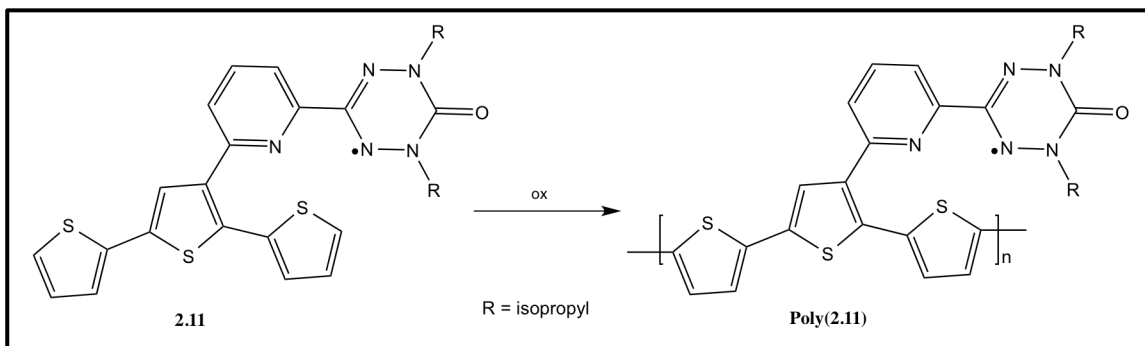


Figure 2.6 Experimental EPR spectrum of compound **2.6** recorded at room temperature ($\nu = 9143 \mu\text{Hz}$, microwave power = 1 mw) (top) and simulated spectrum (bottom)

2.4.2 Synthesis of Verdazyl Radical Functionalized Terthiophene Bridged by Pyridine

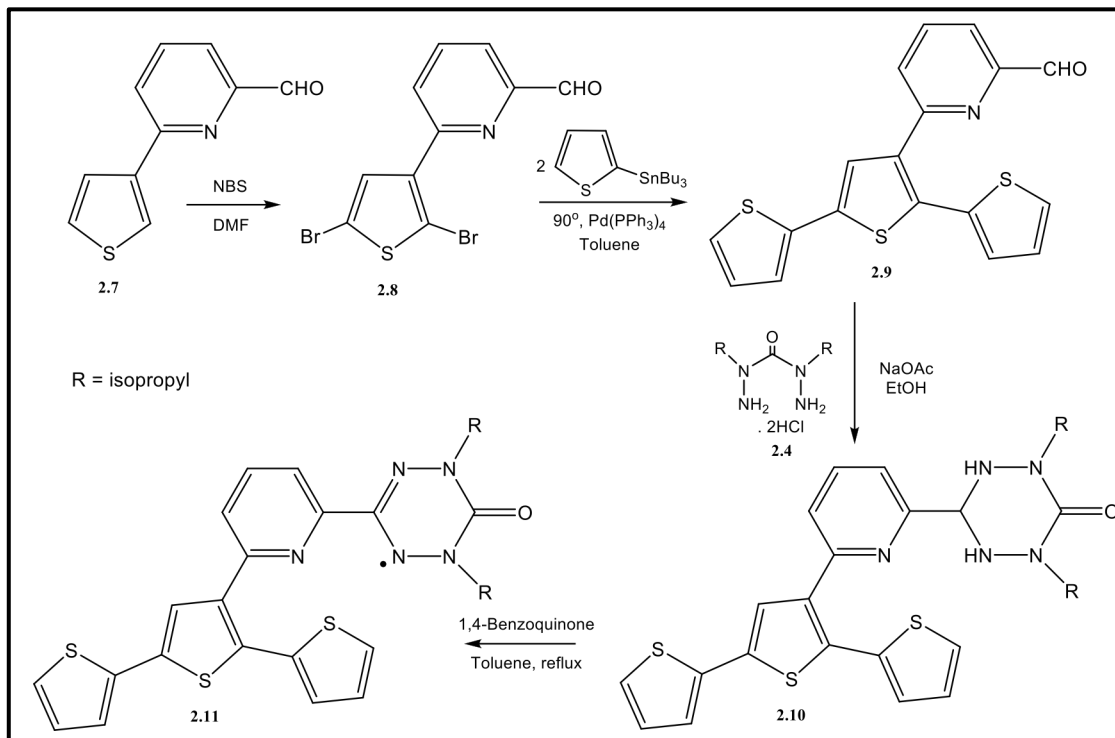
Building of molecule-based materials, which possess more than one property such as electrical conductivity and magnetic interactions, is currently a challenging objective.^{83,84} Such an interesting goal lead us to synthesize molecules where the verdazyl radical and terthiophene units are connected through cross-conjugation via heterocyclic aromatic linkers, such as pyridine. This ligand is interesting because of its ability to be complexed with transition metals.^{74,85} As reported recently, it is anticipated that the transition metal complexes of verdazyl radicals will lead to new molecular magnetic materials, which might show a combination of properties.⁸⁶ The properties of these materials could be affected by the metal-radical interactions, which are being studied for its use in “hybrid” magnetic materials.⁸⁷ Introducing such a linker between the π -donor and π -radical (i.e. terthiophene and verdazyl, respectively) (**2.11**) may affect the electrochemical and optical properties of the corresponding deposited polymer poly(**2.11**) (Scheme 2.5).



Scheme 2.5 Verdazyl radical-oligo/polythiophene cross-conjugated via pyridine

The synthetic route used to prepare the 1,5-diisopropyl-6-oxoverdazyl radical functionalized terthiophene bridged by a pyridine moiety **2.11** is described in Scheme 2.6.

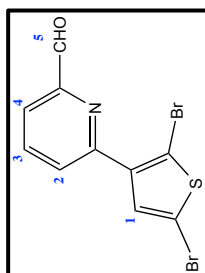
The dibromination at the α , α' positions of the thiophene ring in **2.7** was successfully achieved, with a 50% yield, using NBS in dimethylformamide (DMF) at room temperature. The by-product that was observed from the TLC could be the bromination of pyridine; however, it possesses a low yield compared to the bromination of the thiophene ring.



Scheme 2.6 Synthetic route of terthiophene-3'-pyridine bearing verdazy radical, **2.11**

The ^1H NMR spectrum of compound **2.8** displays characteristics of the thiophene, pyridine rings and the aldehyde group (Figure 2.7), which are summarized in Table 2.4. The singlet at 10.02 ppm corresponds to CHO proton number 5. The doublet peak at 8.08 ppm with a coupling constant of 5.0 Hz corresponds to pyridine proton number 4, and the multiplet at 7.90 ppm corresponds to pyridine protons 2 and 3. The one proton attached to thiophene ring is a singlet peak at 7.47 ppm.

Table 2.4 Assignment of ^1H NMR signals for compound **2.8**

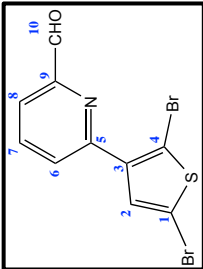


Proton number	δ (ppm)	Multiplicity	Integration	J (Hz)
1	7.47	singlet	1H	-
2,3	7.90	multiplet	2H	-
4	8.08	doublet	1H	5.0
5	10.02	singlet	1H	-

In the ^{13}C NMR spectrum (Figure 2.8), the peak at 193 ppm corresponds to the carbonyl of aldehyde group and peaks between 110 and 160 ppm correspond to aromatic C and CH carbons of the thiophene and pyridine rings. The ^{13}C NMR chemical shifts of **2.8** are presented in Table 2.5.

Table 2.5 Assignment of ^{13}C NMR signals for compound **2.8**

Carbon number	δ (ppm)
1	111.9
2	126.7
3	139.8
4	110.2
5	152.4
6	131.9
7	137.6
8	120.3
9	152.6
10	193.2



The following step was the Stille cross coupling reaction of the dibromothiophene, **2.8**, with two equivalents of the commercially available 2-tributylstannyl thiophene and $\text{Pd}(\text{PPh}_3)_4$ as the catalyst. Terthiophene-3'-pyridine aldehyde (**2.9**) was obtained after purification with a yield of 58 %.

There are two main group of peaks in the ^1H NMR spectrum of **2.9** (Figure 2.9): the singlet at 10.65 ppm corresponding to the aldehydic proton, and the peaks with a chemical shift between 7.0 and 8.0 ppm which correspond to 10 aromatic protons (7 from terthiophene and 3 from pyridine). The position and multicplicity of terthiophene protons was previously mentioned. For the pyridine ring, the doublet peak at 7.92 ppm corresponds to CH proton number 10, and the doublet of doublet at 7.81 ppm corresponds to the proton labeled 9. For the CH peaks (number 8) of pyridine and CH (number 4) of terthiophene are at the same chemical shift thus producing a complex signal. Table 2.6 shows the assignments of ^1H NMR signals for compound **2.9**. Moreover, the ^{13}C NMR spectrum of **2.9** (Figure 2.10) consists of 18 carbons corresponding to 1 aldehydic carbon (194 ppm) and 7 C and 10 CH carbons of terthiophene and pyridine (120-160 ppm). A summary of the ^{13}C NMR assignments for compound **2.9** is given in Table 2.7.

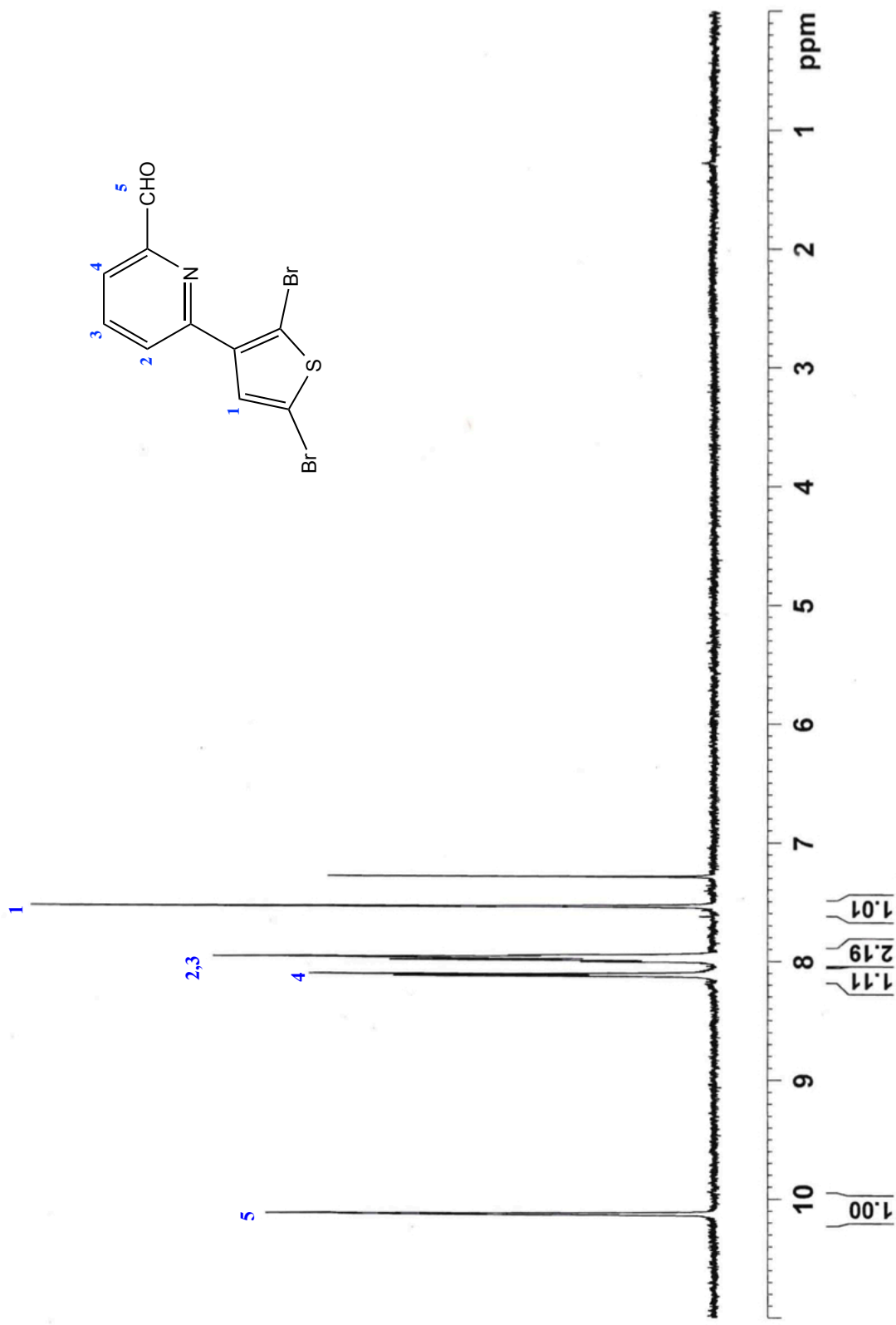


Figure 2.7 500 MHz ¹H NMR spectrum of compound 2.8 in CDCl₃

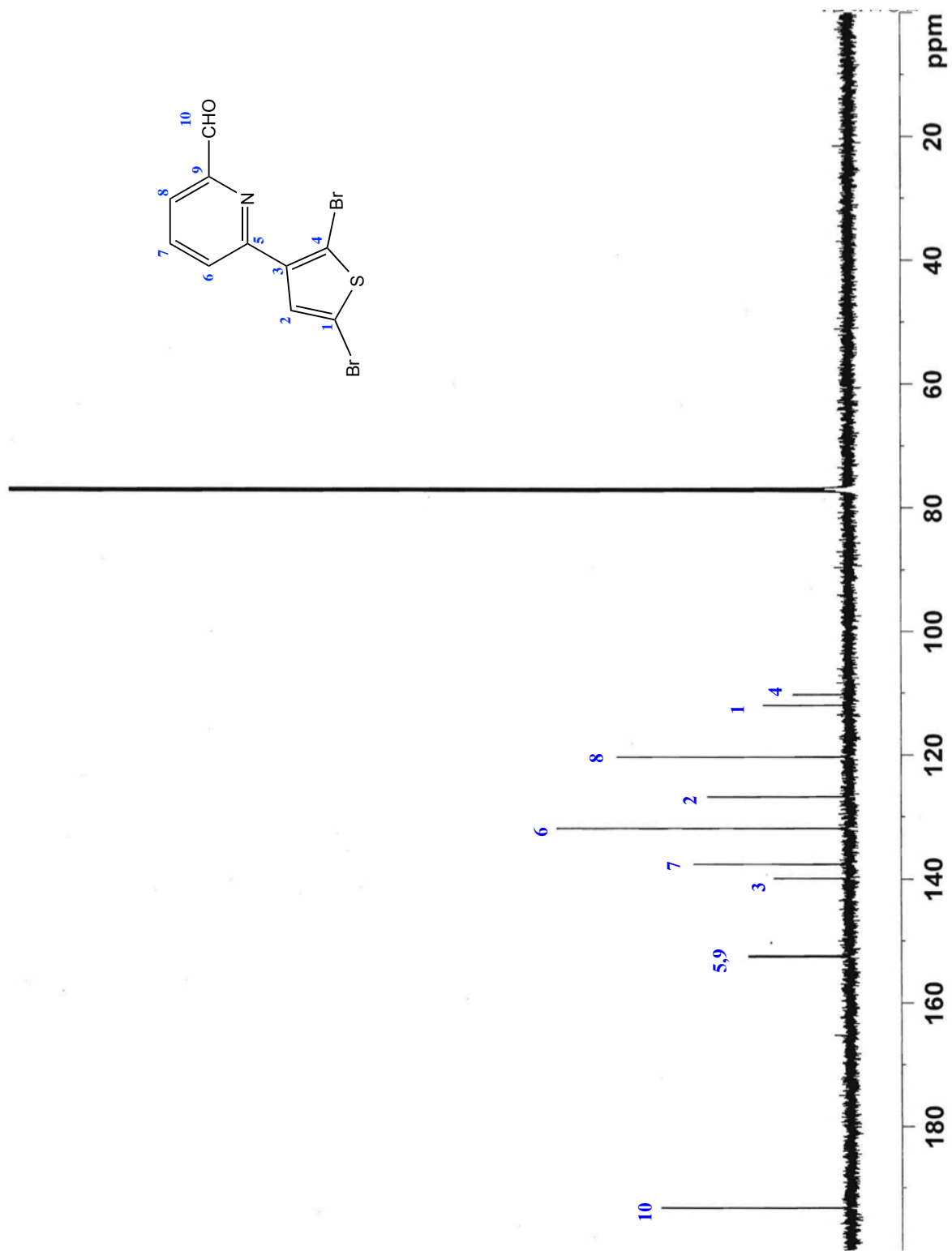
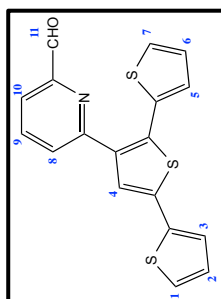


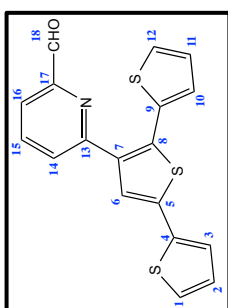
Figure 2.8 500 MHz ¹³C NMR spectrum of compound **2.8** in CDCl₃

Table 2.6 Assignment of ^1H NMR signals for compound **2.9**



Proton number	δ (ppm)	Multiplicity	Integration	J (Hz)
1	7.12	doublet	1H	5.0
2	7.04	doublet of doublet	1H	5.0
3,5	7.30	multiplet	2H	-
4,8	7.60	multiplet	2H	-
6	7.08	doublet of doublet	1H	5.0
7	7.33	doublet	1H	5.0
9	7.81	doublet of doublet	1H	10.0
10	7.92	doublet	1H	10.0
11	10.65	singlet	1H	-

Table 2.7 Assignment of ^{13}C NMR signals for compound **2.9**



Carbons	δ (ppm)
1	125.1
2	126.1
3	127.0
4	132.9
5	137.3
6	128.0
7	128.1
8	137.6
9	134.4
10	124.3
11	127.8
12	127.6
13	155.0
14	136.3
15	120.0
16	136.8
17	154.6
18	193.4

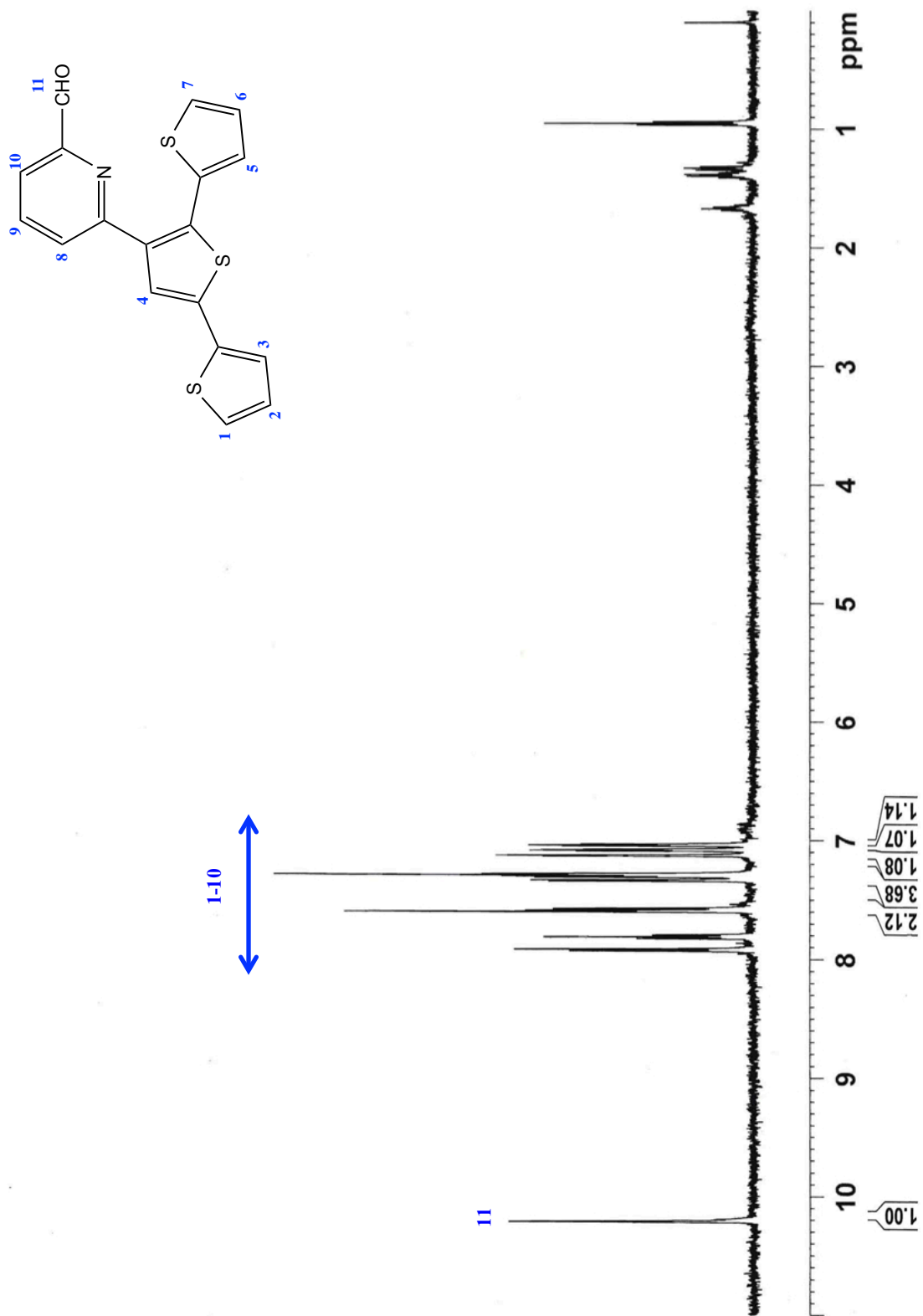


Figure 2.9 500 MHz ^1H NMR spectrum of compound 2.9 in CDCl_3

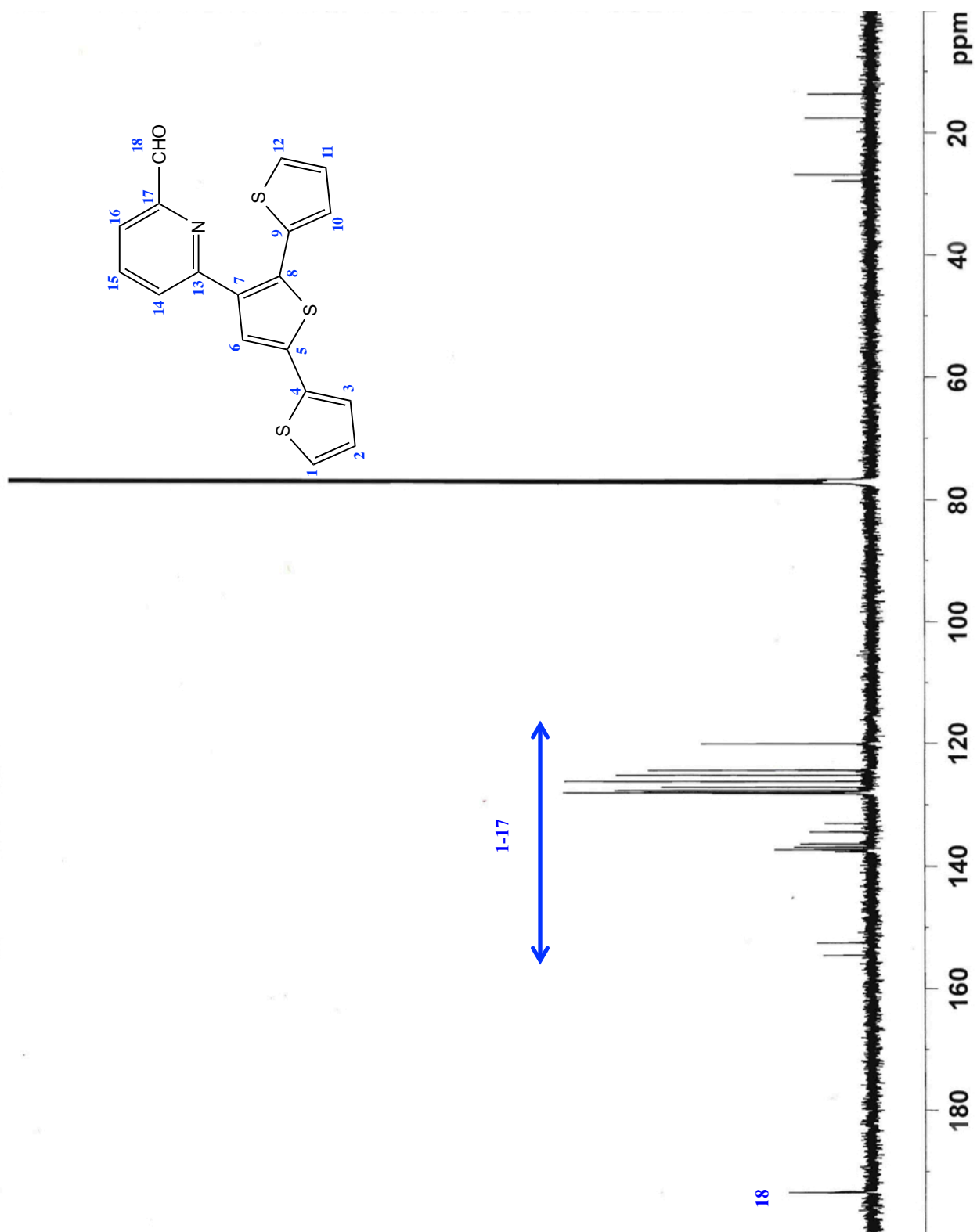


Figure 2.10 500 MHz ^{13}C NMR spectrum of compound 2.9 in CDCl_3

Once the terthiophene pyridine aldehyde, **2.9**, had been synthesized, the next step was the formation of the tetrazane using the same procedure that was used for the synthesis of **2.5**. The heterocyclic tetrazane, **2.10**, was prepared with a yield of 43 %. Figures 2.11 and 2.12 show the ^1H and ^{13}C NMR of tetrazane, **2.10**, respectively.

The ^1H NMR spectrum (Figure 2.11) shows multiple peaks between 7.0 and 8.0 ppm, which correspond to the 7 protons of terthiophene (similar to terthiophene protons in compounds **2.5** and **2.9**) and 3 protons of pyridine (similar to pyridine proton in compound **2.8** and **2.9**). The chemical shifts of the heterocyclic tetrazane and the isopropyl are identical to those of compound **2.5**. To confirm the structure of **2.10**, ^{13}C NMR spectrum was recorded (Figure 2.12). Table 2.10 summarizes the C, CH and CH_3 carbons of the new compound **2.10**.

The final step was the oxidation of tetrazane **2.10** to its corresponding verdazyl radical **2.11**, which was obtained with a yield of 70 %. Radical **2.11** is a red crystal obtained upon sitting for a few days.

Like **2.6**, this verdazyl radical is stable in air and organic solvents allowing us to characterize it without decomposition. Formation of **2.11** is supported by IR spectroscopy since the $\text{C}=\text{O}$ stretching vibration is shifted from 1626 cm^{-1} to 1686 cm^{-1} as shown in Figure 2.13. The dashed line corresponds to tetrazane **2.10** and the solid line corresponds to the verdazyl **2.11**. Moreover, in the verdazyl there is an absence of NH stretching above 3200 cm^{-1} in comparison to the tetrazane that has a broad band in this region.

HRMS experimental data are also in agreement with the theoretical value found for all new prepared compounds **2.8**, **2.9**, **2.10** and **2.11** (Table 2.8).

Table 2.8 HRMS data for compounds **2.8** to **2.11**

Compound	Formula	HRMS calcd.	HRMS found
2.8	$\text{C}_{10}\text{H}_5\text{Br}_2\text{NOS}$	345.8536	345.8529
2.9	$\text{C}_{18}\text{H}_{11}\text{NOS}_3$	354.0081	354.0076
2.10	$\text{C}_{25}\text{H}_{27}\text{N}_5\text{OS}_3$	510.1456	510.1455
2.11	$\text{C}_{25}\text{H}_{24}\text{N}_5\text{OS}_3$	507.1221	507.1247

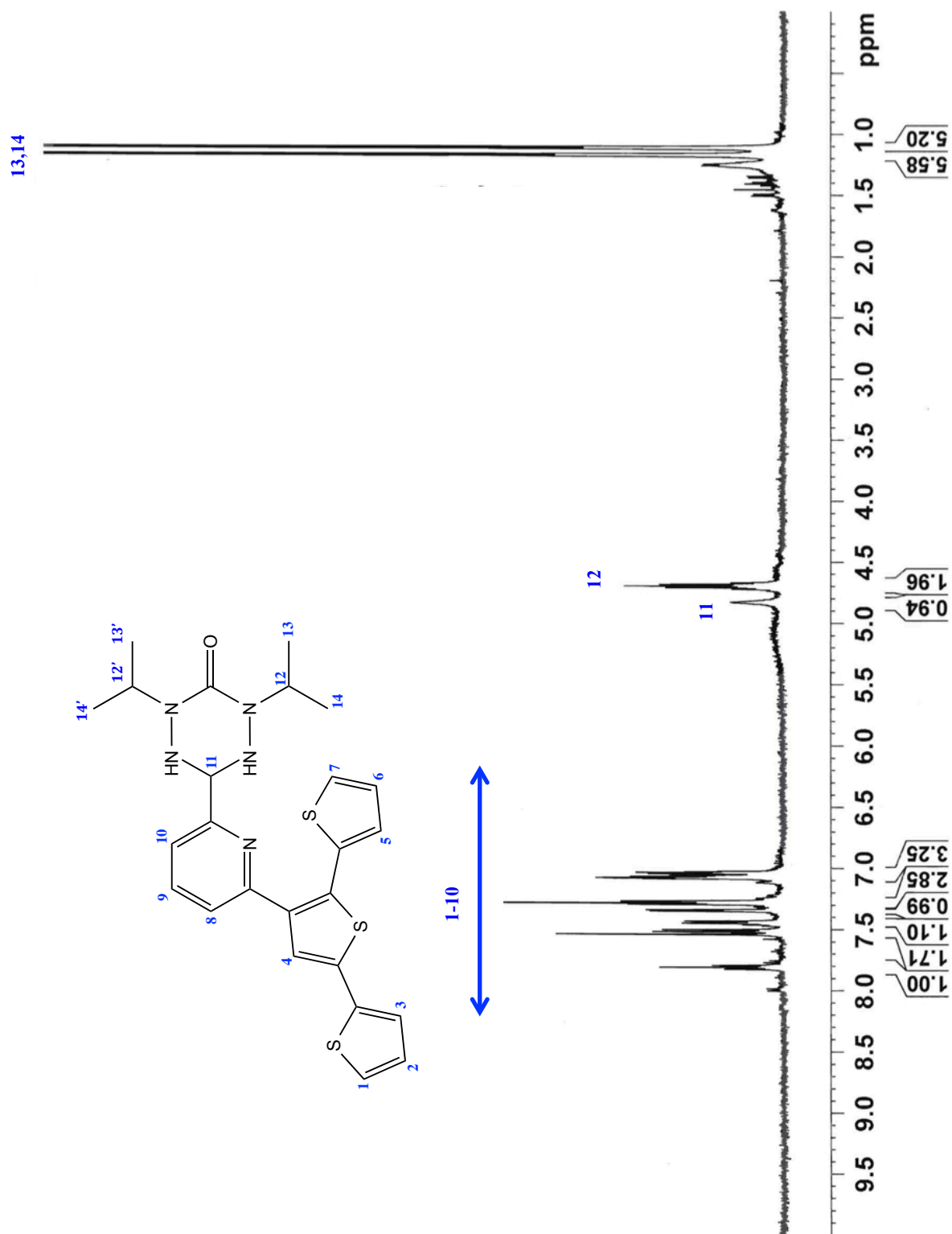
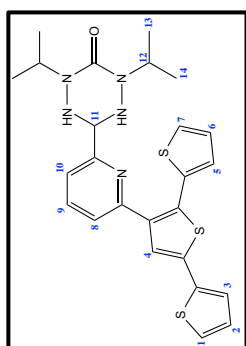


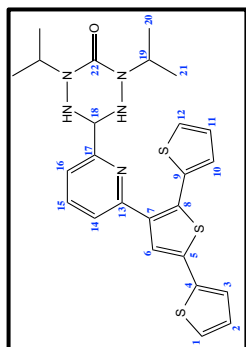
Figure 2.11 500 MHz ^1H NMR spectrum of compound 2.10 in CDCl_3

Table 2.9 Assignment of ¹H NMR signals for compound **2.10**



Proton number	δ (ppm)	Multiplicity	Integration	<i>J</i> (Hz)
1,6	7.10	multiplet	2H	-
2	7.04	doublet of doublet	1H	5.0
3,5	7.30	multiplet	2H	-
4	7.55	singlet	1H	-
7	7.34	doublet	1H	5.0
8	7.44	doublet	1H	10.0
9	7.81	doublet of doublet	1H	5.0
10	7.51	doublet	1H	10.0
11	4.80	singlet	1H	-
12,12'	4.70	multiplet	2H	-
13,13'	1.25	doublet	6H	10.0
14,14'	1.35	doublet	6H	10.0

Table 2.10 Assignment of ¹³C NMR signals for compound **2.10**



Carbon number	δ (ppm)
1	125.2
2	126.8
3	125.1
4	133.3
5	136.1
6	127.5
7	134.7
8	137.0
9	138.6
10	124.3
11	125.5
12	124.1
13	126.0
14	127.9
15	122.1
16	128.0
17	126.9
18	70.8
19,19'	47.7
20,20'	18.7
21,21'	19.5
22	153.1

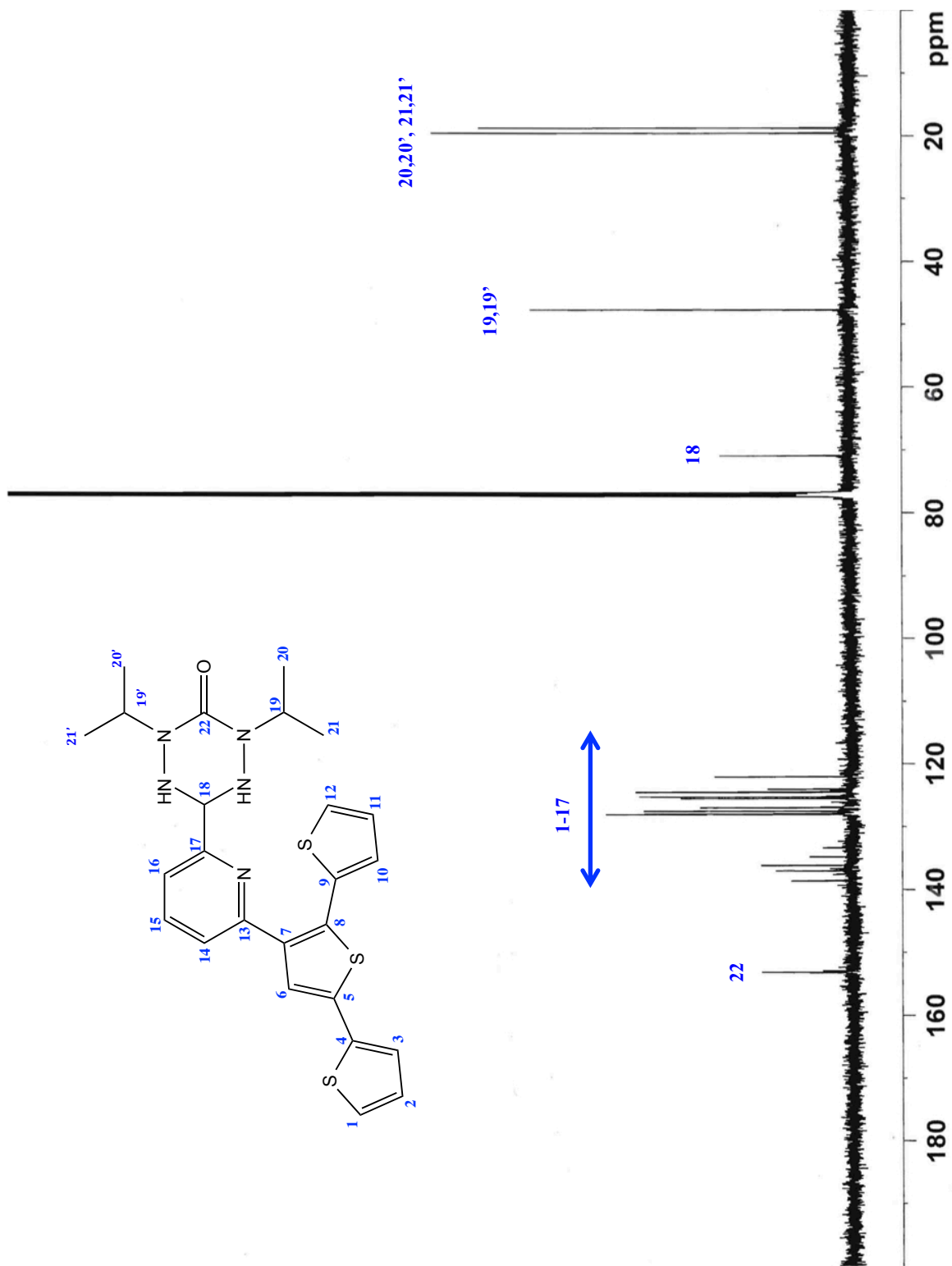


Figure 2.12 500 MHz ^{13}C NMR spectrum of compound **2.10** in CDCl_3

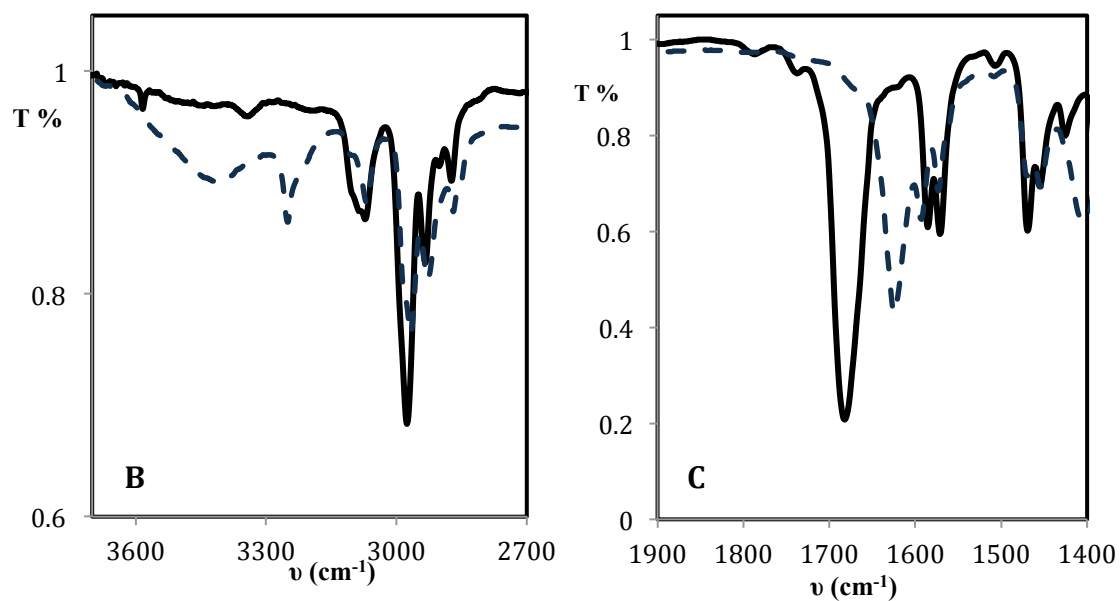
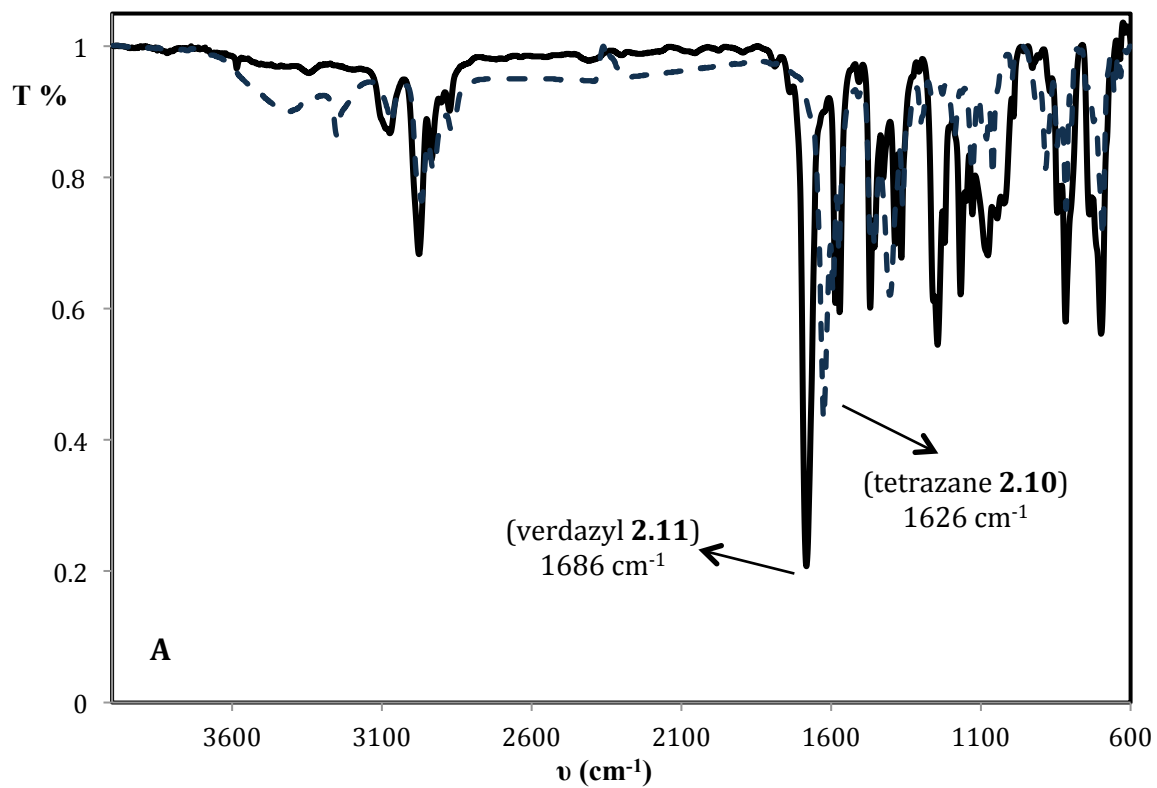


Figure 2.13 A) IR spectra of compounds **2.10** (dashed line) and **2.11** (solid line), B) Expansion of NH region, and C) Expansion of C=O region

The EPR spectrum of 1,5-diisopropyl-6-oxoverdazyl radical functionalized terthiophene through pyridyl linker (**2.11**) recorded at room temperature centered at $g = 2.0010$ is depicted in Figure 2.14. We expected a multi-lined spectrum similar to that found for verdazyl **2.6** in Figure 2.6. However, the broad lines observed in the EPR spectrum of **2.11** are due to: i) unsuccessful solvent degassing during the sample preparation, or ii) unresolved H (two hydrogen atoms in the isopropyl groups) hyperfine interaction. The interaction between the unpaired electron and the two hydrogen atoms (in isopropyl methane) is very small, i.e. $a_H < 1.3$ G. Spectral simulation afforded hyperfine coupling constants as follows: $a(N_{2,4}) = 6.5$ G (2N), $a(N_{1,5}) = 5.3$ G (2N). As mentioned, the EPR spectra of the isopropyl substituted verdazyl radicals are all similar, and the g -value is comparable to the values found in literature.^{81,82}

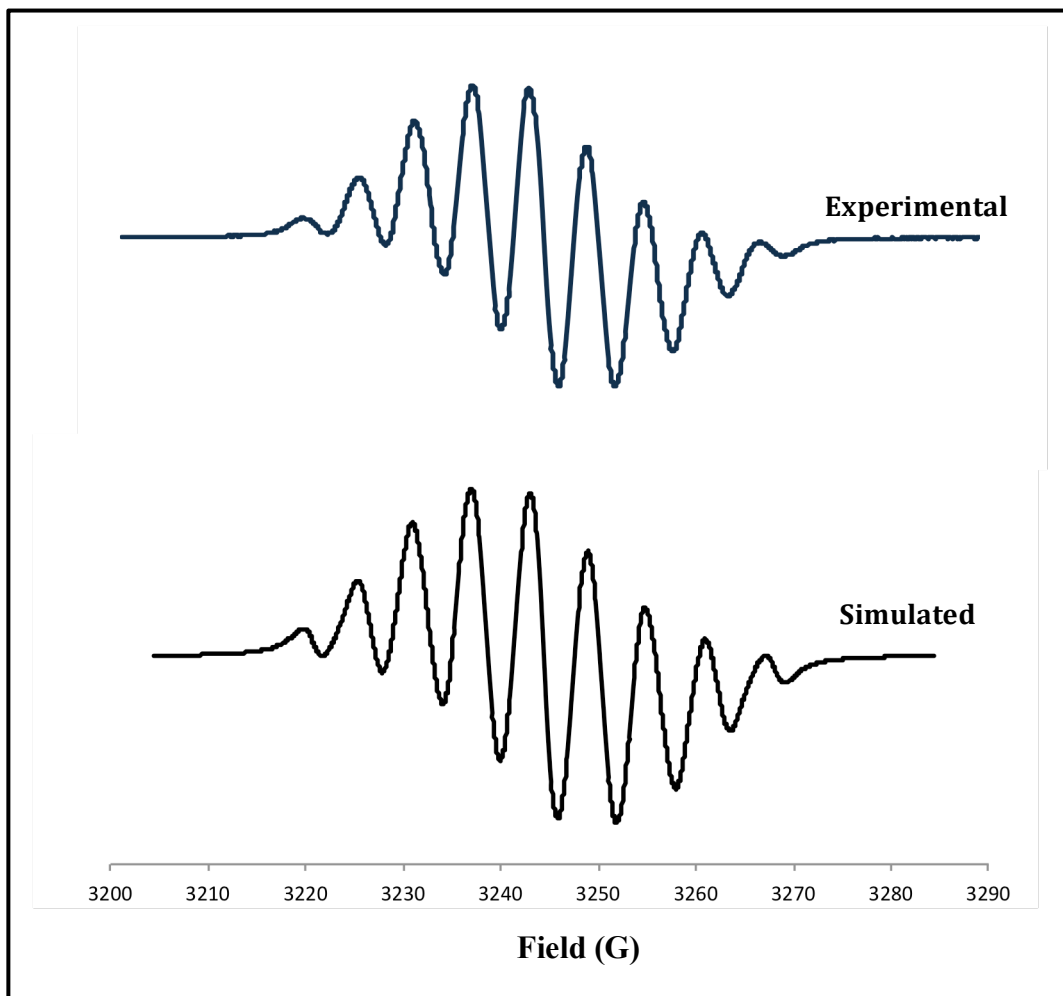


Figure 2.14 Experimental EPR spectrum of compound **2.11** recorded at room temperature ($\nu = 9086$ μHz , microwave power = 1 mw) (top) and simulated spectrum (bottom)

2.5 Summary

All radical precursors have been characterized using classical analytical techniques such as ^1H , ^{13}C NMR, FT-IR, and mass spectroscopy (see experimental section). Verdazyl radicals **2.6** and **2.11** have been successfully prepared in a good yield and characterized using EPR and FT-IR spectroscopies. These radicals are very stable in air and in the presence of organic solvent.

The electrochemical behaviour of verdazyl radicals **2.6** and **2.11**, and their precursors will be examined in Chapter 3.

2.6 Experimental Section

2.6.1 Generalities

Unless stated otherwise, all reactions and manipulations were carried out under an argon atmosphere. Solvents were dried over activated molecular sieves (4 Å), and distilled under an atmosphere of argon prior to use. All reagents were purchased from Sigma-Aldrich and used as received. ¹H proton (and ¹³C carbon) NMR spectra were recorded on a 200 MHz Varian NMR spectrometer and 500 MHz Bruker spectrometer. The NMR samples were prepared by dissolving 20 mg of product in 1 mL of deuterated solvent (DMSO-d₆ or CDCl₃). IR spectra were recorded as KBr pellets using a Bruker Fourier-transform infrared spectrophotometer. EPR spectra were recorded using a Varian E109 EPR Spectrometer. The EPR samples were subjected to a number of freeze-thaw cycles on a vacuum line prior to analysis. The EPR spectra were simulated using the WINSIM program. HRMS experiments were recorded on an Agilent 1260 Infinity liquid chromatograph/6530 accurate mass Q-TOF in high resolution mode in 70:30 acetonitrile/water using positive mode electrospray ionization (HPLC grade solvents).

2.6.2 Synthesis of 2, 4-diisopropyl-6-terthiophene-3-oxotetrazane (2.5)

0.499 g (1.8 mmol) of 2, 4-diisopropylcarbonohydrazide bis-hydrochloride (**2.4**) and 0.382 g (1.8 mmol) of 2,2':5',2''-terthiophene-3'-carboxaldehyde (**2.3**) were dissolved in 10 mL of dry ethanol. To this mixture was added 0.295 g (3.8 mmol) of sodium acetate in ethanol. The solution was left standing at room temperature. The reaction was followed by TLC after 24 hours. The mixture was filtered and evaporated to get the crude product. The purification of the residue by a silica gel column chromatography with 40 % ethyl ether and 60 % CH₂Cl₂ as eluent gave the tetrazane (**2.5**) (R_F = 0.43) as a yellow solid (0.305 g, 0.71 mmol). Yield: 40 %; ¹H NMR (DMSO-d₆, 500 MHz): δ(ppm) = 0.95 (d, *J* = 6.4 Hz, 6H, -C(CH₃)₂), 1.01 (d, *J* = 6.7 Hz, 6H, -C(CH₃)₂), 4.45 (m, 2H, CH(CH₃)₂), 4.56 (t, *J* = 11.5 Hz, 1H, CH-N), 5.25 (d, *J* = 11.5 Hz, 2H, NH), 7.12 (dd, *J* = 3.7 Hz, 1H, Th-H), 7.18 (dd, *J* = 3.7 Hz, 1H, Th-H), 7.29-7.35 (m, 2H, Th-H), 7.56 (d, *J* = 4.7 Hz, 1H, Th-H), 7.60 (s, 1H, Th-H), 7.69 (d, *J* = 4.9 Hz, 1H, Th-H). ¹³C NMR (DMSO-d₆, 500 MHz): δ(ppm) = 18.7, 19.5, 46.7, 67.5, 124.0, 124.6, 126.2, 127.6, 128.0, 128.2,

128.5, 131.9, 133.0, 134.2, 135.5, 135.6, 153.0. IR (KBr pellet); $\nu(\text{cm}^{-1}) = 1607$ (CO ketone). HRMS (ESI) for $\text{C}_{20}\text{H}_{24}\text{N}_4\text{OS}_3$ $[\text{MH}^+]$: calcd. 433.1190; found 433.1186.

2.6.3 Synthesis of 1,5-diisopropyl-3-terthiophene-6-oxoverdazyl (2.6)

0.100 g (0.23 mmol) of 2, 4-diisopropyl-6'-terthiophene-3-oxotetrazane (**2.5**) and 0.037 g (0.345 mmol) of benzoquinone were refluxed in 5 mL of toluene. The reaction was followed by TLC after 3 hours. The mixture was cooled, filtered and the solvent removed by evaporation to get the crude product. Pure **2.6**, a red oil, was obtained by eluting the residue through a silica gel column using 100% CH_2Cl_2 ($R_F = 0.43$) as the eluent. Yield: 70 %; IR (KBr pellet); $\nu(\text{cm}^{-1}) = 1680$ (CO ketone). HRMS (ESI) for $\text{C}_{20}\text{H}_{21}\text{N}_4\text{OS}_3$ $[\text{M}^+]$: calcd. 429.0877; found 429.0870.

2.6.4 Synthesis of 6-(2,5-dibromo-thiophene-3-yl)pyridine-2-carboxaldehyde (2.8)

0.371 g (1.9 mmol) of 6-(3-thienyl)pyridine-2-carboxaldehyde (**2.7**) was dissolved in 5 mL of N,N-dimethylformamide (DMF) in a round bottom flask. Under low light, 1.325 g (7.44 mmol) of N-bromosuccinimide (NBS) was added to the mixture. The mixture was left at room temperature and the progression of the reaction was followed by TLC. After 3 hours, 100 mL of dichloromethane (CH_2Cl_2) was added to the mixture. The organic layer was washed 6 times with 100 mL of distilled water and extracted. The organic layer was then dried with magnesium sulfate (MgSO_4). The solvent was evaporated using a rotary evaporator. The product was purified by silica gel column chromatography using CH_2Cl_2 ($R_F = 0.68$) as the eluent. After evaporation of the solvent, the product was a white solid. Yield: 50 %; ^1H NMR (CDCl_3 , 500 MHz); $\delta(\text{ppm}) = 7.47$ (s, 1H, Th-*H*), 7.90 (m, 2H, Py-*H*), 8.08 (d, $J = 5.0$ Hz, 1H, Py-*H*), 10.02 (s, 1H, CHO). ^{13}C NMR (CDCl_3 , 500 MHz): $\delta(\text{ppm}) = 110.2, 111.9, 120.3, 126.7, 131.9, 137.6, 139.8, 152.4, 152.6, 193.2$. IR (KBr pellet); $\nu(\text{cm}^{-1}) = 1704$ (CO aldehyde). HRMS (ESI) for $\text{C}_{10}\text{H}_5\text{Br}_2\text{NOS}$ $[\text{MH}^+]$: calcd. 345.8536; found 345.8529.

2.6.5 Synthesis of 6-[2, 2': 5', 2'']terthiophen-3'-ylpyridine-2-carboxaldehyde (2.9)

0.615 g (1.77 mmol) of 6-(2,5-dibromo thiophene-3-yl)pyridine-2-carboxaldehyde (**2.8**), 1.980 g (5.31 mmol) of 2-tributylstannyl thiophene, 0.265 g (0.23 mmol) of tetrakis(triphenylphosphine)palladium(0) $\text{Pd}(\text{PPh}_3)_4$ were added to 15 mL of toluene,

which had been dried over molecular sieves and degassed for 1 hour with N₂. The mixture was allowed to stir for 24 hours at 100°C. The progression of the reaction was followed by TLC. After 24 hours, the reaction mixture was filtered through celite (SiO₂) to remove the catalyst. 100 mL of CH₂Cl₂ was added to the mixture and then washed two times with 100 mL portions of a cesium fluoride solution (5%), and five times with 100 mL portions of distilled water. The organic layer was dried over magnesium sulfate (MgSO₄) and the CH₂Cl₂ was removed using a rotary evaporator. The product was purified by silica gel column chromatography using a solvent system of 20 % of pentane and 80 % of CH₂Cl₂ (R_F = 0.46). The yellow fluorescent product was obtained after evaporation of the solvent. Yield: 58 %; ¹H NMR (CDCl₃, 500 MHz); δ(ppm) = 7.04 (dd, *J* = 5.0 Hz, 1H, Th-*H*), 7.08 (dd, *J* = 5.0 Hz, 1H, Th-*H*), 7.12 (d, *J* = 5.0 Hz, 1H, Th-*H*), 7.25-7.31 (m, 2H, Th-*H*), 7.33 (d, *J* = 5.0 Hz, 1H, Th-*H*), 7.55-7.61 (m, 2H, Th-*H* & Py-*H*), 7.81 (dd, *J* = 10.0 Hz, 1H, Py-*H*), 7.92 (d, *J* = 10.0 Hz, 1H, Py-*H*), 10.65 (s, 1H, CHO). ¹³C NMR (CDCl₃, 500 MHz): δ(ppm) = 120.0, 124.3, 125.1, 126.1, 127.0, 127.6, 127.8, 128.0, 128.1, 132.9, 134.4, 136.3, 136.8, 137.3, 137.6, 154.6, 155.0, 193.4. IR (KBr pellet); ν(cm⁻¹) = 1716 (CO aldehyde). HRMS (ESI) for C₁₈H₁₁NOS₃ [MH⁺]: calcd. 354.0081; found 354.0076.

2.6.6 Synthesis of 2, 4-diisopropyl-6-terthiophene-3'-pyridine-2-yl-3-oxotetrazane (2.10)

0.200 g (0.560 mmol) of 2, 4-diisopropylcarbonohydrazide bis-hydrochloride (**2.4**) and 0.119 g (0.560 mmol) of 6-[2, 2': 5', 2'']terthiophen-3'-ylpyridine-2-carboxaldehyde (**2.9**) were dissolved in 10 mL of ethanol. To this mixture 1.13 mmol of sodium acetate in ethanol was added. The solution was allowed to stand at room temperature. The reaction was followed by TLC. After 24 hours, the mixture was filtered and evaporated to get the crude product as a yellow solid. The residue was purified by a silica gel column chromatography. Tetrazane was eluted with a 30 % diethyl ether and 70 % CH₂Cl₂ (R_F = 0.58) solvent mixture. Yield: 43 %; ¹H NMR (CDCl₃, 500 MHz); δ(ppm) = 1.25 (d, *J* = 10.0 Hz, 6H, -C(CH₃)₂), 1.35 (d, *J* = 10.0 Hz, 6H, -C(CH₃)₂), 4.70 (m, 2H, -CH(CH₃)₂), 4.80 (s, 1H, CH-N), 7.04 (dd, *J* = 5.0 Hz, 1H, Th-*H*), 7.05-7.10 (m, 2H, Th-*H*), 7.25-7.30 (m, 2H, Th-*H*), 7.34 (d, *J* = 5.0 Hz, 1H, Th-*H*), 7.44 (d, *J* = 10.0 Hz, 1H, Py-*H*), 7.51 (d, *J* = 10.0 Hz, 1H, Py-*H*), 7.55 (s, 1H, Th-*H*), 7.81 (dd, *J* = 5.0 Hz, 1H, Py-*H*). ¹³C NMR

(CDCl₃, 500 MHz): δ (ppm) = 18.7, 19.5, 47.7, 70.8, 122.1, 124.1, 124.3, 125.1, 125.2, 125.5, 126.0, 126.8, 126.9, 127.5, 127.9, 128.0, 133.3, 134.7, 136.1, 137.0, 138.6, 153.1. IR (KBr pellet); ν (cm⁻¹) = 1649 (CO ketone). HRMS (ESI) for C₂₅H₂₇N₅OS₃ [MH⁺]: calcd. 510.1456; found 510.1455.

2.6.7 Synthesis of 1,5-diisopropyl-3-terthiophene-3'-pyridine-2-yl-6-oxoverdazyl (2.11)

0.050 g (0.098 mmol) of 2,4-diisopropyl-3-terthiophene-3'-pyridine-2-yl-3-oxotetrazane (**2.10**) and 0.016 g (0.147 mmol) of benzoquinone were refluxed in 5 mL of toluene. The reaction was followed by TLC. After 3 hours, the mixture was cooled, filtered and evaporated to give the crude product. The purification of the residue by a silica gel column chromatography with 100 % CH₂Cl₂ (R_F = 0.47) as the eluent produced **2.11** as a red oily product. Yield: 70 %; IR (KBr pellet); ν (cm⁻¹) = 1686 (CO ketone). HRMS (ESI) for C₂₅H₂₄N₅OS₃ [MH⁺]: calcd. 507.1221; found 507.1247.

Chapter 3. Electropolymerization of Terthiophene Bearing a Verdazyl Radical

3 Introduction

3.1 Cyclic Voltammetry

Cyclic voltammetry (CV) is a powerful electroanalytical technique that provides extensive thermodynamic and kinetic information on redox processes. Moreover, CV has the ability to elucidate mechanisms of electrochemical/chemical reactions occurring at the surface of the electrode. A CV experiment is performed in a three-electrode cell, which involves a working electrode (WE), a counter electrode (CE), and a reference electrode (RE) (Figure 3.1). An external potential is applied to the cell. Using a potentiostat combined with a three-electrode system, the potential of the working electrode is controlled relative to the reference electrode and the current is measured between working electrode and the counter electrode.

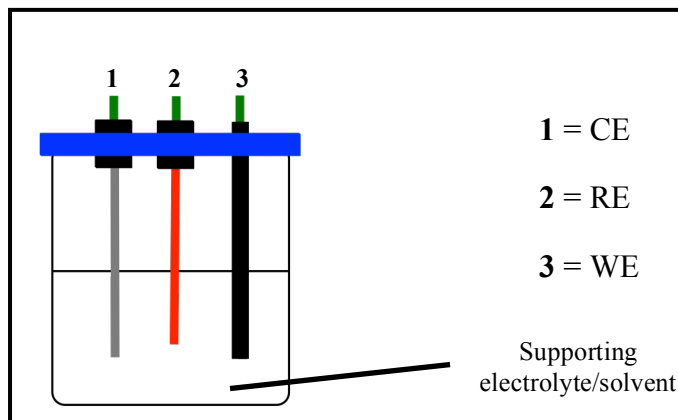


Figure 3.1 Components of an electrochemical cell

The supporting electrolyte (commonly alkali or tetraalkylammonium salts with perchlorate or hexafluorophosphate) is dissolved in a non-aqueous organic solvent such as CH_3CN , CH_2Cl_2 , and DMF.⁸⁸

The redox system can be reversible, quasi-reversible, and irreversible. In a reversible system, the oxidized and reduced species at the electrode surface must be found at

concentrations required by the Nernst equation.⁸⁹ The peak current (i_p) is given by the Randles-Sevcik equation for a redox reaction at 25°C.^{90,91}

$$i_p = (2.69 \times 10^5) n^{3/2} A C D^{1/2} v^{1/2} \quad \text{Equation 3.1}$$

where n is the number of electrons, A is the surface area of the electrode (cm^2), C is the concentration (mol/cm^3), D is the diffusion coefficient (cm^2/s), and v is the scan rate (V/s).

The main characteristics of a reversible system in CV are:

1. The ratio of anodic and cathodic peak currents is equal to one.
2. The separation between the peak potentials has to be $59/n$ mV per number of electron as shown in equation 3.2.

$$\Delta E = E_p^a - E_p^c = 59/n \text{ mV} \quad \text{Equation 3.2}$$

For a one electron reversible system, the theoretical peak separation value is 59 mV; however, the experimentally accepted separation of peak potentials for a reversible system lies between 60 and 70 mV (Figure 3.2).⁹⁰

The standard potential of a reversible redox couple can also be determined from CV between the anodic and cathodic peak potentials (equation 3.3).

$$E^\circ = (E_p^a + E_p^c) / 2 \quad \text{Equation 3.3}$$

Reactions with slow electron transfer (quasi-reversible, Figure 3.3) or those that are coupled with a chemical reaction (irreversible, Figure 3.4) do not exhibit the same characteristics as a reversible redox system. In the case of a quasi-reversible process, the difference between the peak anodic and cathodic potential is greater than 59 mV for a mono-electronic system, at room temperature. For an irreversible system, a single peak potential in the CV is observed, where the electron transfer is extremely slow or coupled with a chemical reaction.⁹²

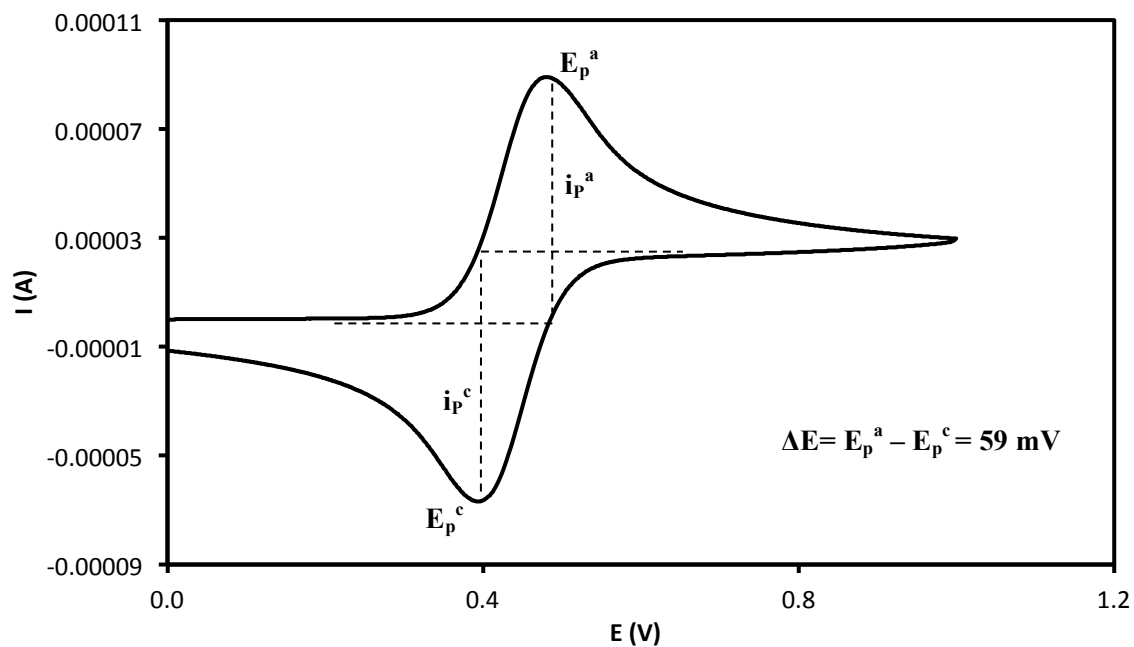


Figure 3.2 Cyclic voltammetry of a reversible system

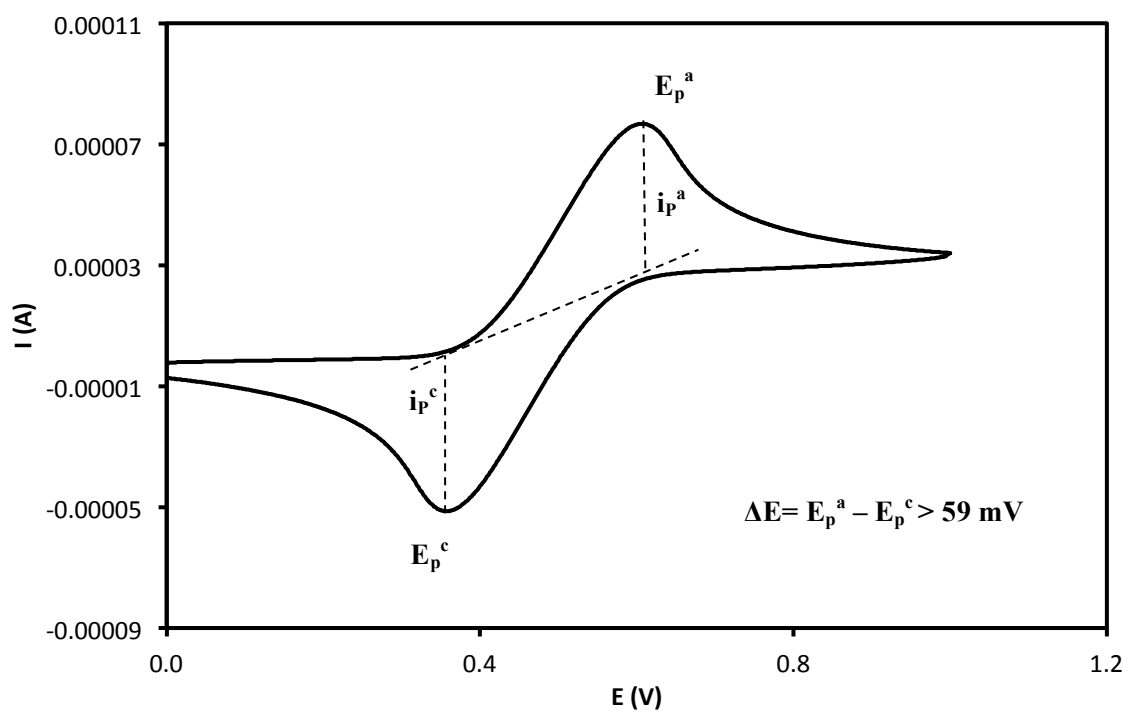


Figure 3.3 Cyclic voltammetry of a quasi-reversible system

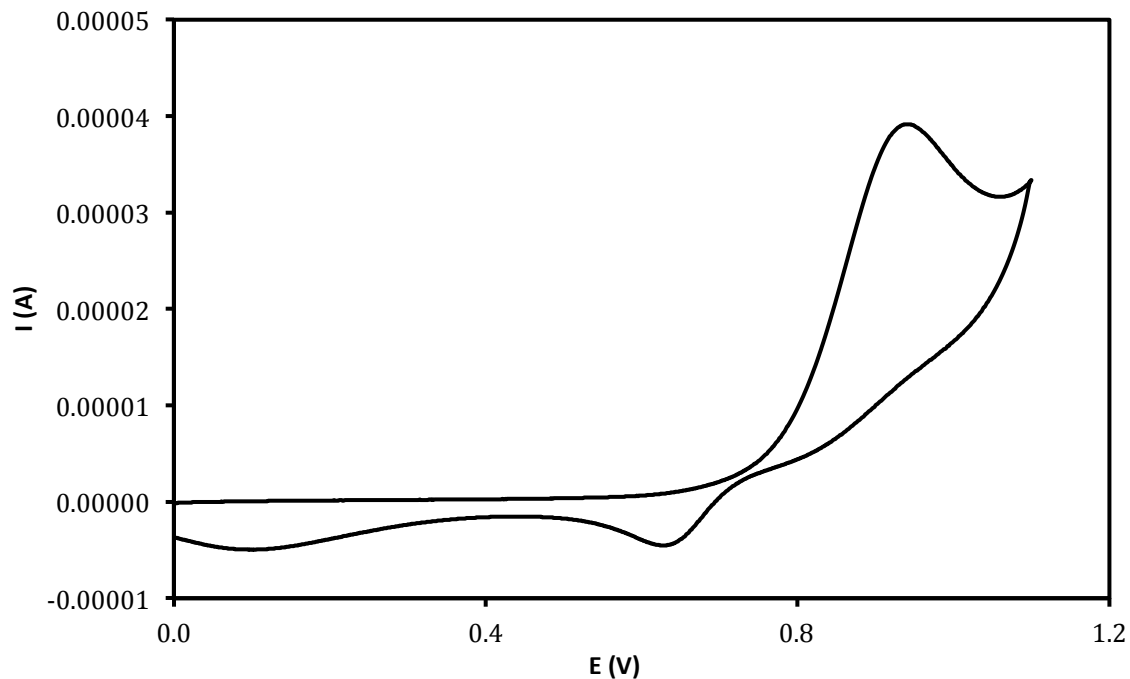


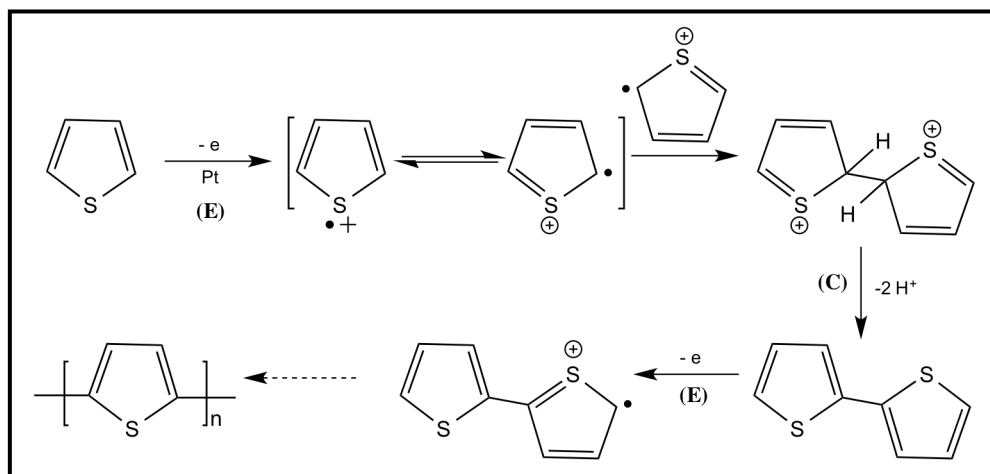
Figure 3.4 Cyclic voltammetry of an irreversible system

3.2 Electropolymerization

The mechanism of the electropolymerization process of thiophene oligomers is explained by an EC reaction,⁹³ which involved an initial electron transfer (E), followed by a chemical reaction (C). In the electrochemical polymerization process several EC cycles are required for the formation of the final polymer.⁹⁴

The monomer is oxidized at the electrode surface to form the corresponding radical cation, which is further dimerized to form a product (Dimer). It is a chain reaction process that affords a dimer, trimer, tetramer, etc, leading to the final corresponding polymer.⁹⁴

The electropolymerization mechanism of heterocyclic compounds was suggested by Díaz *et al.*⁹⁵ based on their work on the oxidation of pyrrole. The mechanism is known as the radical cation - radical cation (RC-RC) coupling mechanism and is depicted in Scheme 3.1 for thiophene.



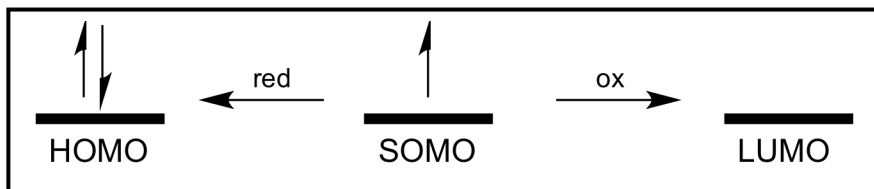
Scheme 3.1 General mechanism of electropolymerization via radical cation-radical cation (RC-RC) coupling

In this mechanism, the first step is the oxidation of thiophene to give the radical cation. This reactive radical cation reacts with another radical cation in the solution to form a dimer dication, which subsequently loses two protons to form the stable neutral dimer. This neutral dimer can also be oxidized to produce the corresponding radical cation dimer that can couple with another radical cation in solution to give a trimer. This process continues until the external potential is removed.⁹⁵

3.3 Electrochemical Properties of Stable Radicals

As mentioned in Chapter 1, the families of stable radicals are used in many applications associated with their unpaired electron(s). The redox properties of stable radicals are related to their use: i) in electron-transfer chemistry,⁹⁶⁻⁹⁸ ii) as building blocks for single-component molecular conductors,⁹⁹⁻¹⁰¹ and iii) their use in organic-based batteries.¹⁰²⁻¹⁰⁸

The electrochemical properties of open shell molecules are different than closed shell molecules. In closed shell molecules, the oxidation process involves the loss of an electron from the highest occupied molecular orbital (HOMO), while the reduction process involves the addition of an electron to the lowest unoccupied molecular orbital (LUMO). However, in the open shell molecules, oxidation and reduction processes involve the loss or gain of an electron from the singly occupied molecular orbital (SOMO) as shown in Scheme 3.2.¹⁰⁹



Scheme 3.2 Oxidation and reduction of neutral radical

3.4 Electrochemistry of Verdazyl Radical

We prepared monomers **2.3**, **2.5**, **2.9** and **2.10** and the two 6-oxoverdazyl radicals functionalized terthiophenes **2.6** and **2.11** as shown below. In this chapter, we will investigate the electrochemical behavior of these monomers, along with the characteristics of the resulting films. The redox properties of all monomers were studied using cyclic voltammetry. Table 3.1 summarizes the oxidation peak potentials of the prepared monomers and their corresponding polymers. These oxidation potentials were calculated versus an internal reference (ferrocene/ferrocenium redox couple).

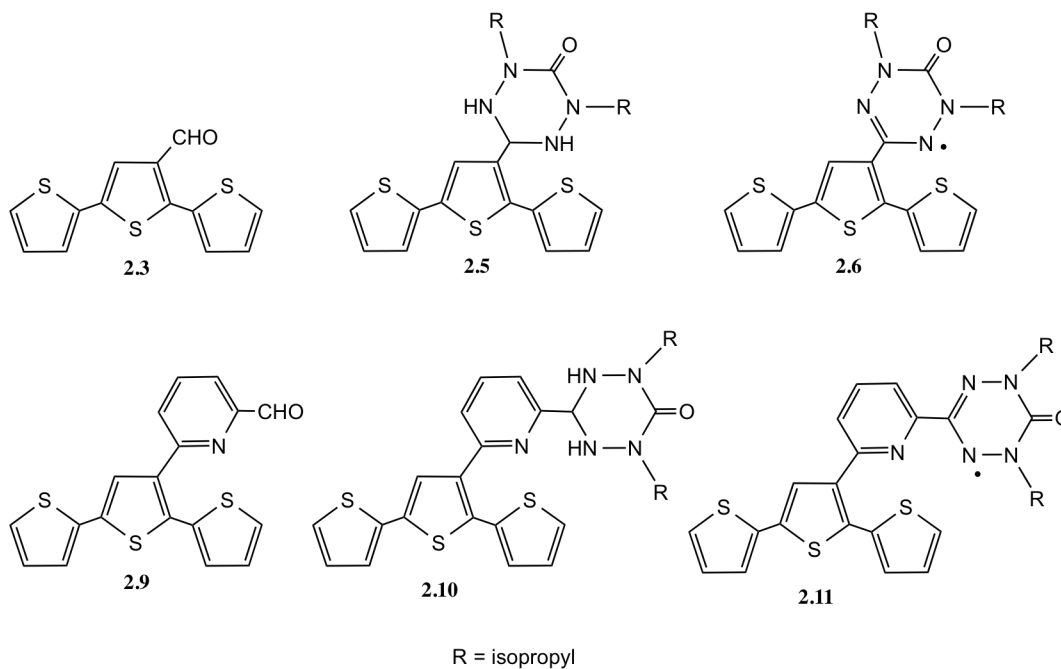


Table 3.1 Electrochemical properties of prepared terthiophene monomers and their corresponding polymers in ACN. [Scan rate of 0.1 V/s, WE = Platinum electrode, RE = Silver wire, and CE = Platinum wire]

Compound	E^1_p or $[E^1_{1/2}]$ (V vs. Fc^+/Fc) \pm 0.02 V	E^2_p or $[E^2_{1/2}]$ (V vs. Fc^+/Fc) \pm 0.02 V
2.3	-	0.80*
2.5	0.52*	0.97*
2.6	[0.16]**	0.87*
2.9	-	0.72*
2.10	0.78*	0.92*
2.11	[0.25]**	0.73*
Poly(2.3) – Pt	-	[0.63]**
Poly(2.5) – Pt	[0.15]**	[0.73]**
Poly(2.6) – Pt	[0.28]**	[0.76]**
Poly(2.9) – Pt	-	[0.61]**
Poly(2.10) – Pt	-	-
Poly(2.11) – Pt	-	-

E^1_p : Oxidation peak potential of tetrazane/verdazyl radical component

E^2_p : Oxidation peak potential of terthiophene component

* First scan

** Reversible system

The reasons behind using terthiophenes rather than monothiophenes are:

- i. Terthiophene has a lower oxidation potential.
- ii. Their corresponding polymers are more stable.
- iii. Their corresponding polymers are highly conducting.

Efforts were made to oxidatively electropolymerize all monomers in a 1 M n-Bu₄NPF₆/ACN solution. This was done through repeated CV cycling beyond the oxidation peak potential of the terthiophene component of each monomer. All monomers **2.3**, **2.5**, **2.6**, **2.9**, **2.10**, and **2.11** were successfully deposited on the surface of the platinum electrode. The electrochemical behaviors of poly(**2.5**) and poly(**2.6**) were also studied using CV. However, poly(**2.10**) and poly(**2.11**) were not stable enough on the surface of the platinum electrode preventing their characterization with CV. The 20 scan electropolymerization CVs of terthiophene-3'-carboxaldehyde species, **2.3** and **2.9** are depicted in Figure 3.5 and Figure 3.6, respectively. During the oxidation process the peak current increases with each successive scan, which indicates the formation of a polymer film on the surface of the platinum electrode. In both curves the first scan is irreversible and in the second scan a new peak starts to develop at a lower oxidation potential, which corresponds to the oxidation potential of the polymer. The oxidation potential of the polymer occurs at lower oxidation potential than its corresponding monomer due to the increase in its length of conjugation.

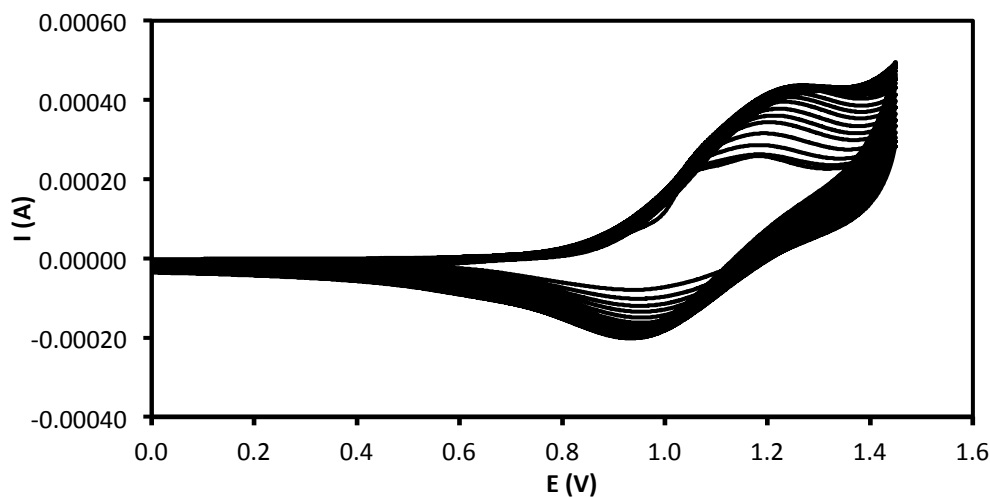


Figure 3.5 A 20 scan electrochemical oxidation of **2.3** in ACN. [Scan rate = 0.1 V/s, WE = Platinum electrode, RE = Silver wire, and CE = Platinum wire]

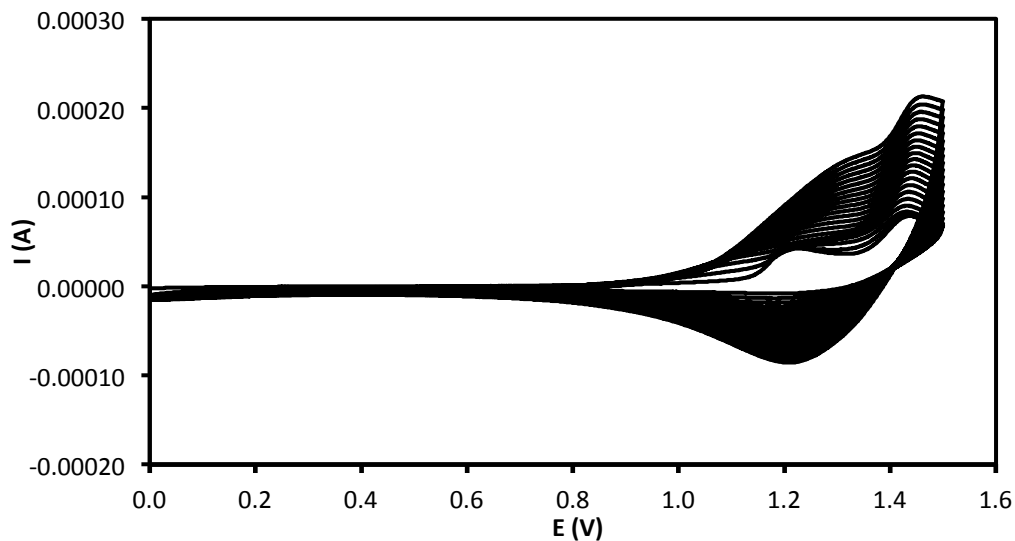


Figure 3.6 A 20 scan electrochemical oxidation of **2.9** in ACN. [Scan rate = 0.1 V/s, WE = Platinum electrode, RE = Silver wire, and CE = Platinum wire]

The electrochemical oxidation of terthiophene bearing 2,4-diisopropyl-3-oxotetrazane, **2.5**, was carried out in a 1 M n-Bu₄NPF₆/ACN solution. The first CV scan of tetrazane **2.5** is depicted in Figure 3.7. Once the anodic potential is applied, both terthiophene and tetrazane are oxidized. From this CV, there are two irreversible peaks in the initial scan. The first peak at 0.52 V (vs. Fc⁺/Fc) corresponds to the oxidation of tetrazane to its radical.

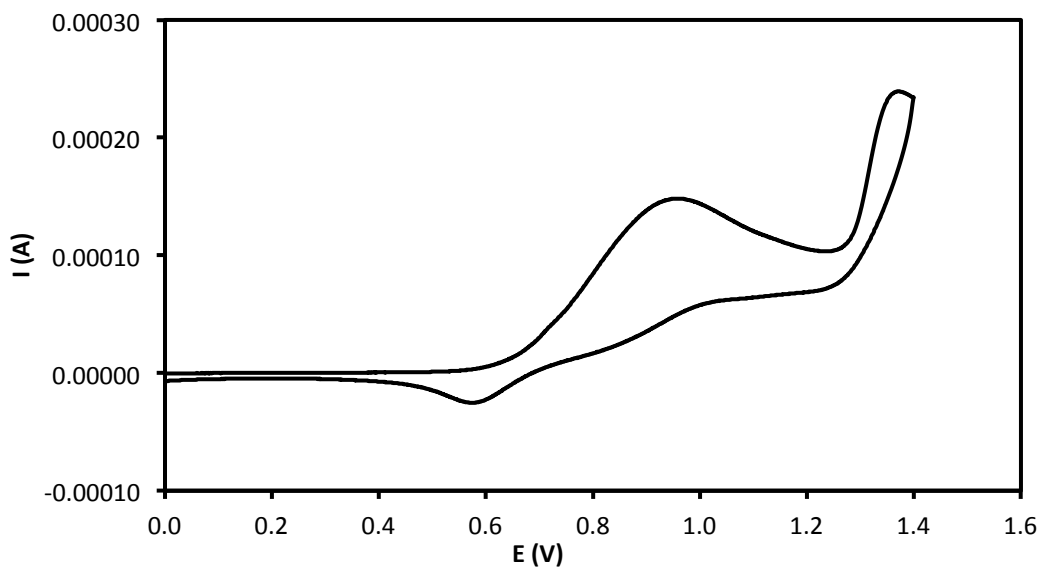
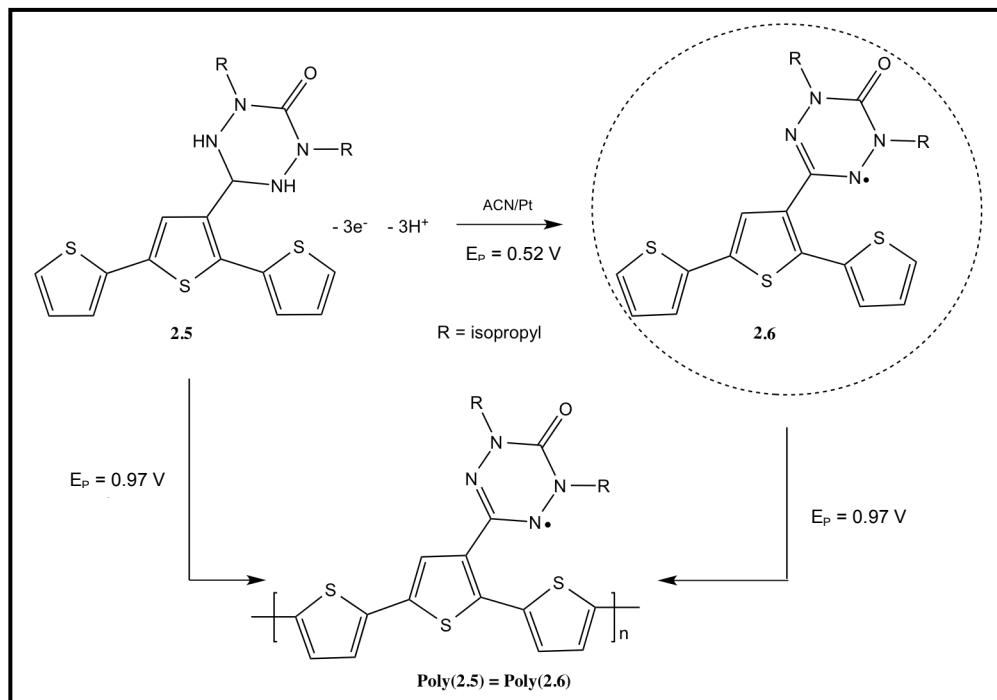


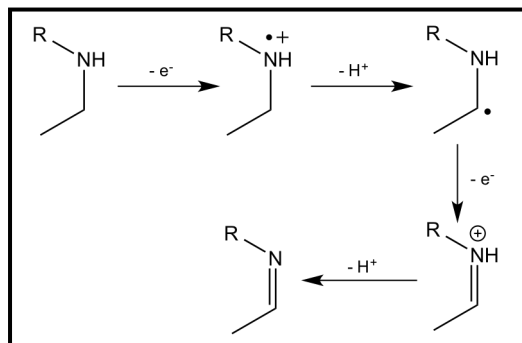
Figure 3.7 The first CV scan of **2.5** in ACN. [Scan rate = 0.1 V/s, WE = Platinum electrode, RE = Silver wire, and CE = Platinum wire]

The peak potential, 0.52 V (vs. Fc^+/Fc), (Figure 3.7) is very broad because there are many electrochemical and chemical reactions occurring at this potential. Until now the mechanism has not been investigated. The second peak at 0.97 V (vs. Fc^+/Fc) corresponds to the oxidation of terthiophene to form poly(terthiophene) (see Scheme 3.3).



Scheme 3.3 Electrochemical oxidation of terthiophene bearing 2,4-diisopropyl-3-oxotetrazane **2.5**

The mechanism of the electrochemical oxidation of amines has been previously investigated.¹¹⁰⁻¹¹² According to the literature, a general mechanism for the oxidation of amines to its radical is presented in Scheme 3.4.¹¹¹ The first step shows the oxidation of the amine to form its radical cation. The radical cation is deprotonated to produce a radical.



Scheme 3.4 Mechanism of the oxidation of aliphatic amines

Figure 3.8 shows a 10 scan electrochemical oxidation of the tetrazane **2.5**. It has been successfully oxidatively electropolymerized to form its corresponding polymer, poly(**2.5**). This CV displays an increase in peak current during the oxidation process, with each successive scan indicating the formation of a polymer film on the surface of the platinum electrode. As mentioned before (Figure 3.7), there are two main irreversible peaks in the first scan of monomer **2.5**. However, during the oxidation process, (i.e. electropolymerization of monomer **2.5**), a new reversible peak was observed at 0.15 V (vs. Fc^+/Fc). This reversible oxidation peak (in Figure 3.8) corresponds to the formation of verdazyl radical by the electrochemical oxidation of tetrazane. During the oxidation process of monomer **2.5**, the tetrazane is converted to verdazyl radical **2.6** (it was not isolated) through the electrochemical oxidation reaction at 0.52 V (vs. Fc^+/Fc). Scheme 3.3 explains the conversion of tetrazane to verdazyl radical by the electrochemical oxidation reaction.

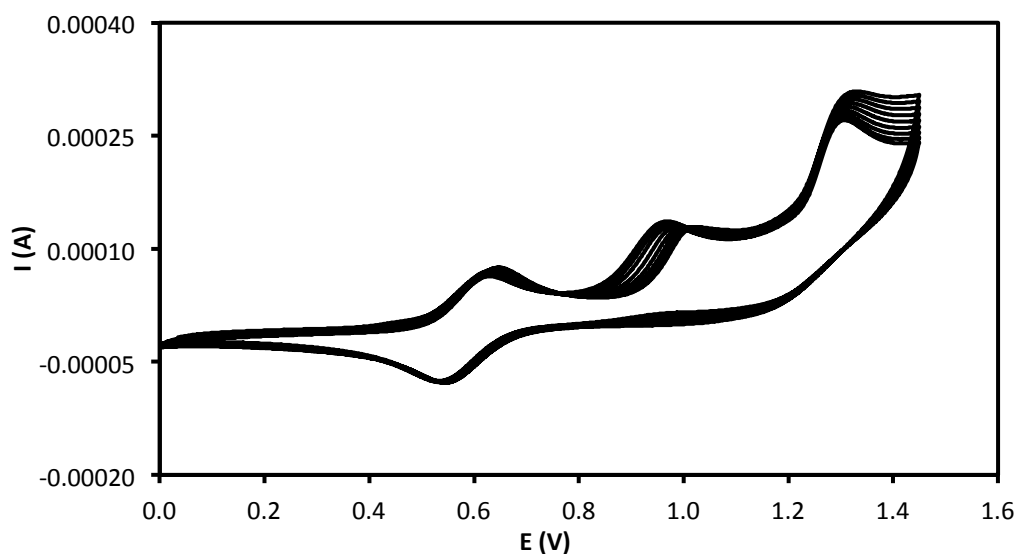


Figure 3.8 A 10 scan electrochemical oxidation of **2.5** in ACN. [Scan rate = 0.1 V/s, WE = Platinum electrode, RE = Silver wire, and CE = Platinum wire]

The electrochemical properties of the verdazyl radical **2.6** were studied using a 1 M $n\text{-Bu}_4\text{NPF}_6/\text{ACN}$ solution. The cyclic voltammogram (CV) of **2.6** is depicted in Figure 3.9. The first CV scan displays two peaks. The first reversible peak at about 0.16 V (vs. Fc^+/Fc) corresponds to the oxidation of verdazyl radical and it is in agreement with values reported in literature.¹¹³ The reversibility of this peak shows the stability of the

cationic species **2.6 π** (see Scheme 3.5). The second irreversible peak at 0.87 V (vs. Fc⁺/Fc) corresponds to the oxidation of terthiophene to form the corresponding polymer.

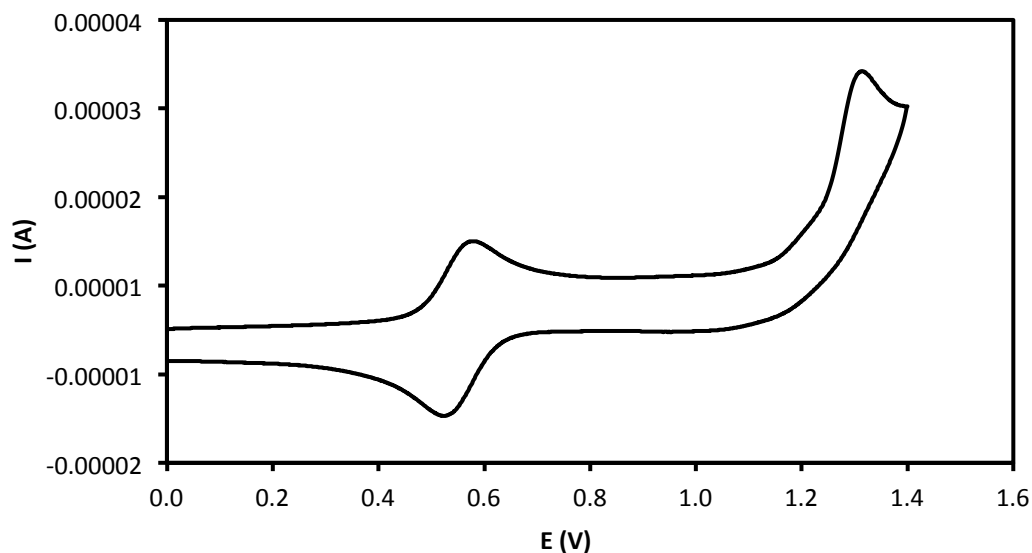
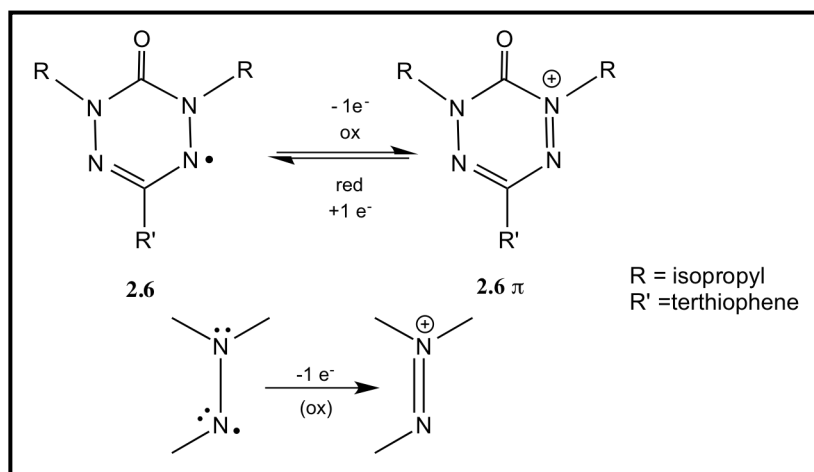


Figure 3.9 The first CV scan of **2.6** in ACN. [Scan rate = 0.1 V/s, WE = Platinum electrode, RE = Silver wire, and CE = Platinum wire]



Scheme 3.5 Electrochemical oxidation of verdazyl **2.6**

The electropolymerization of the 1,5-diisopropyl-6-oxoverdazyl radical functionalized terthiophene monomer **2.6** was successfully done in a 1 M n-Bu₄NPF₆/ACN solution through repeated CV cycling as depicted in Figure 3.10. Through the oxidation process of the verdazyl **2.6**, the peak current increases with each consecutive scan resulting in the formation of the polymer film on the surface of platinum electrode (see Scheme 3.6).

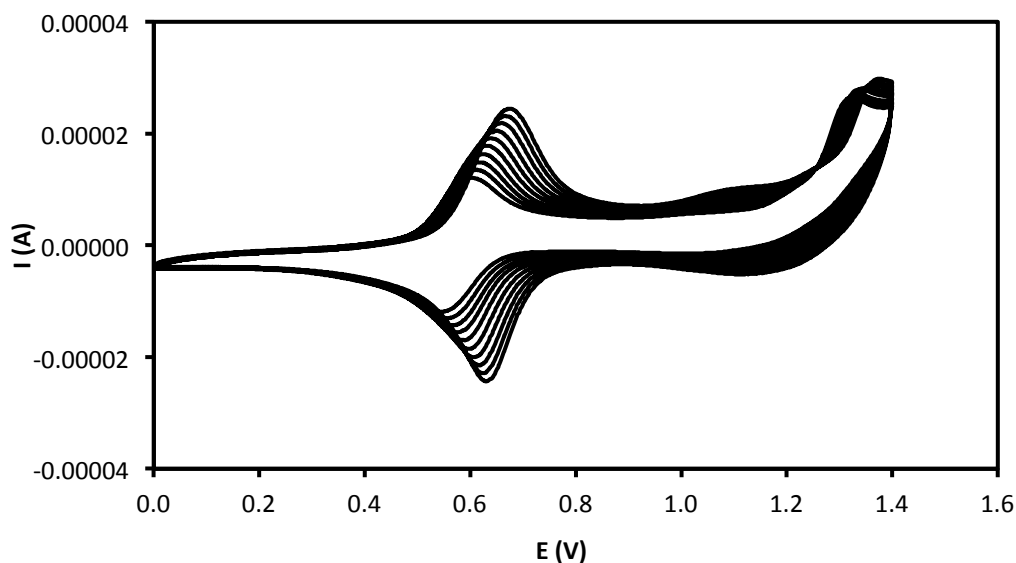
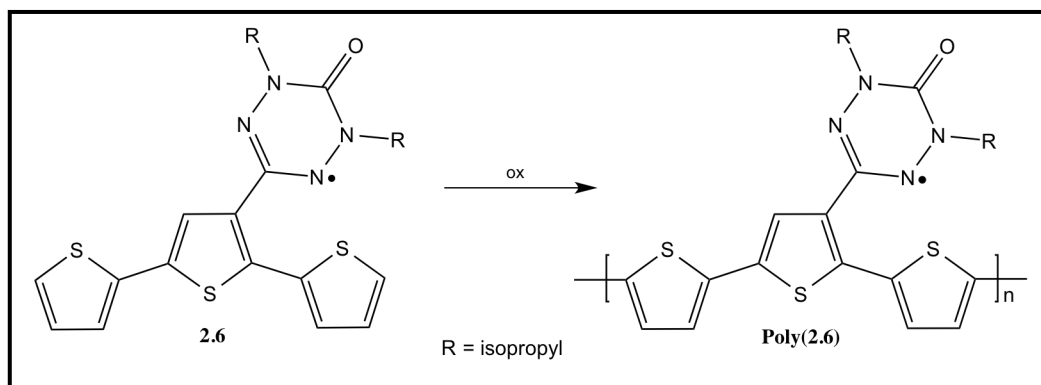


Figure 3.10 A 10 scan electrochemical oxidation of **2.6** in ACN. [Scan rate = 0.1 V/s, WE = Platinum electrode, RE = Silver wire, and CE = Platinum wire]

As the number of scans increases, there are many things to notice (Figure 3.10):

1. The formation of new peak at lower oxidation potential (0.76 V vs. Fc^+/Fc) than that of the monomer (0.87 V vs. Fc^+/Fc), which corresponds to the oxidation potential of the poly(terthiophene).
2. The reversible peak at 0.16 V (vs. Fc^+/Fc), related to the oxidation of verdazyl radical, shifts to higher oxidation potential (0.28 V, vs. Fc^+/Fc) than the initial scan. This positive shift is due to the geometry of the poly(terthiophene) backbone no longer being planar. The loss of the planarity in doped polymer improves the localization of the spin on the heterocyclic tetrazane, which explain the positive shift of the oxidation potential of verdazyl in poly(**2.6**)-Pt.



Scheme 3.6 Formation of poly(terthiophene) bearing verdazyl radical

CV and IR were used to characterize the corresponding polymers poly(**2.5**) and poly(**2.6**). Figures 3.11 and 3.12 illustrate the first CV scan of poly(**2.5**) and poly(**2.6**), in a monomer-free solution. Both CVs exhibit two reversible oxidation peaks. The first peak at 0.15 V for poly(**2.5**) and 0.28 V for poly(**2.6**) (vs. Fc^+/Fc) corresponds to the oxidation potential of the verdazyl radical and the second peak at 0.731 V for poly(**2.5**) and 0.76 V for poly(**2.6**) (vs. Fc^+/Fc) relates to the oxidation potential of poly(terthiophene). Due to the increase in the length of conjugation (electronic delocalization of the π -system), the oxidation potential of the poly(terthiophene) (0.73 V and 0.76 V) is lower than the monomer (0.97 V and 0.87 V).¹¹⁴⁻¹¹⁶ Moreover, the broad irreversible peak of the tetrazane has disappeared (Figure 3.11), (i.e. no irreversible peak at 0.52 V), which confirms that the tetrazane is completely oxidized to form the verdazyl radical. From this result, we conclude that the polymers formed from the electrochemical oxidation of tetrazane **2.5** and verdazyl radical **2.6** have the same structure.

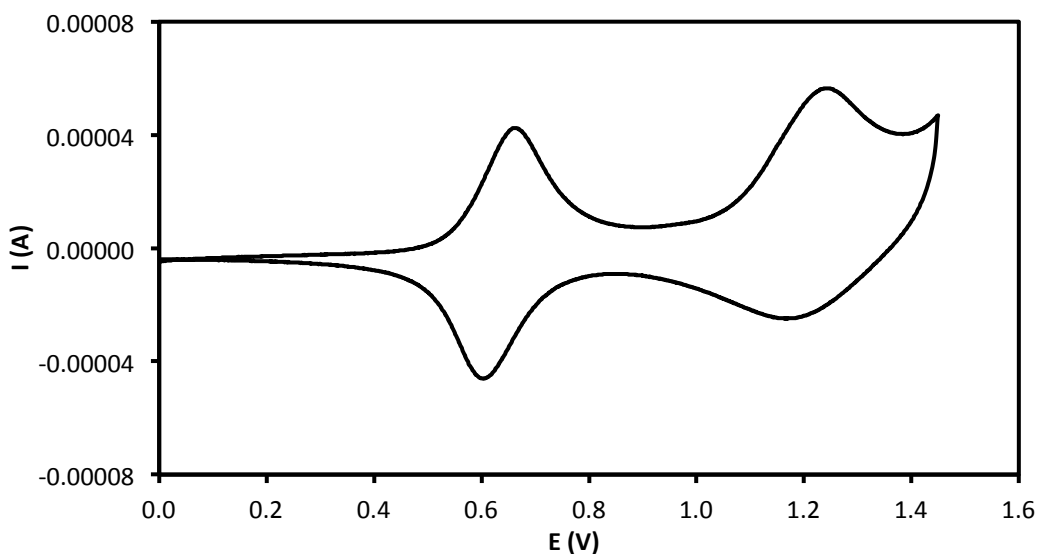


Figure 3.11 One scan CV of poly(**2.5**) in monomer free solution using ACN. [Scan rate = 0.1 V/s, WE = Platinum electrode, RE = Silver wire, and CE = Platinum wire]

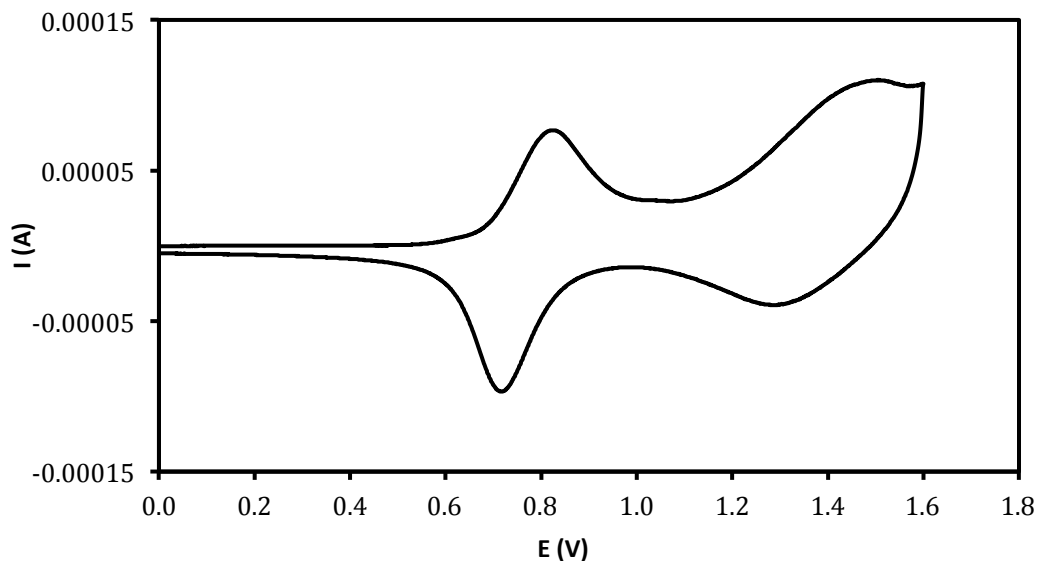


Figure 3.12 One scan CV of poly(**2.6**) in monomer free solution using ACN. [Scan rate = 0.1 V/s, WE = Platinum electrode, RE = Silver wire, and CE = Platinum wire]

To validate the structure of poly(**2.5**) and poly(**2.6**), infrared spectra (IR) of the polymers formed on the surface of a platinum electrode were recorded. The IR spectra of poly(**2.5**) (dashed line) and poly(**2.6**) (solid line) are presented in Figure 3.13. The polymer films were removed from the electrode surface, washed several times with CH_2Cl_2 and dried to remove the solvent. A KBr pellet containing poly(**2.5**) or poly(**2.6**) was prepared. Looking at the carbonyl (C=O) stretching region, the C=O stretching mode for both polymers are identical (1640 cm^{-1}). However, this value is lower than that obtained from the verdazyl monomer (1680 cm^{-1}). This 40 cm^{-1} shift is due to the strong interaction (electron-donating) of the doped form of the resulted π -conjugated polymer and the verdazyl radical in poly(**2.6**). A similar result has been observed when verdazyl radical was chelated to a redox active metal such as ruthenium (Ru),¹¹⁷ where the carbonyl stretching of verdazyl was shifted by 25 cm^{-1} . This was due to the interaction of the $d\pi$ orbital of the Ru with π^* orbital of the verdazyl radical. In our case, the interactions of π -conjugated system of the polymer and the π^* orbital of the radical are very strong, which explain the 40 cm^{-1} shift. Furthermore, the strongest peak in the IR spectra at about 840 cm^{-1} corresponds to the PF_6^- anion that was incorporated into the polymer during the electropolymerization process.¹¹⁸

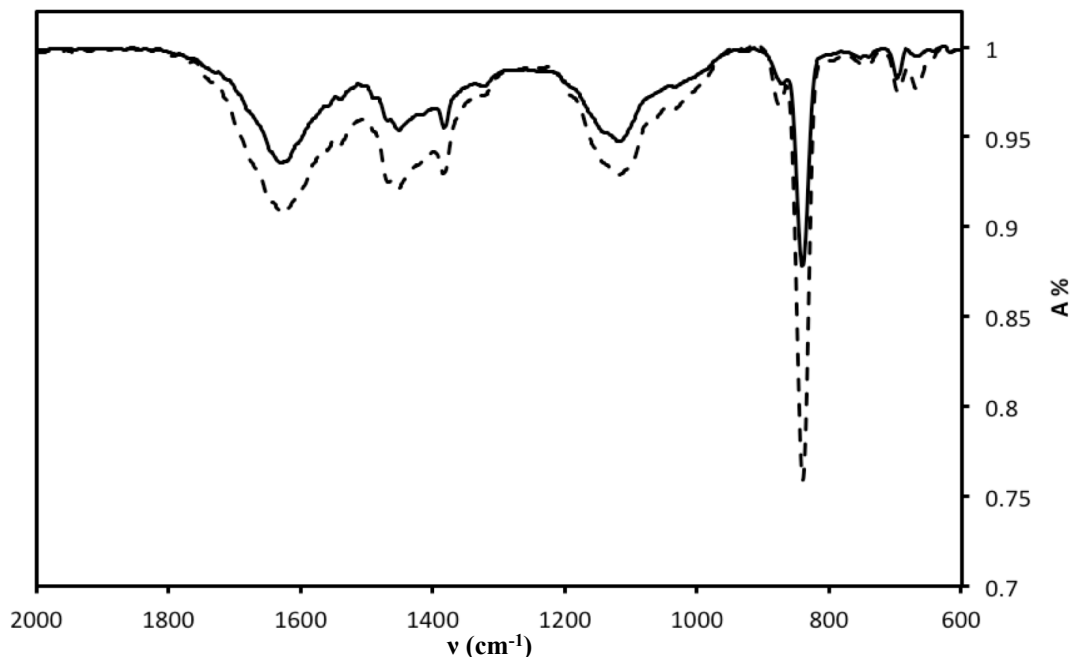


Figure 3.13 IR spectra of poly(**2.5**) (dashed line) and poly(**2.6**) (solid line)

From the characterization of poly(**2.5**) and poly(**2.6**) using CV and IR techniques, it has been shown for the first time that the verdazyl radical can be formed by electrochemical oxidation. The synthesis of verdazyl radical can be done either by chemical (as mentioned in chapter 2) or electrochemical oxidations of tetrazane.

The electrochemical oxidation of tetrazane **2.10** was also studied. Figure 3.14 illustrates the first CV scan of **2.10** using a 1 M n-Bu₄NPF₆/ACN solution. From this CV, there are two main irreversible peaks; the first peak at about 0.78 V (vs. Fc⁺/Fc) corresponds to the oxidation of tetrazane to its radical. As mentioned for tetrazane **2.5**, this 0.78 V peak is also very broad due to the electrochemical and chemical reactions occurring at this potential. The second irreversible peak at about 0.92 V (vs. Fc⁺/Fc) corresponds to the oxidation of terthiophene to form poly(terthiophene) as depicted in Scheme 3.7.

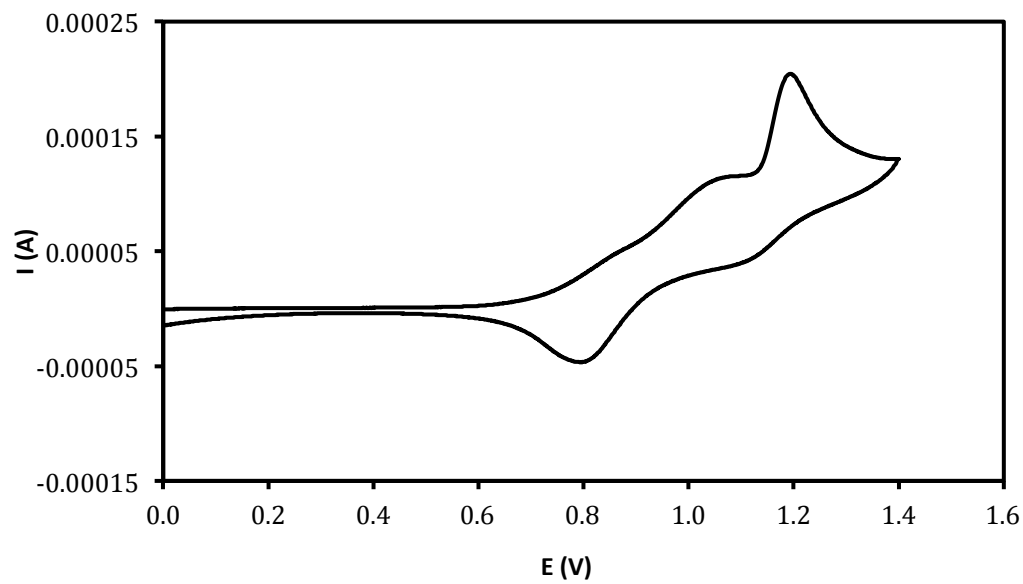
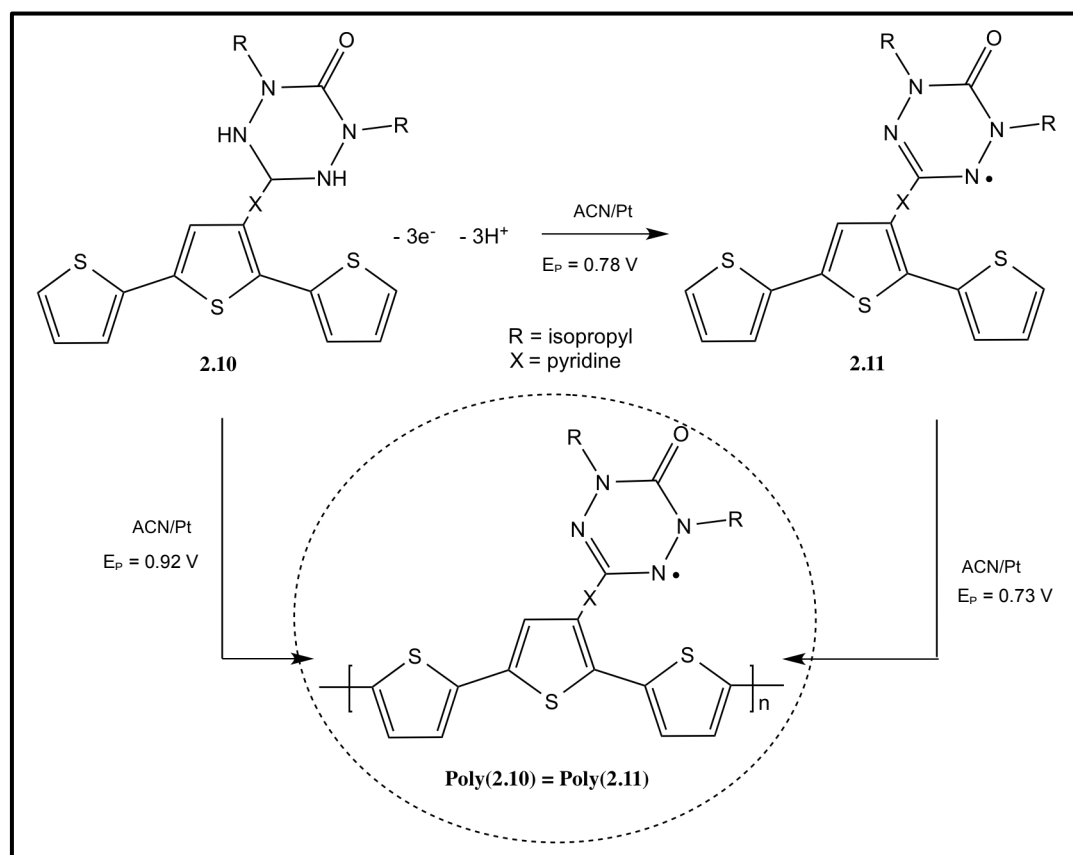


Figure 3.14 The first CV scan of **2.10** in ACN. [Scan rate = 0.1 V/s, WE = Platinum electrode, RE = Silver wire, and CE = Platinum wire]



Scheme 3.7 Electrochemical oxidation of tetrazane **2.10** to its radical **2.11**

Figure 3.15 shows the electropolymerization of the tetrazane **2.10** using a 1 M $n\text{-Bu}_4\text{NPF}_6/\text{ACN}$ solution. It has been successfully oxidatively electropolymerized to form its corresponding polymer, poly(**2.10**). This CV shows an increase in peak current during the oxidation process, with each successive scan indicating the formation of a polymer film on the surface of the platinum electrode. The electropolymerization of **2.10** also shows the formation of a new reversible peak at about 0.64 V (vs. Fc^+/Fc), which relate to the oxidation of verdazyl radical. As a result, the tetrazane, **2.10**, is converted to verdazyl radical **2.11** through the electrochemical oxidation reaction at 0.78 V (vs. Fc^+/Fc), Scheme 3.7. Unfortunately, poly(**2.10**) was not stable enough on the surface of the platinum electrodes to allow its characterization with CV and IR.

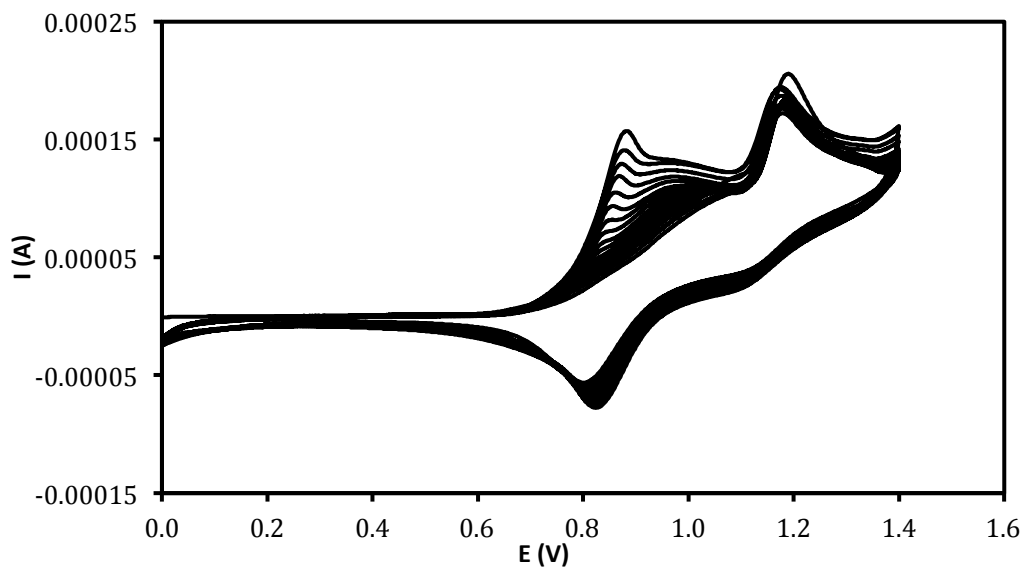


Figure 3.15 The electropolymerization of **2.10** in ACN. [Scan rate = 0.1 V/s, WE = Platinum electrode, RE = Silver wire, and CE = Platinum wire]

The electrochemical properties of the verdazyl radical **2.11** were also studied using a 1 M $n\text{-Bu}_4\text{NPF}_6/\text{ACN}$ solution. The first CV scan of **2.11** is depicted in Figure 3.16. This CV displays two main peaks. The first reversible peak at about 0.25 V (vs. Fc^+/Fc) corresponds to the oxidation of verdazyl radical. The reversibility of this peak shows the stability of the cationic species **2.11 π** , Scheme 3.8. The second irreversible peak at 0.73 V (vs. Fc^+/Fc) corresponds to the oxidation of terthiophene to form the corresponding poly(terthiophene).

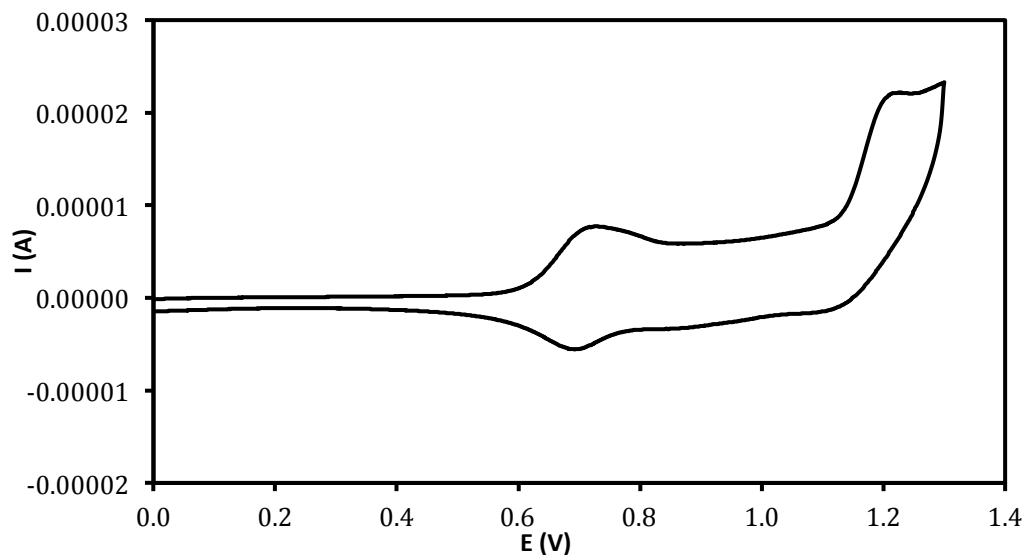
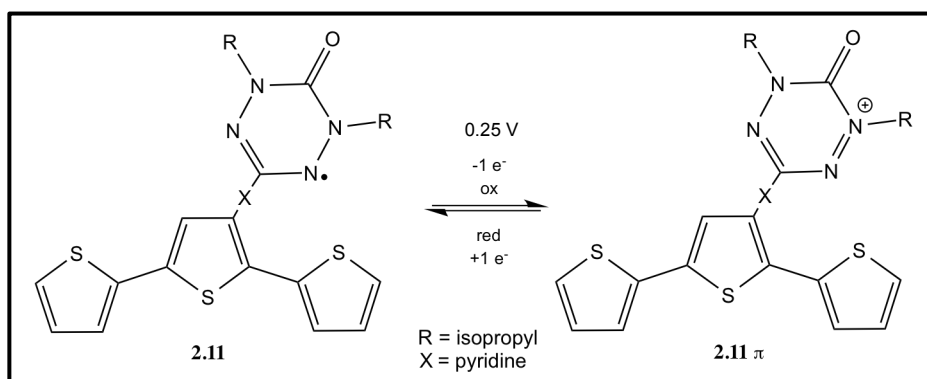


Figure 3.16 The first CV scan of **2.11** in ACN. [Scan rate = 0.1 V/s, WE = Platinum electrode, RE = Silver wire, and CE = Platinum wire]



Scheme 3.8 Electrochemical oxidation of verdazyl **2.11**

Figure 3.17 shows a 10 scan electropolymerization of verdazyl radical **2.11** using a 1 M $n\text{-Bu}_4\text{NPF}_6/\text{ACN}$ solution. During the oxidation process, the peak current increases with each successive scan, which shows the formation of a polymer film on the surface of platinum electrode (Scheme 3.9). Unfortunately, poly(**2.11**) was also not stable enough on the surface of the platinum electrode. Its characterization with CV and IR could not be carried out.

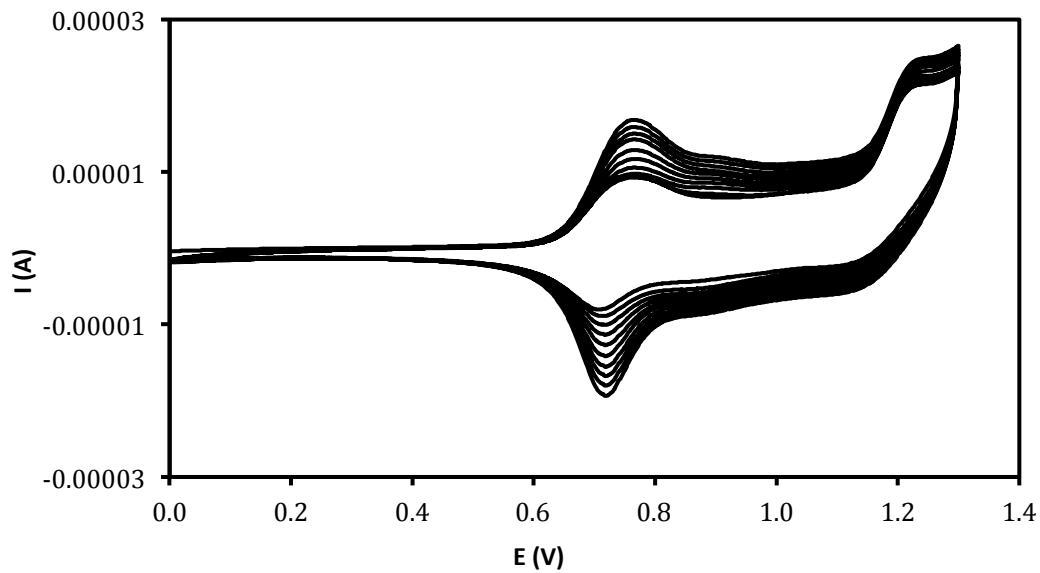
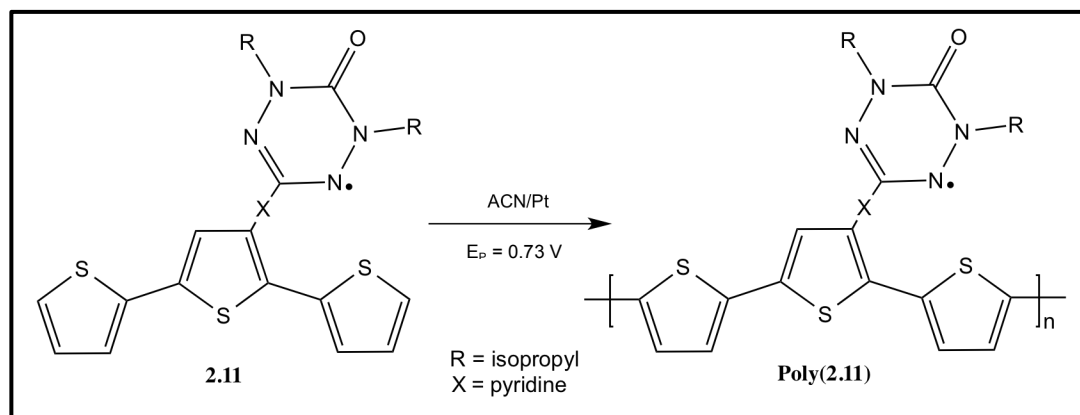


Figure 3.17 A 10 scan electrochemical oxidation of **2.11** in ACN. [Scan rate = 0.1 V/s, WE = Platinum electrode, RE = Silver wire, and CE = Platinum wire]



Scheme 3.9 Formation of poly(**2.11**) at the surface of platinum electrode

3.5 Summary

The electropolymerization of all monomers **2.3**, **2.5**, **2.6**, **2.9**, **2.10**, and **2.11** were successfully achieved in a 1 M n-Bu₄NPF₆/ACN solution. For all monomers, the peak current increase with each successive scan indicating the deposition of the polymer on the surface of the platinum electrode. Furthermore, the oxidation potential of the polymer appeared at lower oxidation potential than its corresponding monomer due to the increase in the length of conjugation of terthiophene.

For the first time, we were able to synthesize the verdazyl radical using the electrochemical oxidation of tetrazane at 0.52 V. This was confirmed by the characterization of the resulting polymers (poly(**2.5**) and poly(**2.6**)) using both CV and IR spectroscopy.

3.6 Experimental Section

3.6.1 Generalities:

All voltammetric experiments were done in acetonitrile (ACN) containing 1M n-Bu₄NPF₆. A platinum working electrode was used (diameter 1.6 mm). Platinum wire was used as an auxiliary (counter) electrode and silver wire was used as a reference electrode. All oxidation peak potentials/oxidation potentials were reported versus an internal reference ferrocene/ferrocenium redox. The working electrode (Pt) was polished on alumina before use. Infrared spectra (IR) of samples prepared as KBr pellets were measured with a BOMEM Fourier-transform infrared spectrophotometer.

3.6.2 Electrochemical oxidation of all new monomers

In a cell, (1.935 g, 5 mmol) of supporting electrolyte, n-Bu₄NPF₆ was dissolved in 5 mL of dry acetonitrile (ACN). A platinum electrode was used as the working electrode (WE). Platinum wire was used as a counter electrode (CE) and silver wire was used as a reference electrode (RE). The Pt electrode (WE) was polished with alumina before use. Also, all three electrodes were cleaned very well with distilled water, and acetone and were placed in the glassy cell. The background scan was run. After that, 20 mg of the monomer was added to the cell. The anodic potential was applied to perform the electrochemical oxidation.

3.6.3 Infrared spectroscopy (IR) of the polymers

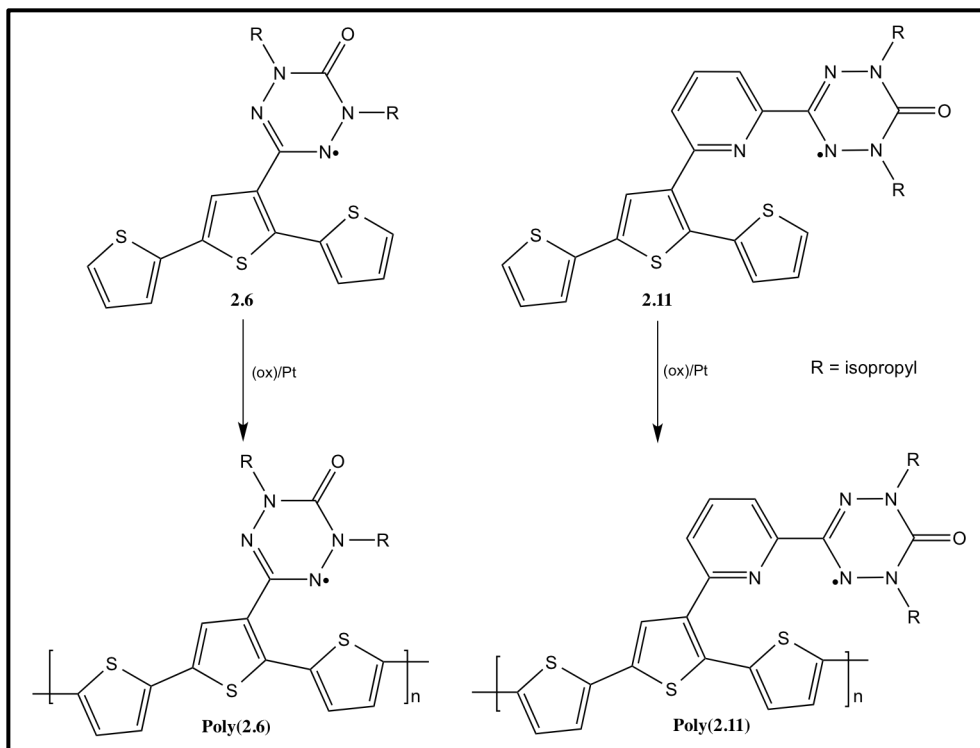
All polymers were taken off the electrode surface. They were then washed with CH₂Cl₂ and dried under vacuum. The KBr pellet was prepared by mixing a minimum amount of the polymer with KBr powder. A portion of the mixture was placed in a KBr press to form a pellet. The IR of the KBr pellet was recorded using a BOMEM Fourier-transform infrared spectrometer.

Chapter 4. Conclusions and Future Work

4 Conclusions

The family of verdazyl radicals has been extensively studied due to their efficiency as ligands for transition metals, spin labels, as well as components of magnetic and conducting materials. Most examples of stable radicals were discovered by accident, and some effort has been placed towards the design of stable radicals. The family of verdazyl radical is the only class of organic radicals that have high stability comparable to nitroxides.

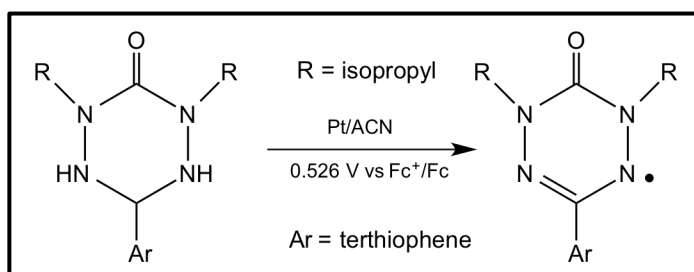
Materials with multiple properties have attracted a great deal of attention for their wide application in several fields such as photovoltaic cells, magnetic materials and energy storage. We are interested in the preparation of new conducting materials, which combine properties of stable free radicals and polythiophenes. So, two 1,5-diisopropyl-6-oxoverdazyl radical functionalized terthiophenes have been successfully prepared **2.6** and **2.11** (Scheme 4.1).



Scheme 4.1 Verdazyl radical functionalized oligo/polythiophenes

Radical functionalized terthiophenes **2.6** and **2.11** are very stable in the presence of air and organic solvents. Their oxidation using electrochemical methods affords the corresponding poly(**2.6**) and poly(**2.11**). Poly(**2.6**) has been characterized by CV and IR. The characterization of poly(**2.11**) is underway.

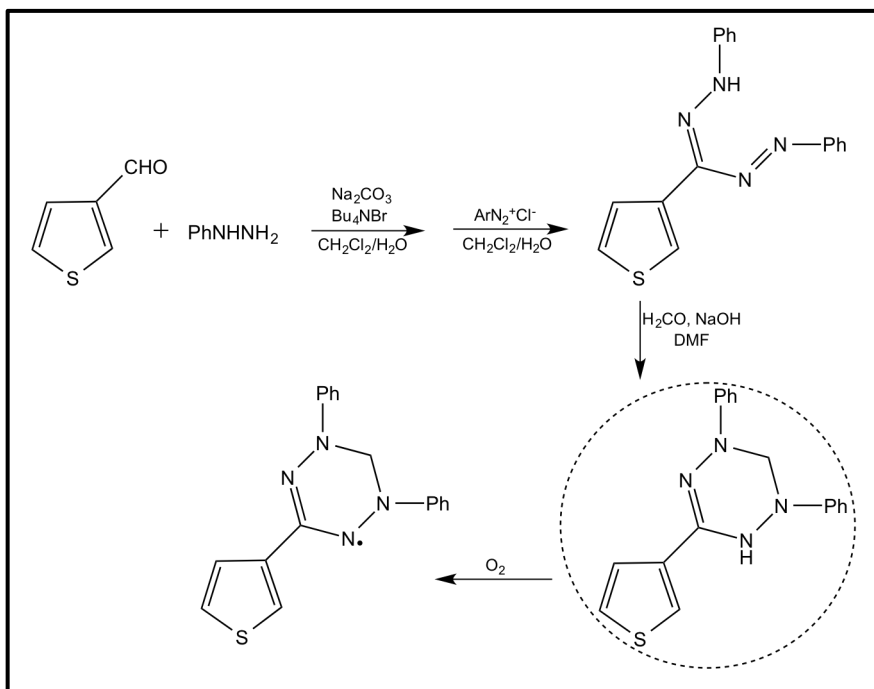
Surprisingly, the electrochemical oxidation of the radical precursors (6-membered heterocyclic ring) yields the verdazyl radical. To the best of our knowledge, it is the first synthesis of verdazyl radical using electrochemical method (Scheme 4.2). It is a new green synthetic route for verdazyl radicals.



Scheme 4.2 Electrosynthesis of verdazyl radicals

In addition to IR and CV, further characterizations of poly(**2.6**) and poly(**2.11**) using EPR, UV-vis and molecular orbital calculations are currently underway. Furthermore, magnetic properties of these polymers may find a great interest in the preparation of magnetic materials.

Attempts to prepare new radical functionalized oligo/polythiophene as described in Scheme 4.3 are currently in progress. In this type of verdazyl radical, the formazan has to be formed to give the verdazyl radical. The synthesis of formazan can be done according to literature procedures¹¹⁹ under biphasic conditions through the coupling reaction of an aryldiazonium chloride salt with arylhydrazones in the presence of a base.



Scheme 4.3 Synthetic route of thiophene bearing formazan radical

References

1. Hicks, R. G. *Org. Biomol. Chem.* **2007**, *5*, 1321.
2. Griller, D.; Ingold, K. U. *Acc. Chem. Res.* **1976**, *9*, 13.
3. Gomberg, M. *J. Am. Chem. Soc.* **1900**, *22*, 757.
4. Neumann, W. P.; Uzick, W.; Zarkadis, A. K. *J. Am. Chem. Soc.* **1986**, *108*, 3762.
5. Neumann, W. P.; Penenory, A.; Stewen, U.; Lehing, M. *J. Am. Chem. Soc.* **1989**, *111*, 5845.
6. Kahr, B.; Vanengen, D.; Gopalan, P. *Chem. Mater.* **1993**, *5*, 729.
7. Ballester, M.; Riera, J.; Castaner, J.; Badia, C.; Monso, J. M. *J. Am. Chem. Soc.* **1971**, *93*, 2215.
8. Ballester, M. *Acc. Chem. Res.* **1985**, *18*, 380.
9. Armet, O.; Veciana, J.; Rovira, C.; Riera, J.; Castaner, J.; Molins, E.; Rius, J.; Miravittles, C.; Olivella, S.; Brichfeus, J. *J. Phys. Chem.* **1987**, *91*, 5608.
10. Reid, D. H. *Tetrahedron* **1958**, *3*, 339.
11. Sogo, P. B.; Nakazak, M.; Calvin, M. *J. Chem. Phys.* **1957**, *26*, 1343.
12. Lewis, I. C.; Singer, L. S. *J. Chem. Phys.* **1969**, *73*, 215.
13. Altwicker, E. R. *Chem. Rev.* **1967**, *67*, 475.
14. Fehir, R. J.; McCusker, J. K. *J. Phys. Chem. A* **2009**, *113*, 9249.
15. Coppinger, G. M. *J. Am. Chem. Soc.* **1957**, *79*, 501.
16. Dietz, F.; Tyutyulkov, N.; Baumgarten, M. *J. Chem. Phys. B.* **1998**, *102*, 3912.
17. Novak, I.; Kovac, B. *Chem. Phys. Lett.* **2005**, *413*, 351.
18. Miura, Y.; Isogai, M.; Kinoshita, M. *Bull. Chem. Soc. Jpn.* **1987**, *60*, 3065.
19. Miura, Y.; Kurokawa, S.; Nakatsuji, M.; Ando, K.; Teki, Y. *J. Org. Chem.* **1998**, *63*, 8295.
20. Miura, Y.; Yamamoto, A.; Katsura, Y.; Kinoshita, M. *J. Chem. Soc., Chem. Commun.* **1980**, 37.
21. (a) Miura, Y.; Fuchikami, T.; Momoki, M. *Chem. Lett.* **1994**, 2127; (b) Miura, Y.; Kitagishi, T.; Ueno, S. *Bull. Chem. Soc. Jpn.* **1994**, *67*, 3282; (c) Miura, Y.; Momoki, M.; Fuchikami, T.; Teki, Y.; Itoh, K.; Mizutani, H. *J. Org. Chem.* **1996**, *61*, 4300; (d) Miura, Y.; Nakamura, S.; Teki, Y. *J. Org. Chem.* **2003**, *68*, 8244; (e) Miura, Y.; Nishi, T.; Teki, Y. *J. Org. Chem.* **2003**, *68*, 10158.

22. (a) Miura, Y.; Yamano, E.; Tanaka, A.; Ogo, Y. *Chem. Lett.* **1992**, 1831; (b) Miura, Y.; Yamano, E.; Tanaka, A.; Yamauchi, J. *J. Org. Chem.* **1994**, *59*, 3294; (c) Miura, Y.; Oka, H.; Yamano, E.; Teki, Y.; Takui, T.; Itoh, K. *Bull. Chem. Soc. Jpn.* **1995**, *68*, 1187.
23. Keana, J. F. W. *Chem. Rev.* **1978**, *78*, 37.
24. Fremy, E. *Ann. Chim. Phys.* **1845**, *15*, 408.
25. Piloty, O.; Scherwin, B. G. *Ber.* **1901**, *34*, 1870.
26. Clark, D. E. *Chemical Health & Safety* **2001**.
27. Lebedev, O. L.; Kazarnovskii, S. N. Zhur. *Obshch. Khim.* **1960**, *30*, 1631.
28. Neugebauer, F. A.; Fischer, H. *Angew. Chem. Int. Ed.* **1973**, *12*, 455.
29. Glazer, R. L.; Poindexter, E. H. *J. Chem. Phys.* **1971**, *55*, 4548.
30. Mukai, K.; Yamamoto, T.; Kohon, M.; Azuma, N.; Ishizu, K. *Bull. Chem. Soc. Jpn.* **1974**, *47*, 1797.
31. Neugebauer, F. A.; Brunner, H. *Tetrahedron* **1974**, *30*, 2841.
32. Mukai, K.; Shikata, H.; Azuma, N.; Kuwata, K. *J. Magn. Res.* **1979**, *35*, 133.
33. Kuhn, R.; Trischmann, H. *Angew. Chem. Int. Ed. Engl.* **1963**, *2*, 155.
34. Kursmitteilung, F. A.; Neugebauer, F. A.; Fischer, H. *Angew. Chem. Int. Ed. Engl.* **1980**, *19*, 724.
35. Milcent, R.; Barbier, G. *J. Heterocycl. Chem.* **1994**, *31*, 319.
36. Neugebauer, F. A.; Fischer, H.; Krieger, C. *J. Chem. Soc. Perkin. Trans.* **1993**, *2*, 535.
37. Neugebauer, F. A.; Fischer, H.; Siegel, R.; Krieger, C. *Chem. Ber.* **1983**, *116*, 3461.
38. Pare, E. C.; Brook, D. J.; Brieger, A.; Badik, M.; Schinke, M. *Org. Biomol. Chem.* **2005**, *3*, 4258.
39. Callabretta, R.; Gallina, C.; Giordano, C. *Synthesis* **1991**, 536.
40. Nalwa, H.S. *Handbook of Organic Conductive Molecules and Polymers* **1997**, *3*.
41. Nishide, H.; Miyasaka, M.; Yamazaki, T.; Tsuchida, E. *Polyhedron* **2001**, *20*, 1157.
42. Miyasaka, M. *Macromolecules* **2000**, *33*, 8211.
43. Oms, O.; Norel, L.; Chamoreau, L-M.; Rousseliere, H.; Train, C. *New J. Chem.* **2009**, *33*, 1663.
44. Bunce, N. J. *J. Chem. Educ.* **1987**, *64*, 907.

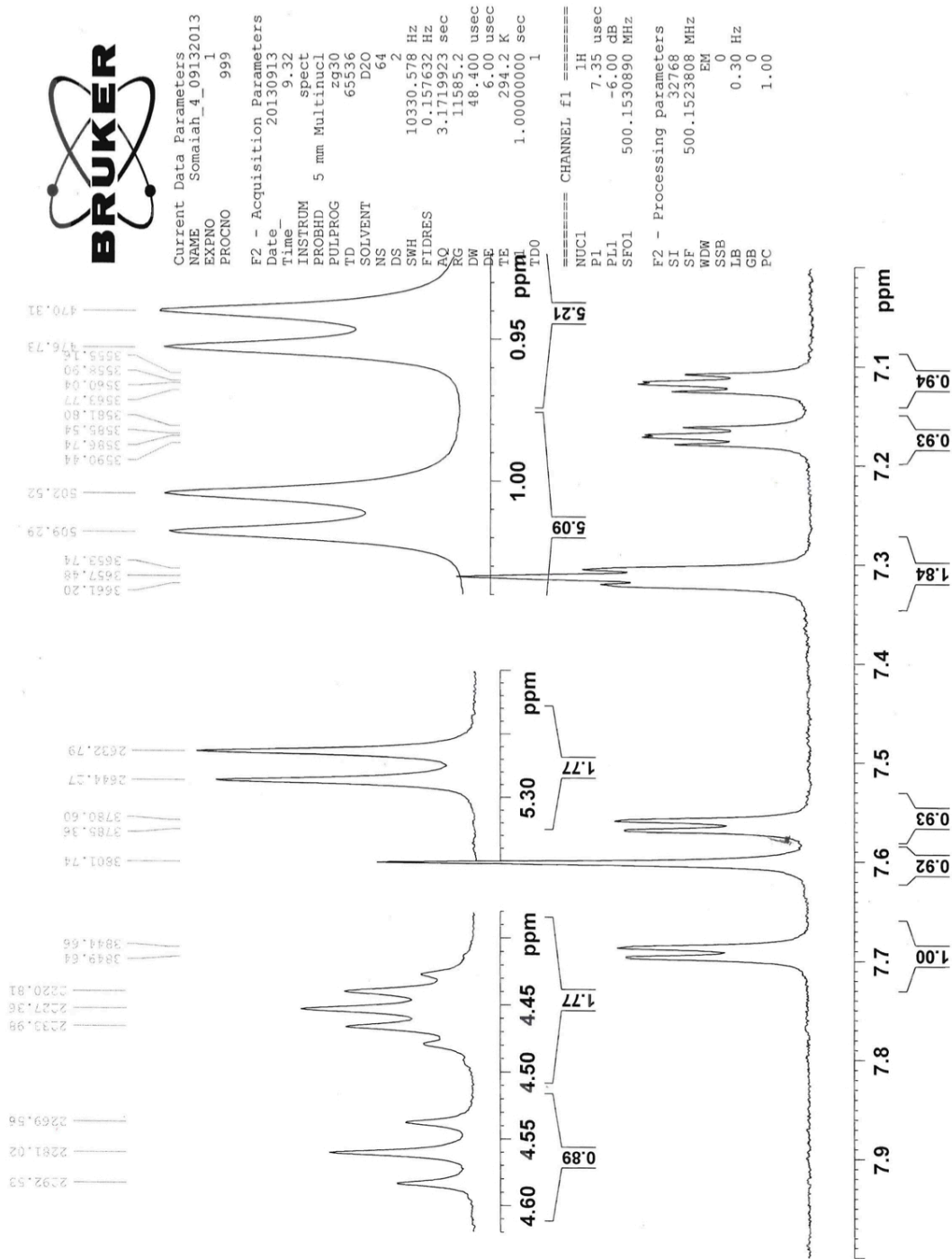
45. Bowry, V. W.; Ingold, K. U. *J. Am. Chem. Soc.* **1992**, *114*, 4992.
46. Janzen, E. G.; Blackburn, B. J. *J. Am. Chem. Soc.* **1969**, *91*, 4481.
47. Rosenthal, I.; Mossoba, M. M.; Riesz, P. *Can. J. Chem.* **1982**, *60*, 1486.
48. Janzen, E. G.; Evans, C. A.; Liu, J. I. P. *J. Mag. Res.* **1973**, *9*, 513.
49. Berliner, L. J. *Spin Labelling: Theory and Applications*. Academic Press: New York, **1979**.
50. Swartz, H. M.; Bolton, J. R.; Borg, D. C. *Biological Applications of Electron Spin Resonance*. Wiley-Interscience: New York, **1972**.
51. Vishnyakova, E. A. *Biochimica et Biophysica Acta* **2000**, *1467*, 380.
52. Yamada, B.; Kageoka, M.; Otsu, T. *Macromolecules* **1991**, *24*, 5234.
53. Brook, D. J. R.; Lynch, V.; Conklin, B.; Fox, M. A. *J. Am. Chem. Soc.* **1997**, *119*, 5155.
54. Chen, E. K. Y.; Teertstra, S. J.; Chan-Seng, D.; Otieno, P. O.; Hicks, R. G.; Georges, M. K. *Macromolecules* **2007**, *40*, 8609.
55. Yang, A.; Kasahara, T.; Chen, E. K. Y.; Hamer, G. K.; Georges, M. K. *Eur. J. Org. Chem.* **2008**, 4571.
56. Yamada, B.; Yoshikawa, E.; Shiraiishi, K.; Miura, H.; Otsu, T. *Polymer* **1991**, *32*, 1892.
57. Yamada, B.; Tanaka, H.; Konishi, K.; Otsu, T. *Macromol. Sci., Pure and Appl. Chem.* **1994**, *A31*, 351.
58. Yamada, B.; Nobukane, Y.; Miura, Y. *Polym. Bull. (Berlin)* **1998**, *41*, 539.
59. (a) Lemaire, M. T.; Barclay, T. M.; Thompson, L. K.; Hicks, R. G. *Inorg. Chim. Acta.* **2006**, 359, 2616; (b) Koivisto, B. D.; Hicks, R. G. *Coord. Chem. Rev.* **2005**, *249*, 2612.
60. Brook, D.; Cardius J. R.; Benjamin C. H.; Michael H.; Gordon T. Y. *Chem. Commun.* **2010**, *46*, 6590.
61. Brook, D.; Abeyta, V. *J. Chem. Soc., Dalton Trans.* **2002**, *22*, 4219.
62. Norel, L.; Chamoreau, L. M.; Journaux, Y.; Oms, O.; Chastanet, G.; Train, C. *Chem. Commun.* **2009**, 2381.
63. Norel, L.; Pointillart, F.; Train, C.; Chamoreau, L. M.; Boubekeur, K.; Journaux, Y.; Brieger, A.; Brook, D. J. R. *Inorg. Chem.* **2008**, *47*, 2396.

64. McKinnon, S. D. J.; Patrick, B. O.; Lever, A. B. P.; Hicks, R. G. *J. Am. Chem. Soc.* **2011**, *133*, 13587.
65. Panico, R.; Powell, W.; Richer, J. *A guide to IUPAC Nomenclature of Organic Compounds*; Blackwell Scientific Publications: Oxford, **1993**.
66. Gronowitz, S. *The Chemistry of Heterocyclic Compounds, Thiophene and its Derivatives*; Wiley: New York, **1993**; Vol. 44.
67. Epiotis, N.; Cherry, W.; Bernardi, F.; Hehre, W. *J. Am. Chem. Soc.* **1976**, *98*, 4361.
68. Belen'kii, L. I.; Suslov, I. A.; Chuvylkin, N. D. *Chem. Heterocycl. Compd.* **2003**, *39*, 36.
69. Bauer, H. H.; Christian, G. D.; O'Reilly, J. E. *Instrumental Analysis*; Allyn and Bacon: Boston, **1978**; Chapter 13.
70. Weckhuysen, B. M.; Heidler, R.; Schoonheydt, R. A. *Mol. Sieves* **2004**, *4*, 295.
71. Odom, B.; Hanneke, D.; D'Urso, B.; Gabrielse, G. *Phys. Rev. Lett.* **2006**, *97*, 3.
72. Lunde, A.; Shiotani, M.; Shimada, S. *Principles and Applications of ESR Spectroscopy* Springer-Verlag: London, New York **2011**.
73. Murphy, D. M. *EPR (Electron Paramagnetic Resonance) Spectroscopy of Polycrystalline Oxide System* John Wiley & Sons: Weinheim, Germany **2009**.
74. Barr, C. L.; Chase, P. A.; Hicks, R. G.; Lemaire, M. T.; Stevens, C. L. *J. Org. Chem.* **1999**, *64*, 8893.
75. Gu, Z.; Tang, P.; Zhao, B.; Luo, H.; Guo, X.; Chen, H.; Yu, G.; Liu, X.; Shen, P.; Tan, S. *Macromolecules* **2012**, *45*, 2359.
76. Lee, K.; Morino, K.; Sudo, A.; Endo, T. *J. Polym. Sci. A1* **2011**, *49*, 1190.
77. Lee, K.; Lee, H.; Kuramoto, K.; Tanaka, Y.; Morino, K.; Sudo, A.; Okauchi, T.; Tsuge, A.; Endo, T. *J. Polym. Sci. A1* **2011**, *49*, 234.
78. Bolduce, A.; Lachapelle, V.; Skene, W. G. *Macromol. Symp.* **2010**, *297*, 87.
79. Neugebauer, F. A.; Fischer, H.; Siegel, R. *Chem. Ber.* **1988**, *121*, 815.
80. Duling, D. R. Simulation of Multiple Isotropic Spin Trap EPR Spectra, *J. Magn. Reson., Ser. B*, **1994**, *104*, 105.
81. Brook, D. J. R.; Yee, G. T. *J. Org. Chem.* **2006**, *71*, 4889.
82. Gilroy, J. B.; McKinnon, S. D. J.; Kennepohl, P.; Zsombor, M. S.; Ferguson, M. J.; Thompson, L. K.; Hicks, R. G. *J. Org. Chem.* **2007**, *72*, 8062.

83. Awaga, K.; Coronado, E.; Drillon, M. *MRS Bull.* **2002**, 52.
84. Palacio, F.; Miller, J. S. *Nature* **2000**, 408, 421.
85. Hicks, R. G.; Lemaire, M. T.; Thompson, L. K.; Barclay, T. M. *J. Am. Chem. Soc.* **2000**, 122, 8077.
86. Barclay, T. M.; Hicks, R. G.; Lemaire, M. T.; Thompson, L. K. *Inorg. Chem.* **2001**, 40, 5581.
87. Chahma, M.; Macnamara, K.; van der Est, A.; Alberola, A.; Polo, V.; Pilkington, M. *New J. Chem.* **2007**, 31, 1973.
88. Zoski, C. *Handbook of Electrochemistry*, 1st ed.; Elsevier: Amsterdam, **2007**.
89. Atkins, A.; Paula, J. *Physical Chemistry*, 7th ed.; W.H. Freeman: New York, **2002**.
90. Bard, A.; Faulkner, L. *Electrochemical Methods: Fundamentals and Applications*, 2nd ed.; John Wiley & Sons: New Jersey, **2001**.
91. Skoog, D.; West, D.; Holler, F.; Crouch, S. *Fundamentals of Analytical Chemistry*, 8th ed.; Thomson: Belmont, **2004**.
92. Nicholson, R.; Shain, I. *Anal. Chem.* **1964**, 36, 706.
93. Nadjo, L.; Saveant, J.-M. *Electroanal. Chem.* **1973**, 48, 113.
94. Sadki, S.; Schottland, P.; Brodie, N. S. G. *Chem. Soc. Rev.* **2000**, 29, 283.
95. Genies, E.; Bidan, G.; Diaz, A. *J. Electroanal. Chem.* **1983**, 149, 101.
96. Ratera, I.; Ruiz-Molina, D.; Renz, F.; Ensling, J.; Wurst, K.; Rovira, C.; Gutlich, P.; Veciana, J. *J. Am. Chem. Soc.* **2003**, 125, 1462.
97. Sporer, C.; Ratera, I.; Ruiz-Molina, D.; Zhao, Y. X.; Vidal-Gancedo, J.; Wurst, K.; Jaitner, P.; Clays, K.; Persoons, A.; Rovira, C.; Veciana, J. *Angew. Chem. Int. Ed.* **2004**, 43, 5266.
98. Heckmann, A.; Lambert, C. *J. Am. Chem. Soc.* **2007**, 129, 5515.
99. Beer, L.; Brusso, J. L.; Cordes, A. W.; Haddon, R. C.; Itkis, M. E.; Kirschbaum, K.; MacGregor, D. S.; Oakley, R. T.; Pinkerton, A. A.; Reed, R. W. *J. Am. Chem. Soc.* **2002**, 124, 9498.
100. Chi, X.; Itkis, M. E.; Patrick, B. O.; Barclay, T. M.; Reed, R. W.; Oakley, R. T.; Cordes, A. W.; Haddon, R. C. *J. Am. Chem. Soc.* **1999**, 121, 10395.
101. Boere, R. T.; Moock, K. H. *J. Am. Chem. Soc.* **1995**, 117, 4755.
102. Nakahara, K.; Iwasa, S.; Satoh, M.; Morioka, Y.; Iriyama, J.; Suguro, M.;

- Hasegawa, E. *Chem. Phys. Lett.* **2002**, 359, 351.
103. Nishide, H.; Iwasa, S.; Pu, Y. J.; Suga, T.; Nakahara, K.; Satoh, M. *Electrochim. Acta* **2004**, 50, 827.
104. Suga, T.; Pu, Y. J.; Oyaizu, K.; Nishide, H. *Bull. Chem. Soc. Jpn.* **2004**, 77, 2203.
105. Buhrmester, C.; Moshurchak, L. M.; Wang, R. L.; Dahn, J. R. *J. Electrochem. Soc.* **2006**, 153, A1800.
106. Katsumata, T.; Satoh, M.; Wada, J.; Shiotsuki, M.; Sanda, F.; Masuda, T. *Macromol. Rapid Commun.* **2006**, 27, 1206.
107. Nakahara, K.; Iwasa, S.; Iriyama, J.; Morioka, Y.; Suguro, M.; Satoh, M.; Cairns, E. J. *Electrochim Acta* **2006**, 52, 921.
108. Li, H. Q.; Zou, Y.; Xia, Y. Y. *Electrochim. Acta* **2007**, 52, 2153.
109. Lazar, M. *Free Radical in Chemistry* Boca, Florida: CRC Press **1989**.
110. Zhang, L.; Su, L.; Wang, S.; Wan, C.; Zha, Z.; Du, J.; Wang, Z. *Chem. Commun.* **2011**, 47, 5488.
111. Adenier, A.; Chehimi, M. M.; Gallardo, I.; Pinson, J.; Vila, N. *Langmuir* **2004**, 20, 8243.
112. Hampson, N. A.; Lee, J. B.; Morley, J. R.; Scanlon, B. *Can J. Chem.* **1969**, 47, 3729.
113. Chemistruck, V.; Chambers, D.; Brook, D. J. R. *J. Org. Chem.* **2009**, 74, 1850.
114. Sarac, S.; Evans, U.; Serantoni, M.; Clohessy, J.; Cunnane, V. *Surf. Coat. Technol.* **2004**, 182, 7.
115. Brillas, E.; Oliver, R.; Estrany, F.; Rodríguez, E.; Tejer, S. *Electrochim. Acta* **2002**, 47, 1623.
116. Roncali, J.; Garnier, F.; Lemaire, M.; Gerreau, R. *Synth. Met.* **1986**, 15, 323.
117. McKinnon, S. D. J.; Patrick, B. O.; Lever, A. B. P.; Hicks, R. G. *Chem. Commun.* **2010**, 46, 773.
118. Allison, J. D.; Walton, R. A. *J. Am. Chem. Soc.* **1984**, 106, 163.
119. Gilroy, J. B.; McKinnon, S. D. J.; Koivisto, B. D.; Hicks, R. G. *Org. Lett.* **2007**, 9, 4837.

Appendices: ^1H and ^{13}C NMR Spectra Expansion



Appendix 1 ^1H NMR spectrum expansion of compound 2.5 in DMSO



Current Data Parameters
NAME Somalah_4C_09132013
EXPNO 1
PROCNO 999

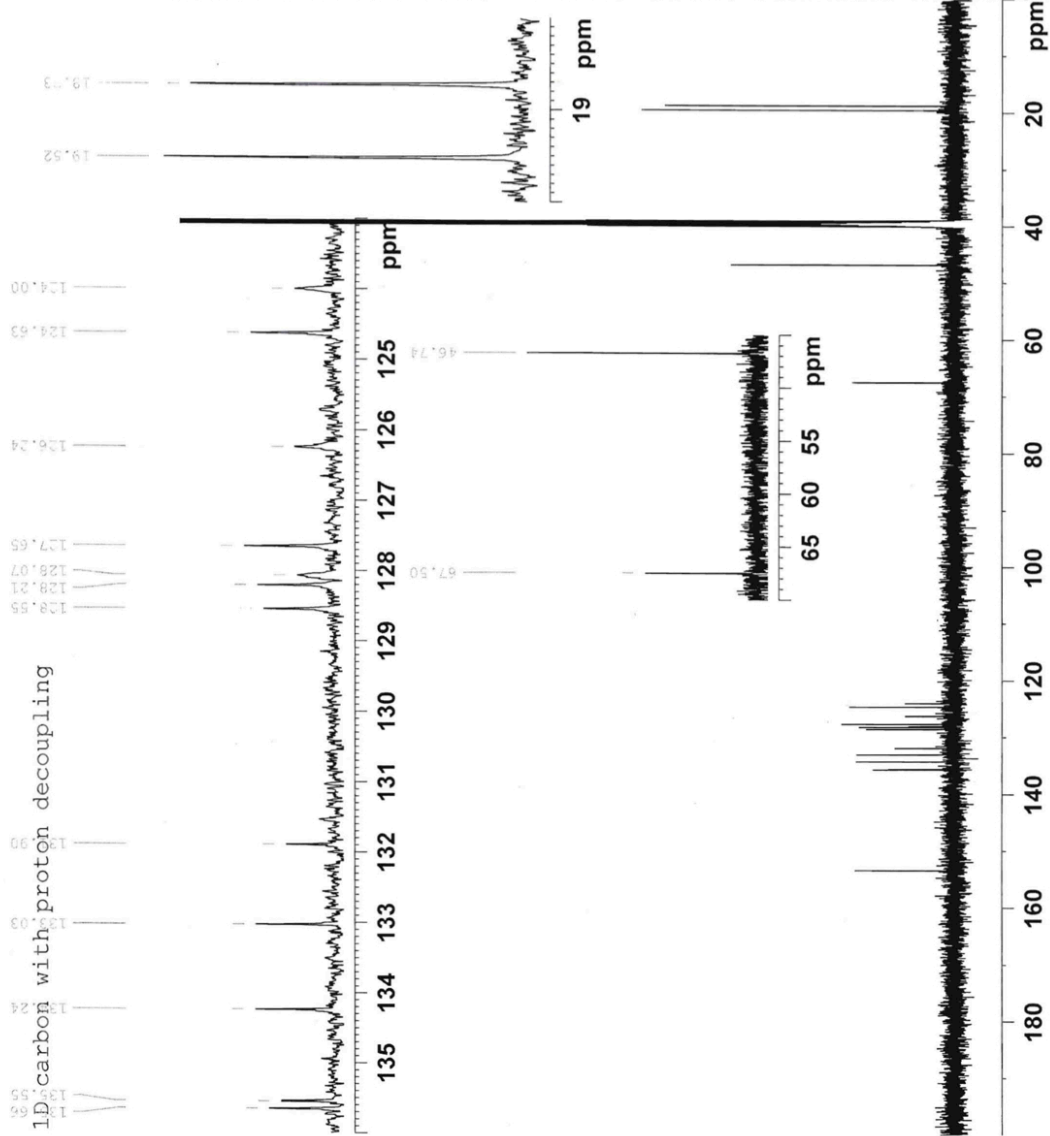
F2 - Acquisition Parameters

Date_ 20130913
Time_ 10.08
INSTRUM spect
PROBHD 5 mm Multinucl
PULPROG zgpg30
TD 65536
SOLVENT CDCl3
NS 2048
DS 4
SWH 30030.029 Hz
FIDRES 0.458222 Hz
AQ 1.0912244 sec
RG 8192
DW 16.650 usec
DE 6.00 usec
TE 294.8 K
D1 2.00000000 sec
d11 0.03000000 sec
DELTA 1.89999998 sec
TDO 1

==== CHANNEL f1 =====
NUC1 13C
P1 13.00 usec
PL1 -4.10 dB
SFO1 125.7753940 MHz

==== CHANNEL f2 =====
CPDPRG2 waltz16
NUC2 1H
PCPD2 80.00 usec
PL2 -6.00 dB
PL12 14.74 dB
PL13 17.66 dB
SFO2 500.1520010 MHz

F2 - Processing parameters
SI 32768
SF 125.7634675 MHz
WDW EM
SSB 0
GB 1.00 Hz
PC 1.00



Appendix 2 ^{13}C NMR spectrum expansion of compound 2.5 in DMSO

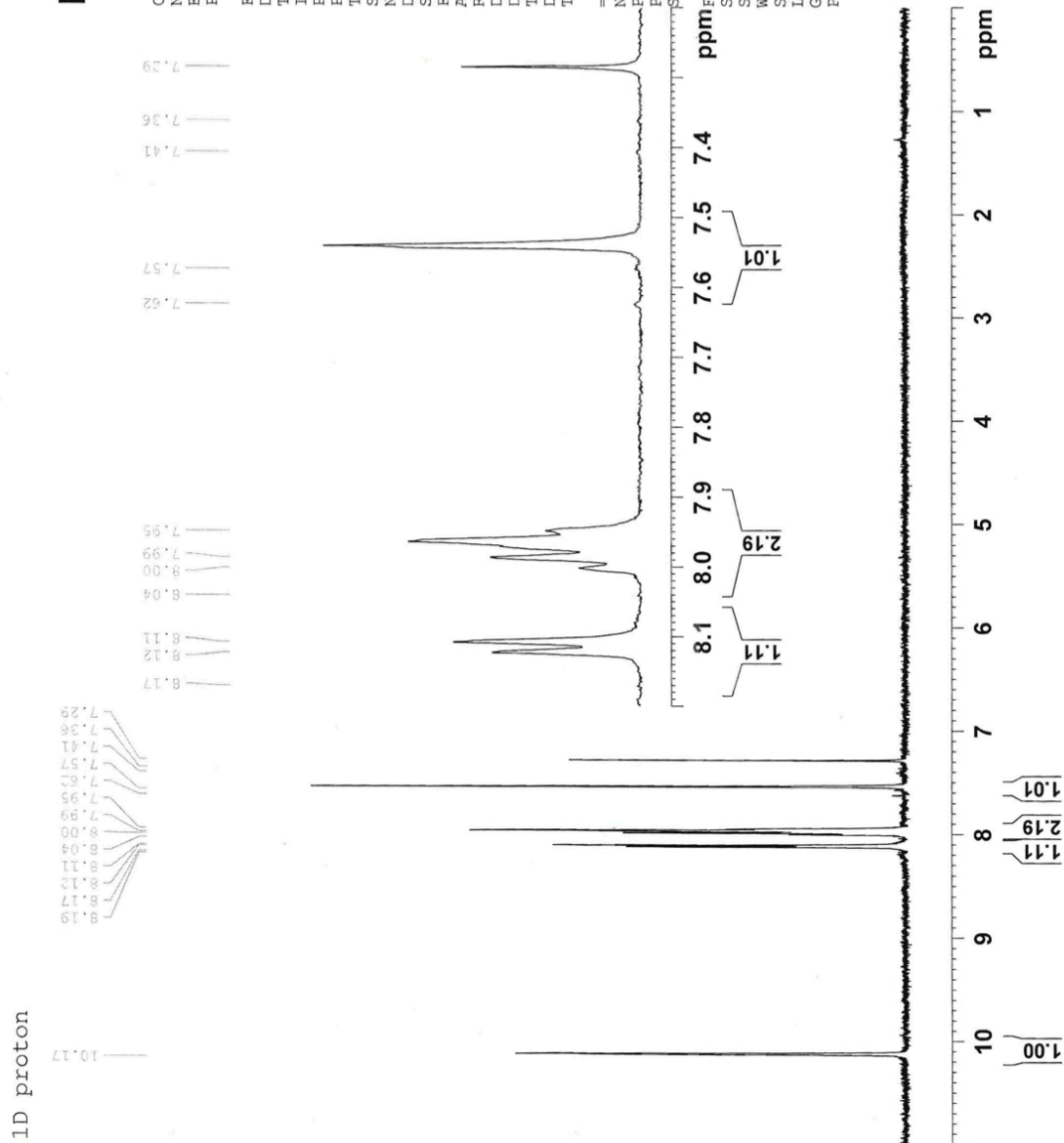


Current Data Parameters
NAME Somaiah_IH_09132013
EXPNO 1
PROCNO 999

F2 - Acquisition Parameters
Date_ 20130913
Time_ 14.54
INSTRUM spect
PROBHD 5 mm Multinucl
PULPROG zg30
TD 65536
SOLVENT D2O
NS 64
DS 2
SWH 10330.578 Hz
FIDRES 0.157632 Hz
AQ 3.1719923 sec
RG 46341
DW 48.400 usec
DE 6.00 usec
TE 295.2 K
D1 1.00000000 sec
TD0 1

==== CHANNEL f1 =====
NUC1 1H
P1 7.35 usec
PL1 -6.00 dB
SFO1 500.1530890 MHz

F2 - Processing parameters
SI 32768
SF 500.1500000 MHz
WDW EM
SSB 0
LB 0.30 Hz
GB 0
PC 1.40



Appendix 3 ^1H NMR spectrum expansion of compound 2.8 in CDCl_3



1D proton



Current Data Parameters
NAME Somaiah_2_H_09132013
EXPNO 1
PROCNO 999

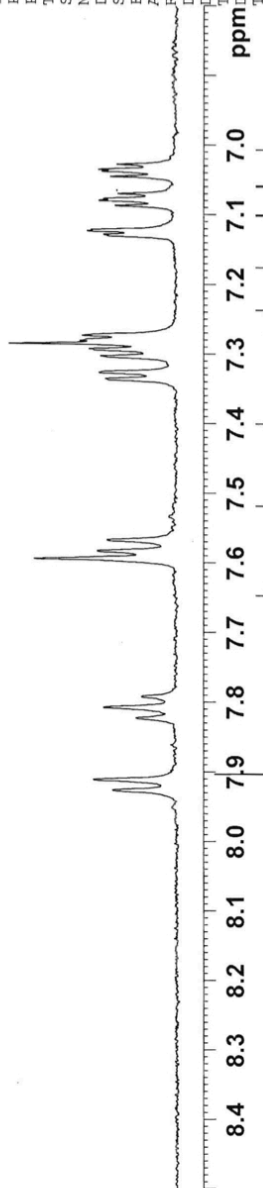
F2 - Acquisition Parameters

Date_ 20130914
Time_ 16.26
INSTRUM spect
PROBHD 5 mm Multinucl
PULPROG zg30
TD 65536
SOLVENT D2O
NS 64
DS 2
SWH 10330.578 Hz
FIDRES 0.157632 Hz
AQ 3.1719923 sec
RG 46341
DW 48.400 usec
DE 6.00 usec
TE 297.2 K
TD0 1.00000000 sec
I 1

==== CHANNEL f1 =====
NUC1 1H
P1 7.35 usec
PL1 -6.00 dB
SFO1 500.1530890 MHz

F2 - Processing parameters

SI 32768
SF 500.1500000 MHz
WDW EM
SSB 0
LB 0.30 Hz
GB 0
PC 1.40

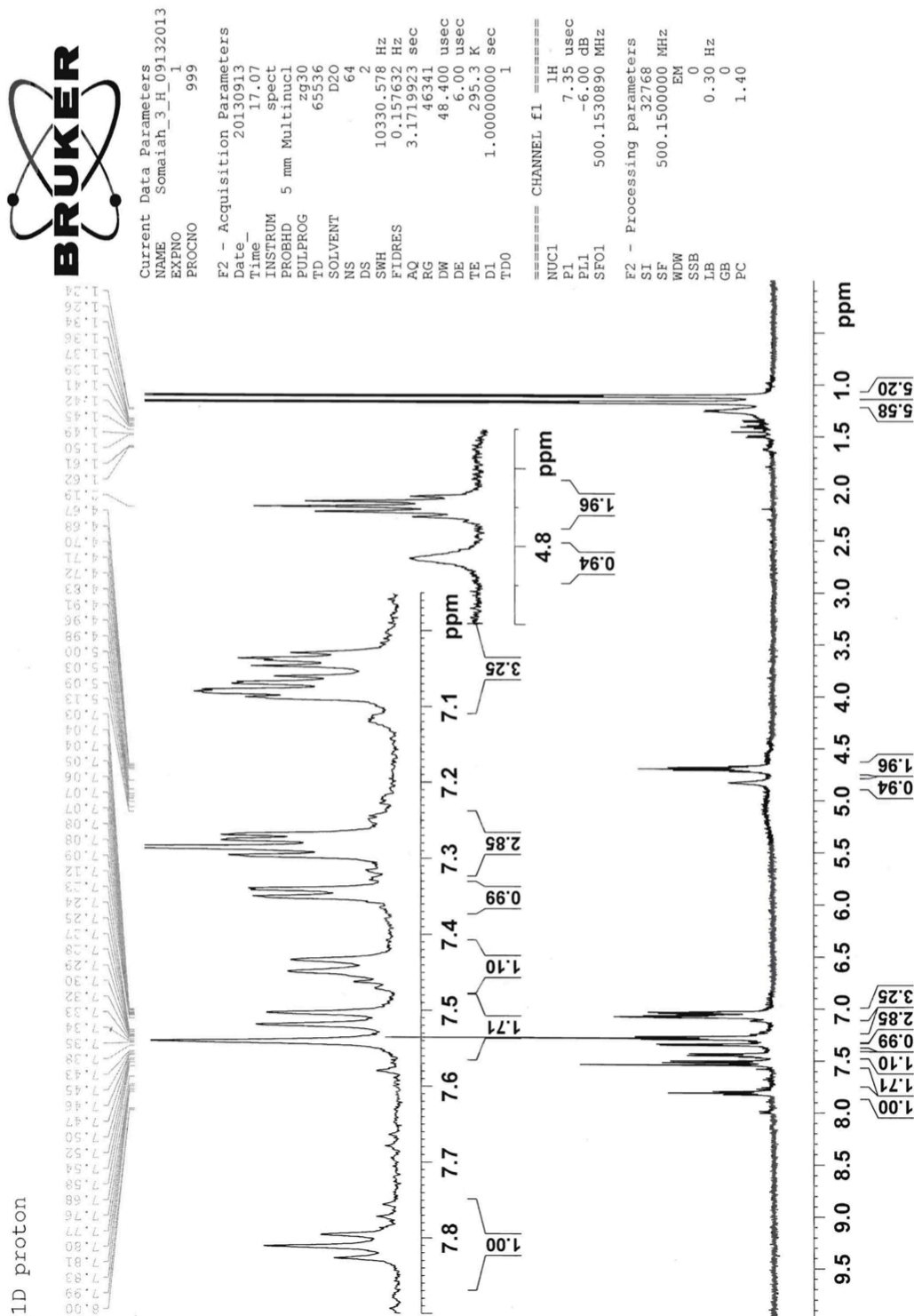


1.14
1.07
1.08
3.68
2.12

1.14
1.07
1.08
3.68
2.12

10 ppm
9
8
7
6
5
4
3
2
1
ppm

Appendix 5 ^1H NMR spectrum expansion of compound 2.9 in CDCl_3



Appendix 7 ^1H NMR spectrum expansion of compound **2.10** in CDCl_3

